DISSERTATION

A CIRCUITOUS JOURNEY OF VIRUS CHARACTERIZATION AND SURVEILLANCE IN NORTH AND CENTRAL AMERICA.

Submitted by

Rebekah J. McMinn

Department of Microbiology, Immunology, and Pathology

In partial fulfillment of the requirements

For the Degree of Doctor of Philosophy

Colorado State University

Fort Collins, Colorado

Summer 2023

Doctoral Committee:

Advisor: Gregory D. Ebel

Sandra Quackenbush
Aaron Brault
Jennifer Neuwald

ABSTRACT

A CIRCUITOUS JOURNEY OF VIRUS CHARACTERIZATION AND SURVEILLANCE IN NORTH AND CENTRAL AMERICA.

The burden of ticks and the pathogens they carry is increasing worldwide. Powassan virus (POWV, *Flaviviridae*: *Flavivirus*), the only known North American tick-borne flavivirus, is of particular concern due to rising cases and the severe morbidity of human disease. In this dissertation we evaluated the recent emergence of POWV from a culmination of field (chapter 2), *in vitro* (chapter 3), and *in-vivo* (chapter 4) studies. In addition, we determined the applicability of a vector-enabled surveillance method (xenosurveillance) in Central America (chapter 5).

We first used a genetic approach to evaluate the emergence of lineage II POWV, known as deer tick virus (DTV), in parts of North America where human cases occur. We detected DTV-positive ticks from eight of twenty locations in the northeastern United States with an average infection rate of 1.4%. High-depth whole genome sequencing of eighty-four new and archival POWV and DTV samples allowed us to assess geographic and temporal phylodynamics. We observed both stable infection in the northeastern United States and patterns of geographic dispersal within and between regions. Bayesian skyline analysis demonstrated DTV population expansion over the last fifty years. This is concordant with the documented expansion of *Ixodes scapularis* tick populations and suggests increasing risk of human exposure as the vector spreads. Finally, we isolated sixteen novel viruses in cell culture and demonstrated limited genetic change after passage, a valuable resource for future studies investigating this emerging virus. We then assessed *in vitro* phenotypes of POWV on human neuronal cells using 16 genetically diverse isolates obtained from a broad geographic and temporal range. We determined over a 10,000-fold range in peak viral titer and significantly decreased cell mortality for two Midwest DTV isolates, though no clear correlation between *in vitro* phenotype and geo-temporal characteristics could be made. We then

performed whole genome sequencing of virus post neuronal cell passage to identify potential residues of interest. Again, no residues could be linked to phenotype, though several interesting residues with increased frequency post-neuronal cell culture were identified.

Based on the significant *in vitro* diversity observed, we sought to assess pathogenesis and tick transmission phenotypes between isolates. We noted neurological disease in mice in both lineages of POWV, with potential low-virulence strains derived from coastal New York. Additionally, we observed an early neuroinvasion phenotype for a Midwest DTV isolate. The ability to infect *I. scapularis* ticks was determined by feeding on infected host mice (viremic) and through an artificial infection method. Surprisingly, infection rates in ticks via viremic or artificial infection remained consistent between all five isolates tested, resulting in 12-20% infection rate. Taken together, these data demonstrate potential genotype-independent ability to infect ticks and conversely, strain-dependent differences in pathogenesis.

In chapter 5, we evaluated a vector-enabled surveillance method ('xenosurveillance') in rural Guatemala. Surveillance methods that permit rapid detection of circulating pathogens are desperately needed. Xenosurveillance is a novel surveillance approach that takes advantage of mosquito feeding behavior to identify blood-borne pathogens that may be circulating in human and animal hosts. This approach circumvents invasive blood sampling of individuals and results in an abundant sample source derived from both humans and animals. In this study, twenty households from two villages (Los Encuentros and Chiquirines) in rural, southwest Guatemala were enrolled and underwent weekly prospective surveillance for 16 weeks. When febrile illness was reported in a household, recently blood-fed mosquitoes were collected from within dwellings and blood samples taken from each member of the household. Mosquitoes were identified to species and blood sources identified by sequencing. Shotgun metagenomic sequencing was used to identify circulating viruses. *Culex pipiens* (60.9%) and *Aedes aegypti* (18.6%) were the most abundant mosquitoes collected. Bloodmeal sources were most commonly human (32.6%) and chicken (31.6%), with various other mammal and avian hosts detected. Several mosquito-specific viruses were detected, including Culex orthophasma virus. Human pathogens were not

detected. While more intensive sampling may be needed to detect human pathogens, sampling mosquitoes that feed on humans and domestic animals may prove valuable for monitoring pathogens with zoonotic potential.

ACKNOWLEDGMENTS

I've been lucky enough to work with an amazing group of people in the Ebel lab over the past six years. Dr. Emily Gallichotte has been the mentor I can turn to for anything, and I know she will have good advice to give. I've learned a lot from her over the past few years, and truly, she's made me a better scientist. Dr. Emma Harris (the Ebel lab creeper) is the kindest person you'll ever meet and has always offered me unwavering help and support both on tick experiments and xenosurveillance. Dr. Reyes Murrieta has played several roles in my life: lab mate, mentor, adventure buddy, friend, housemate, and sometimes adversary. I've really valued his mentorship over the years and the comradery we have, even if he does push my buttons. Thank you to Emily 'Fitz' Fitzmeyer, who has been a peer, friend, and confidant. Thank you to all the members of the Ebel lab, past and present, who have made the lab a welcoming and supportive place to learn. Finally, thank you to Dr. Greg Ebel, who works his ass off to be the best mentor and P.I. he can be. I truly appreciate all the effort he puts in to building a supportive lab community. I know through experience that he will have my back when I need it.

I would not be here without the support of the academic community in MIP. My committee members: Drs. Sandra Quackenbush, Aaron Brault, and Jennifer Neuwald have been incredibly supportive and patient, even when I didn't think I deserved it. Thank you to Drs. Mark Zabel and Zaid Abdo for believing in me from the beginning. Thanks to Susi Bennett for answering all my biosafety and shipping questions and just being a great person to chat to in BSL3. Thank you to Heidi Runge and Stephie Zellner who have the incredibly difficult job of keeping all us stressed-out grad students on track.

Thank you to my dad, Joel McMinn, who has always encouraged learning, observing, and questioning in every part of life. To my annoyance, he still models this behavior constantly. And to my mom, Pat McMinn who knows how to inject a little humor into daily life and care less what people think. To my brother, Josh McMinn, who has been the most supportive big brother a girl could ask for. I'm not sure why he let his kid sister tag along for so long, but I'm so incredibly grateful for his generosity and

encouragement. To Elisti, Caleb, and Sierra McMinn, who let me invade their lives the last few months, I am so lucky to have gotten that time with them and grateful for their love and support.

I'm incredibly thankful for my friends outside of the lab. I credit Megan Miller for getting me here. Since I met her in Montana, she's the first person I go to for advice and has been a friend to me through very hard times. I must thank Melissa Vivian, Jonny Tran and Kirsten Hein for generating some very fun let-loose nights downtown and for just being great friends. Thanks to Reyes and Dee for their career guidance, game nights, and infectious adventurous spirit. To Vince Ngo who has always been a friend and hype-man since high school. In typical Colorado fashion, I rely on outdoor sports to keep me sane. Climbing has become incredibly important to me, especially as an outlet during grad school. To my friends and devoted climbing partners: Megan, Melissa, Dominique, Arielle, and Tom. Thanks for the campouts, the crag-hunting, and most importantly, the catches.

Finally, to my dog Domino, who's a pain in my ass and the best part of my day.

TABLE OF CONTENTS

LIST OF TABLES

LIST OF FIGURES

CHAPTER 1: LITERATURE REVIEW

1.1 History of Powassan virus

In 1958, a 5-year-old boy died of severe encephalitis in Powassan, Ontario, Canada with unknown cause. The cause was attributed to a group B arbovirus serologically related to Russian spring-summer virus, a subtype of tick-borne encephalitis virus (TBEV)[1]. The isolated virus was named 'Powassan virus' (POWV), and became the first and only North America member of the TBE antigenic complex: antigenically-related tick-borne viruses within the genus *Flavivirus*[2]. In the years following, extensive field and serological surveys were conducted in the area and uncovered neutralizing antibodies from humans and rodents[3,4]. POWV was also identified in *Dermecenter andersoni* ticks collected in 1952 in northern Colorado, providing evidence that this virus is indeed transmitted by ticks[5]. The complete viral genome was published in 1993, which confirmed the placement of POWV in the TBE complex, although it was identified as the most distantly related of the group[6]. To date, POWV is the only known tick-borne flavivirus in North America.

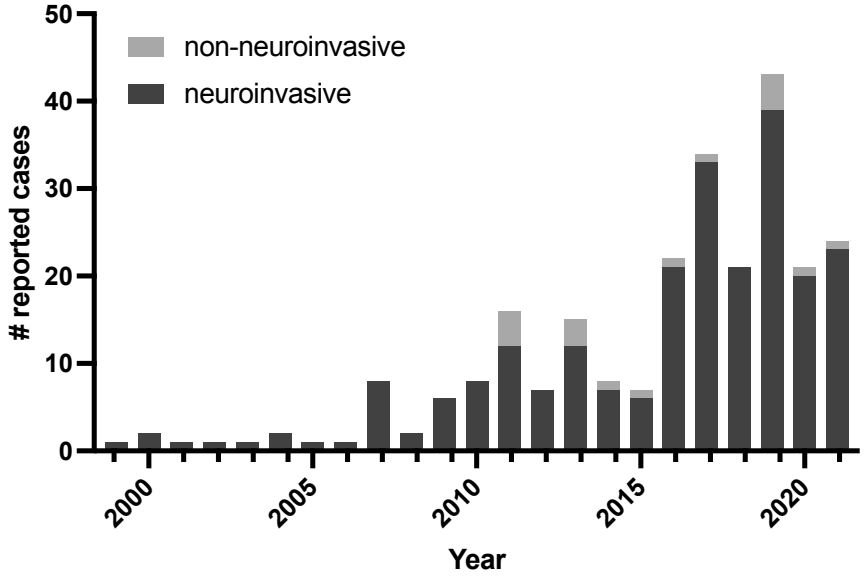

Figure 1.1. Reported cases on ArboNet in the United States 2009-2021. Human cases of POWV have been reported with increased frequency in the years since DTV was first reported in *I. scapularis*. Increased recognition, prevalence, and tick populations are all suspected to play a role.

In the 1970s, POWV was isolated from *Haemaphysalis* and *Dermacentor* ticks collected from the Primorsky Krai region in eastern Russia. Since then, positive serology and/or virus isolation from humans, voles, and ticks, as well as confirmed cases in humans are evidence of the endemicity of POWV in Russia[7]. However, the role of these tick and rodent vectors in maintaining virus transmission has not been described. Russian isolates have high sequence identity to each other and to Canadian strains of POWV (99.8%)[6,7], evidence for the introduction of POWV from Canada to Russia. Mandl et al. proposed POWV was likely introduced to Russia via mink exportation in the 20th century[6].

In 1997, Telford et al. identified a subtype of POWV in *Ixodes scapularis* ticks referred to as 'deer tick virus' (DTV)[8]. Prior to this, approximately 20 cases of POWV had been reported in North America. While DTV is serologically indistinguishable from POWV, nucleotide sequencing of the virus determined DTV to be a genetically distinct sublineage[8,9]. Thus, canonical POWV was designated as lineage I and DTV as lineage II. For the remainder of this dissertation, 'POWV' refers to both virus lineages unless specially indicated as 'lineage I', whereas 'DTV' refers solely to lineage II virus.

The identification of DTV in an aggressive human-biting vector that is increasing in range and density[10,11] has significant implications for disease in humans. Moreover, confirmed DTV infections in patients with severe neurological disease demonstrated the virus had similar pathogenicity to lineage I virus[12]. In the United States, cases have increased from 0.9 cases per year (1958-2007) to 16.7 cases per year (2008-2021)[13,14] (Figure 1.1). While this increase may be in part due to improved diagnostic ability, serological evidence in deer[15], reports of high infection rates in ticks[16–18], and human cases and DTV-infected ticks identified in states with no prior history[14,17,19,20] provide evidence of increasing POWV prevalence. Numerous studies have reported on the expanded range and density of ticks and the pathogens they carry in North America[10,11,21]. Therefore, DTV is an emerging virus of medical importance.

1.2 POWV through the TBEV lens

POWV is the only North American member of the tick-borne encephalitis (TBE) complex (Fig 1.2). The TBE complex is composed of viruses which are antigenically related (indicated by serological

cross-reactivity) and transmitted between tick and mammal hosts. Tick-borne encephalitis virus (TBEV) is the most widely studied of the TBE complex viruses, with over 10,000 clinical human cases reported annually[22]. Current observations of TBEV transmission and disease underscore the importance of studying the molecular and phenotypic epidemiology of POWV and provide context to the hypothesis presented in this dissertation.

TBEV is widely distributed across Europe and Asia (Fig 1.2). Several forms of TBEV disease have been characterized: febrile, meningeal, meningoencephalitic, poliomyelitic, polyradiculoneuritic, and chronic. The meningeal form of disease is most common, causing headaches, nausea, and photophobia in patients for one to two weeks. However, a large portion of TBEV infections are likely asymptomatic[22,23]. The three main subtypes of TBEV are associated with location and disease severity. The European subtype (TBEV-EU) is characterized by biphasic disease with fever in the first phase and generally mild neurological disorders in the second phase resulting in a case fatality rate (CFR) of 1-2%. The Siberian subtype (TBEV-SIB) can cause severe febrile disease with a CFR of 6-8%. Chronic infections have also been linked to this subtype. The far eastern subtype (TBEV-FE), also known as Russian spring-summer virus, is the most severe subtype of TBEV and is found in far-eastern Russia and Asia. Patients infected with this subtype often develop meningoencephalitis characterized by severe neurological disorders including epilepsy, cognitive disorders, paralysis, and coma. TBEV-FE disease can cause permanent damage to the brain and spinal cord, and result in death for 20-30% of patients[23–25].

TBEV has been isolated from over 15 different tick species including *Dermacentor*, *Ixodes*, and *Haemaphysalis* species and many small to medium sized rodents, particularly voles[23,26]. Potential associations have been identified between disease severity and tick vector and vertebrate host species in the Far-East. Mild disease was observed with human TBEV-FE infections when *Haemaphysalis concinna* was the predominant local species, as opposed to the more commonly associated *Ixodes persulcatus* tick. When *H. concinna* and *I. persulcatus* were co-prevalent, both mild and severe disease in humans was observed. In addition, low-virulence strains were shown to be associated with the common vole (*Microtus arvalis*)[23]. Associations between pathogenicity and vector species have similarly been demonstrated for

mosquito-borne viruses[27]. These observations highlight the role vertebrate and arthropod hosts may play in shaping disease potential in humans.

Figure 1.2. Known geographic distribution of TBE complex viruses pathogenic in humans. Tick-borne flaviviruses are widely distributed in Europe and Asia. POWV is the only known tick-borne flavivirus in North America. POWV = Powassan, DTV = deer tick, LIV = louping ill, TBEV-EU/SIB/FE = tick borne encephalitis European/Siberian/far eastern subtypes, OHFV = Omsk hemorrhagic fever, KSIV = Karshi, KFDV = Kyanasaur forest disease, LGTV = Langat (Figure created using Mapchart.net)

1.3 POWV disease in humans.

POWV is transmitted to humans through the bite of an infected *Ixodes* tick, with most cases occurring during peak tick season in the summer and fall[25]. Disease in humans is most frequently reported in Massachusetts, Minnesota, Wisconsin, and New York[14]. The number of reported cases has been increasing over the past decade with human infections detected in states with no prior history of disease[14,20] In the past few years, cases have been reported in Ohio, Virginia, North Dakota, and Quebec (Fig 1.1 and 1.3). While TBEV causes over 10,000 human cases every year[22], cases of POWV remain rare, with less than 40 reported annually. Despite their antigenic relationship, similar neurological pathogenicity in humans, and comparable prevalence in tick populations (0.1-5%)[28], the reason for the vast difference in disease burden is unknown and may be attributed to strain-dependent factors.

POWV infection can lead to severe disease, resulting in permanent neurological disorders in 50% and death in 11% of reported cases[13,29]. Symptoms arise one to five weeks after exposure and include

fever, sore throat, drowsiness, and disorientation[30]. In severe cases, infection can develop into neurological disease, such as encephalitis and meningitis. In these cases, symptoms include seizures, vomiting, and neurological deficits such as slow speech and paralysis[30,31] which can be prolonged or permanent. A review of 99 cases reported from 2006 to 2016 found 90% to be neuroinvasive: 72% presented with encephalitis, 16% with meningitis, and 2% with other neurological disorders. All non-neuroinvasive cases presented with febrile illness. 11% of patients succumbed to the disease, all of whom presented with neuroinvasive disease[29]. In some cases, patients of severe disease develop long-term sequelae such as partial paralysis[30,31] headaches, impaired motor function, incoordination, memory loss, and impaired cognitive abilities[31,32]. A follow up of fourteen cases in New York between 2002 and 2012 found five patients had died within a year of hospital discharge, all of whom were over 60[32].

Although both POWV and DTV can cause severe neurological disease in humans[12], they are serologically indistinguishable[9], making it difficult to identify the causative genotype for many human patients. DTV is suspected to be the major cause of human disease in the U.S. as *I. scapularis* are more likely to bite humans than the enzootic tick vectors associated with lineage I POWV. With increased sequencing of recent human samples, DTV is nearly always identified as the causative genotype; however, these descriptions have been mainly from cases in New York and Massachusetts, states with dense populations of DTV-associated deer ticks[12,32–36]. Thus, the major source of human disease in other parts of the U.S. has not been confirmed.

Serological studies suggest that there are likely many asymptomatic or undiagnosed infections. After discovering POWV in 1958, McLean et al. conducted serological surveys in humans and animals in the regions surrounding Powassan, Ontario. In surveying a total of 1008 healthy residents of Northern Ontario, 11 (1.1%) had POWV neutralizing antibodies; however, seropositivity was only identified near Powassan and Manitoulin Island and not broader Ontario. In regions where POWV antibodies were detected, seropositivity ranged from 0.5 to 4%[4,37]. In New York, Deibel et al. screened nearly 3000 serum samples from 1966 through 1977 for evidence of arboviral infection from patients with undiagnosed CNS infections. Eight of these samples were positive for Powassan virus, evidence that neuroinvasive cases

were going undiagnosed[38]. In 2015, Frost et al. screened 95 patient serum samples with suspected tick-borne disease infection and 50 patient serum samples from patients receiving routine chemical tests. From this cohort, eleven patients had POWV-reactive antibodies, two of which did not have suspected tick-borne infection. None of these patients had symptoms of neuroinvasive disease[39]. In 2019, after a cluster of human cases was reported in Sussex county, New Jersey, researchers estimated 0.31% seroprevalence rate equating to nine potentially undetected human infections in the area[40]. These findings suggest POWV infection is more widespread than observed from reported cases.

1.4 Animal models of disease

POWV disease has been assessed in many animals including hamsters, horses, rabbits, rhesus macaques, squirrels, groundhogs, and Peromyscus mice[41–45]. Inbred laboratory strains of mice, such as BALB/c and C57BL/6 mice, have been frequently used as a neuroinvasive disease model because they develop similar neurological signs as observed in humans. Such mice strains have used to assess POWV transmission and disease[9,46–54].

Both C57BL6 and BALB/c mice develop febrile illness and neurological disease similar to disease in humans. Weight loss is the first sign of disease, starting around day five post infection followed by generalized febrile illness observed by ruffled fur, hunched posture, and reduced activity. Signs of neurological disease including weakness, tremors, seizures, and paralysis, usually develop one to two days following onset of febrile illness. Disease in BALB/c mice is somewhat more severe with mortality rates range from 60-100%[55], while infection of C57BL/6 mice results in 0-40% mortality[54]. Following infection with 10^1-10^5 DTV, viral RNA is detected in the blood, brain, sciatic nerve, kidney, spleen, lymph node, and testis. The highest viral load is observed in the brain. Interestingly, dose-dependent differences in viral load were not observed in any of these tissues except blood. Viral RNA was detected in the blood one to six days post-infection, with the peak occurring at day one for high doses, day two for mid-range doses, and day three for low doses. Many mice develop meningoencephalitis which positively

correlates with mortality, but not viral load[46,55]. Male and female mice were similarly susceptible to neurological disease, though microscopic lesions were not found in the cerebral cortex of female mice. Additionally, female mice had slightly greater survival at higher doses compared to males[55]. Tick saliva has been shown to enhance POWV neuroinvasion at low viral doses[48,51]. Though both DTV and POWV cause neurological disease in humans and mice, few studies have directly compared POWV and DTV[9,53]. VanBlargan et al. demonstrated decreased mortality of DTV-infected mice compared to POWV; however, historical, highly passaged isolates were used for this study[53]. Contemporary, low-passage strains of POWV have not been evaluated for their pathogenic potential. Thus, the true scope of the pathogenic potential of POWV has not been well characterized.

1.5 Ecology and life cycle of *Ixodes* ticks

Ixodes is a genus of ticks within *Ixodidae*: 'hard ticks' recognized by their scutum and exposed mouthparts. The life cycle of *Ixodes* takes place over the course of many months or years, depending on species, feeding behavior, host availability, and climate. Tick life stages include the inactive egg and active immature stages (larvae, nymphs) and mature (adult male and female). At each active life stage, *Ixodes* ticks rely on a bloodmeal. For many *Ixodes sp.,* bloodmeals are taken from two to three hosts over the tick's life. To find suitable hosts, host-seeking ticks climb up grass or other structure and hold first pair of legs outstretched in a behavior called questing. Ticks feed for several days after which replete (fully fed) ticks fall off the host and begin the process of molting (for larvae, nymphs) or oviposition (adult females) in the humid layers of decaying vegetation[56,57]. The molting process takes several weeks in which histolytic enzymes break down and rebuild tissues[58,59]. Adult *Ixodes* mate on or off the host, after which the mated female produces 350-5000 eggs (depending on volume of blood ingested) which are oviposited two to three weeks after repletion, before the female dies[60].

Ixodes ticks remain attached to their host and blood-feed for three to ten days, depending on life stage and species. Within the first few hours of this process, physical and chemical reactions are used to

form a strong attachment and prevent host rejection. Toothed chelicerae are used to saw through the epidermis, while barbs on the hypostome (used for sucking and saliva secretion) help latch it in place[61]. A 'cement cone' is formed around the mouthparts, made of glycine-rich proteins produced in the salivary glands. The cement forms a solid attachment to the host and protects the mouthparts from the host's immune system[59]. During feeding, ticks intermittently ingest blood and secrete saliva during feeding. A period of 'fast-feeding' combined with increased salivation occurs in the last 12-24 hours of engorgement[62,63]. Active compounds including anticoagulants, vasodilators, anti-inflammatory and immune-modulators, antimicrobials, and digestive enzymes are produced and secreted through the saliva into the host[56,57]. Blood is ingested by sucking through the hypostome from the blood pool that forms from local tissue damage. Adult females ingest several milliliters of blood, and excess water is secreted to concentrate the bloodmeal. Digestion of the bloodmeal takes place intracellularly in the midgut, while the tick is attached to the host, and lasts several weeks to months after detaching[56,57]. The formation of a peritrophic matrix on the apical surface of midgut cells, akin to mosquitoes, has been identified in *Ixodes*

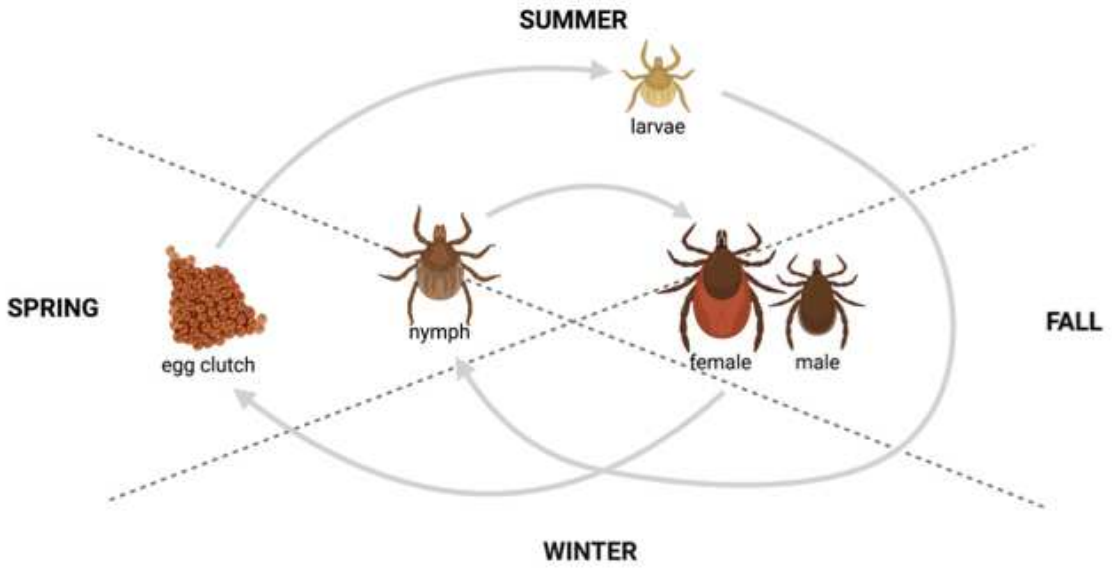

Figure 1.3. Life cycle of *I. scapularis*. Mated and replete adult females overwinter and oviposit large egg batches in the spring. Eggs hatch and larvae host seek in the summer, usually overwintering to host-seek as nymphs in the spring. Replete nymphs molt to adult male or female in the fall, which will mate on or off host. (Figure adapted from Nonaka et al. 2010 using Biorender.com)

ticks. The peritrophic matrix acts as a mechanical barrier to toxic substances in addition to providing structural support of the expanding midgut. Formation of the peritrophic matrix begins approximately 12 hours after attachment and is renovated as the midgut expands over the course of blood feeding[64,65].

The distribution and host preferences of the most relevant POWV-associated ticks in North America are described below:

I. scapularis (blacklegged or deer tick) are a widely distributed species present east of the Rocky Mountains in North America, and the vector of many medically important pathogens that infect humans and animals. Importantly, many studies have described the increasing range and density of this species[11]. *I. scapularis* often feed on small to medium size rodents as larvae and nymphs, and larger animals such as deer as adults. In the southern U.S., immature stages preferentially feed on lizards and other reptiles[66]. These ticks are exophilous and live independently of their hosts in between feeding periods.

I. cookei (woodchuck tick) are found east of the Rocky Mountains, particularly in northern U.S. and southern Canada. These ticks often feed on groundhogs, as their name suggests, though have also been associated with other small to medium size rodents. Though infrequently, they have also been known to bite humans and birds. These ticks are not often found by flagging due to their propensity to inhabit burrows. Collection of these ticks usually requires animal trapping[67,68].

I. marxi (squirrel tick) are found in the eastern U.S. and are particularly associated with squirrels but have also been identified on other small to medium size rodents. This species are nidicolous, often found in the nest of their host[68].

1.6 Virus transmission to, within, and between ticks

For viruses to be successfully transmitted by ticks, they must establish infection, disseminate to different tissues, survive the molting process, and be passed to other ticks and/or vertebrate hosts. For tick-borne viruses, barriers to infection and transmission, and mechanisms of overcoming those barriers have not been extensively studied. This is partly because ticks have much larger and more repetitive genomes[69], longer and more invasive blood feeds, and less recognition in human disease compared to mosquitoes. As a result, studying tick-borne viruses in the laboratory can be challenging. As follows, much of the information on infection, dissemination, and transmission of tick-borne flaviviruses has been gleaned from studies on mosquitoes, mosquito-borne viruses, and tick-borne bacteria.

Upon being ingested into the tick midgut, the virus may replicate in midgut epithelium cells before passing through the midgut wall into the hemocoel. Barriers to infection have been demonstrated in the midgut for Thogotoviruses (family: *Orthomyxoviridae*). Viruses unable to survive after ingestion in a bloodmeal were rescued and successfully tick-transmitted after inoculation into the hemocoel. In addition, viruses able to enter and replicate in the midgut epithelium could not disseminate into distal tissues. The molecular mechanisms of these barriers are not well studied, although several methods have been speculated: (1) surface receptors may be required for entry and replication in midgut epithelium cells, (2) intracellular digestion of the bloodmeal may limit access to essential enzymes and prevent viruses from initiating infection, and (3) the timing and concentration of virus uptake may be important to bypass peritrophic matrix produced on the surface of midgut epithelium hours after engorgement begins[70]. Notably, the peritrophic matrix is a well characterized barrier for many arthropod-borne viruses (arboviruses), including dengue, West Nile, Saint Louis encephalitis, and eastern equine encephalitis viruses, in mosquitoes[71].

After escaping the midgut and entering the hemocoel, viruses may enter and replicate in the salivary gland acinar cells to be released into the saliva (salivary gland escape)[72]. In mosquitoes, salivary gland entry and escape barriers are documented for flaviviruses and alphaviruses. The molecular

mechanisms of these barriers have not been described but may be receptor-dependent and involve inducing cellular apoptosis[71]. Very little is known about this process in ticks. Some viruses, as demonstrated for Thogoto virus, may bypass this barrier and be excreted into the saliva straight from the hemocoel[59]. *Borrelia burgdorferi*, the bacterial agent of Lyme disease, only disseminates into the salivary glands during blood-feeding, resulting in transmission to the vertebrate host ~48 hours after attachment[73]. In contrast, infection of tick salivary glands immediately after molting has been demonstrated for several tick-borne viruses, including POWV[59,74], thus activation of dissemination upon blood-feeding is not required. Moreover, POWV has been shown to be capable of transmission to a vertebrate host within 15 minutes of attachment[47]. Together, these results suggest POWV is likely prepared in the salivary glands and readily released into the saliva, though the mechanisms of entry and escape are unknown.

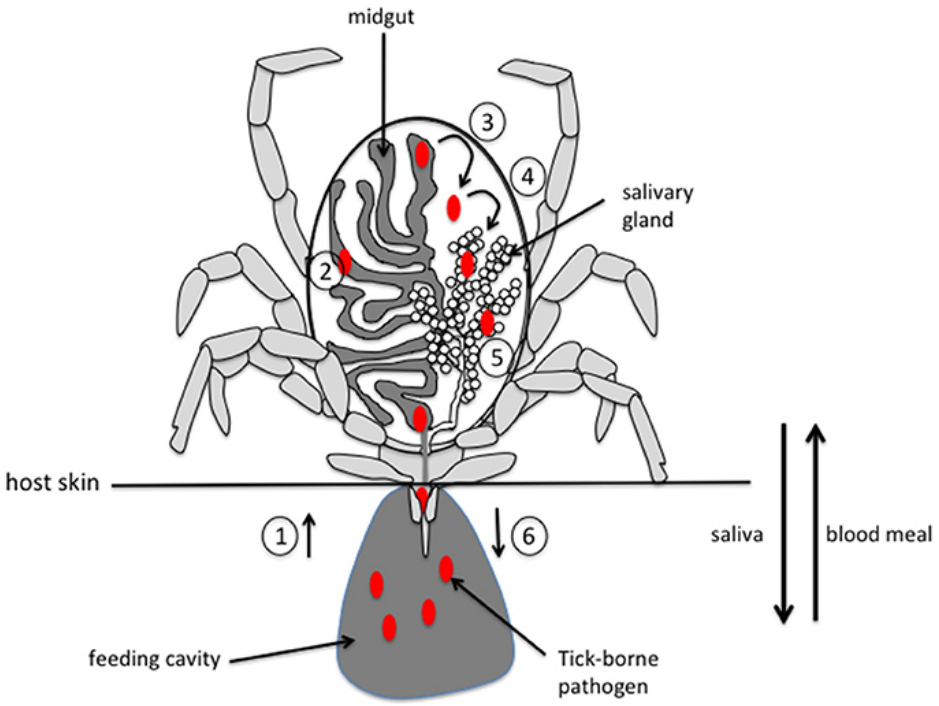

Figure 1.4. Virus infection and dissemination in an Ixodid tick. The ingested infectious bloodmeal is taken into the midgut (1)(2) and passes through the midgut lining into the hemocoel (3). From the hemocoel, virus can enter the salivary gland acini (4) and be secreted into the saliva for subsequent transmission (6). Figure: Simo et al. 2020

Over the course of the viral life cycle in arthropods, virus will encounter multiple antiviral responses, which it must evade or counteract to survive. Such antiviral responses likely include

autophagy, Toll, immune deficiency, and RNA interference (RNAi) pathways; although our knowledge of arthropod immunity centers around fruit flies and mosquitoes[69,75]. Recent studies have described significant differences in immune genes predicted in ticks[75], thus tick antiviral responses are not well described. In mosquitoes, RNAi, specifically the small interfering RNA (siRNA) pathway, is thought to be the major line of defense against viruses. Ticks have been shown to have an altered set of RNAi-associated proteins, yet the siRNA pathway appears to be active against tick-borne Langat virus (LGTV; *Flavivirus*). Proteins of the tick siRNA pathway recognize and cleave viral RNA into small 22-nucleotide fragments (viRNAs) which are used as guide strands for continued degradation of viral genomes. LGTV and POWV-derived viRNAs were found to largely map to the 5' and 3' ends of the viral genome (untranslated regions; UTRs)[76,77], suggesting the UTRs may play a role in counter-defense of tick RNAi. The 3' UTR of most flaviviruses expresses a stable structural RNA known as subgenomic flavivirus RNA (sfRNA) which have been shown to interfere with RNAi pathways through an unknown mechanism. This effect has been demonstrated for mosquito-borne (dengue and West Nile) and tick-borne (LGTV, TBEV) flaviviruses[76]. Though the mechanisms of virus infection and dissemination are vastly unknown in ticks, clearly, tick-borne viruses encounter multiple interhost barriers to survival.

For a virus to perpetuate in a population, it must survive to the next life stage, and be successfully transmitted to other vertebrate or tick hosts. Four methods of virus transmission in ticks have been observed: horizontal (viremic and co-feeding) and vertical (transstadial and transovarial), though many gaps remain in our knowledge of their cellular and molecular mechanisms.

Viremic transmission is the infection of a naïve tick from a viremic animal. Transmission of POWV from infected animals to naïve ticks has been observed in *D. andersoni*[74], and *I. scapularis*[47,77,78]. Costero et al. found 10% of *I. scapularis* larvae, 40% of nymphs, and 57% of adults to be infected two to three weeks post-feeding on a viremic animal[78]. In contrast, Ebel et al. found 90% of larvae were infected with POWV immediately post-detachment[47]. Taken together, these results suggest ingestion of virus does

not always result in established infection. In addition, infection success may increase with life stage, possibly due to longer feeding times and volume of ingested blood/virus.

Co-feeding (non-viremic) transmission is the transfer of viruses between ticks feeding in proximity on a host. Viruses are secreted into the host, enter the bloodstream, and re-enter a co-feeding tick as blood is ingested; thus, viremia is not required. Though co-feeding transmission has not been shown for POWV, it has been demonstrated for other TBE complex viruses such as TBEV and LIV[79]. In mice, 50 to 80% of naïve ticks were infected with TBEV after co-feeding with infected ticks. Notably, the rate of infection via co-feeding varied significantly by host species. Hedgehogs and pheasants, in the case of TBEV, did not support co-feeding transmission[79], suggesting other factors at the tick-host interface play a role in the local migration of virus in the host. Salivary gland extract has been shown to enhance co-feeding transmission[80,81], likely due to the pharmacologically active compounds in saliva which augment blood flow. Labuda et al. demonstrated that local infection and migration of immune cells at the skin site may also facilitate the transfer of virus between co-feeding ticks[82]. It is likely that POWV can be transmitted horizontally between ticks through co-feeding, though the efficiency of transmission in small-medium size rodents is yet to be determined.

Transstadial transmission (TST) is the process of surviving and maintaining infection through the degradation, rearrangement, and rebuilding of tissues that occurs during molting[58,83]. Some have speculated that viruses disseminate into hemocytes before molting, which protects them from tissue degradation (histolysis)[70,84]. TST from larvae to nymphs[47], nymphs to adults, and larvae to adults has been observed for POWV[77,78,85]. Infection rates observed in nymph or adult ticks after one molt are similar to those observed prior to molting[47,78], however the infection rate of adults after two molts was much lower[78]. This latter result could be a factor of time or decreased viral titer, as virus had to maintain infection an additional 9 weeks in these ticks. The extrinsic incubation period (the time needed for a virus to be capable of transmission to a new host) is thought to occur during the molt. Drops in viral titer have been observed mid-molt, but recover before molt completion, and ticks are able to transmit virus

immediately post-molting[47,74,77,78]. Even such, Grubaugh et al. observed evidence of wide genetic bottlenecks in TST events as seen by the preservation of observed variants post-molt[77]. Persistent infection through tick life stages seems to be a key feature for successful transmission in ticks, as many studies have described TST capability for other tick-borne pathogens[70]. In conclusion, the barriers for TST may be low for POWV and other tick-borne pathogens, though additional research is needed to understand cellular mechanisms of TST.

Vertical transmission from mother to progeny is often referred to as transovarial transmission (TOT) in ticks, however the true mechanism of virus transmission in ticks is not clear. TOT refers specifically to infection inside the developing ovum. Eggs can also be contaminated with virus during oviposition or when the egg's waxy coat is deposited via Gene's organ, referred to as transovum transmission (TVT). Infection of Gene's organ was demonstrated in *Dermacentor* ticks experimentally infected with POWV. Furthermore, the restriction of Gene's organ resulted in decreased infectivity of egg masses. When egg masses were washed, infectivity also decreased. Taken together, these results suggest virus is present on the outside of the egg. However, in either case, there was not a complete loss of virus in eggs masses, suggesting other vertical transmission mechanisms may be at work[74]. For many tick-borne viruses, including TBEV, KFDV, LIV, and OHFV, low levels of vertical transmission have been observed[70]. For TBEV, 20% of egg batches were shown to contain virus, though less than 1% filial (hatched larvae) infection was observed[86]. Similar infection rates were observed for POWV in *D. variabilis*[74], *H. longiconis*[85], and *I. scapularis*[78]. Some have suggested efficient vertical transmission may come at a cost to vector fitness[79,87], and infection of larvae may be enhanced by co-feeding transmission[79]. Though only one study has assessed vertical transmission of POWV in a known natural tick vector (*I. scapularis*[78]), transmission rates remain consistent between different flaviviruses and vector species. Therefore, it's likely that POWV is vertically transmitted in a similar fashion to other flaviviruses, though the resulting low filial infection rates suggest this route alone may not sustain viral transmission as modeled previously[88].

POWV is capable of horizontal oral, transstadial, and vertical transmission, and though co-feeding transmission is yet to be determined, it is likely. These mechanisms likely work in conjunction to facilitate natural transmission cycles. Given the time tick-borne viruses must survive in the vector host, it's not surprising that POWV may be very well adapted to ticks. The described POWV transmission studies have used either lineage I (LB strain) or DTV (SPO strain), both of which are highly passaged historical strains. While both lineages can undergo multiple tick transmission mechanisms, strain-dependent differences in the ability of virus to be transmitted by these routes have not yet been described. With the emergence of POWV in North America, the use of low-passage, contemporary, genetically and geographically diverse isolates is essential for an accurate representation of tick transmission.

1.7 Ecology of POWV in North America

Prior to the discovery of DTV in 1997, POWV was identified in *I. marxi*[89], *I. cookei*[90–92], and *I. spinipalpus*[92] in Northeastern U.S. and Canada. Virus isolation from *I. cookei* and *I. marxi* ticks and their natural hosts (woodchucks and squirrels respectively) provided strong evidence for the sylvatic transmission cycle of lineage I virus[30,89,91–95]. Although there has been fewer reported tick surveys in Ontario since the 1960s, serological surveys demonstrate exposure of POWV in Ontario woodchucks as late as 2016[93]. In New York, lineage I virus has been isolated from *I. cookei* as recent as 2019. Virus and POWV neutralizing antibodies have also been detected in skunks collected in the northeastern U.S.[91] and California[96]. The importance of these hosts to POWV transmission cycle is unclear, as experimental infections of woodchucks, squirrels and skunks demonstrated only low levels of viremia in a few woodchucks and skunks[41]. Interestingly, POWV or POWV-reactive sera has been detected in New Mexico, Alaska[97], British Columbia, and Alberta[74,98]. POWV was also isolated from *Dermecentor andersoni* in Colorado in 1952[5], although subsequent attempts to detect POWV in field-collected *Dermacentor* have not been successful[95,99,100]. Experimental infections have also demonstrated

Dermacentor variabilis to be a competent vector of POWV. Given this data, POWV seems to be more broadly distributed in North America than appreciated by human caseloads (Fig 1.5).

In 1997, DTV was identified in *I. scapularis* from Massachusetts and Connecticut. Since then, infected *I. scapularis* ticks have been detected in Minnesota, Wisconsin and nearly every state in New England[101]. Recently, virus has been detected in ticks collected from Virginia[20] and Oklahoma[17], states with little or no prior history of human cases. In 1997, 0.5-1% of *I. scapularis* were determined to be DTV positive in the Northeast[8,102]. Since 2008, 0.2-5% DTV-infected *I. scapularis* have been reported in Connecticut[103,104], New York[16,104–107], Pennsylvania[18,108,109], Maine[110], Wisconsin[99,100,102], Minnesota[111], Vermont[112] and recently, Virginia[20,113] and Oklahoma[17]. The Pennsylvania Department of Health reported some counties with infection rates as high as 11-67%, though sample size and collection methods were not reported[18].

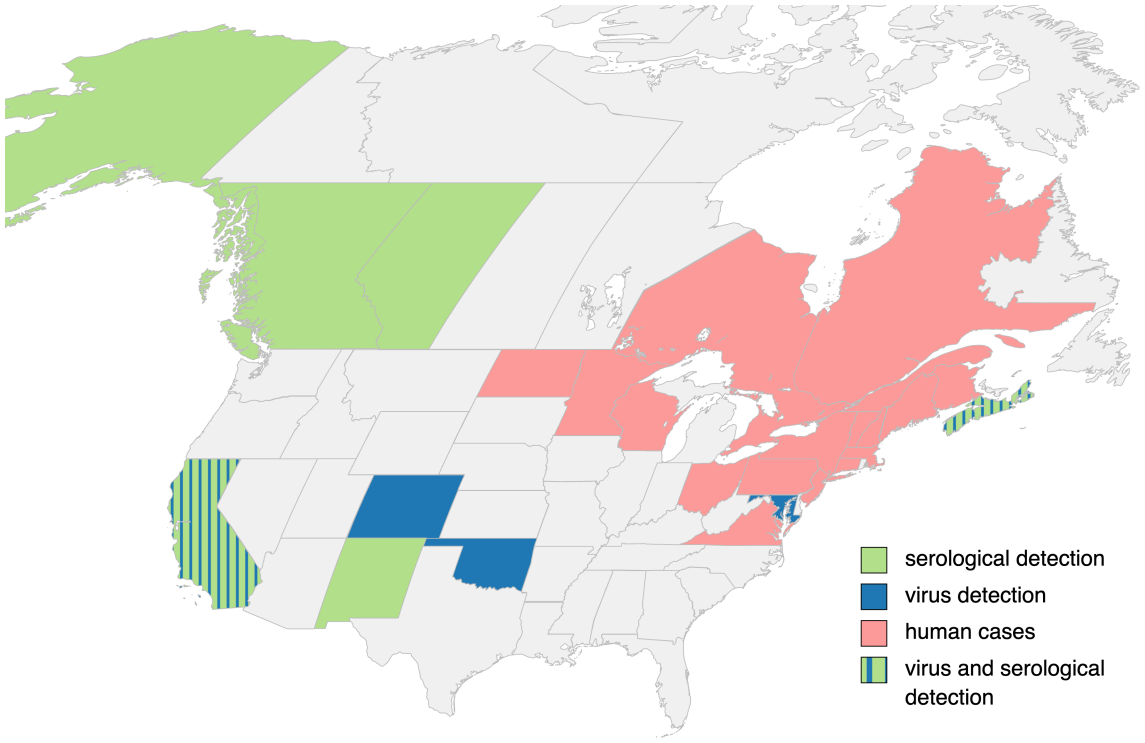

Figure 1.5. Detection of POWV in North America. Human cases have so far been detected in the Northeastern and Midwest U.S. and Southeast Canada. Serological surveys and virus isolation are evidence of a much broader distribution than appreciated by human caseloads. (Figure created using Mapchart.net)

The landscape of POWV is complicated by sympatric distribution of tick vector species and virus. Two instances of crossover between viral lineages have been observed. In Ontario, a single DTV-infected *I. cookei* tick collected off a Canada goose was found in 2012[93]. DTV has not been reported in *I. scapularis* collected in Ontario[93,114], though this could be due to infrequent tick surveys or underreporting. In New York, lineage I virus was isolated from two *I. scapularis* ticks collected in 2019, in addition to two *I. cookei* ticks collected from woodchucks[107]. Due to the overlapping range of vector species and broad host range of *I. scapularis*, crossover between genetic lineages seems likely; although, the extent and consequence of crossover is unknown.

The associated mammal hosts for lineage II virus have not yet been elucidated. This is in part due to the opportunistic feeding behavior of *I. scapularis*. *P. leucopus* (white-footed mice) are abundant hosts for *I. scapularis* and are known to play an important role as a reservoir for *Borrellia burgdorferi*[115]. Thus, this rodent species has been implicated as a relevant host for DTV[8]. Antibodies reactive against DTV antigen were detected in *P. leuocopus*, but not *M. pennsylvanicus* (Meadow vole), trapped in Wisconsin, Rhode Island, and Massachusetts[116]. Additionally, DTV-infected ticks were found infested on these mice, though virus has never been directly isolated. Experimental infections of *P. leucopus* found low levels of viremia early in infection, suggesting white-footed mice may not be a good reservoir for POWV[50]. Similar findings were observed for DTV infection in woodchucks, squirrels, and skunks: virus was detected in a few animals of each species, but viremia was low and not prolonged[41]. Most recently, shrews have been implicated as a potentially important host for DTV[117]. Goethert et al. used bloodmeal analysis on nymphal *I. scapularis* and found a statistically significant association of DTV infection with having taken a shrew bloodmeal, but no such correlation was found with mice[117].

Many questions remain about the ecology of POWV, especially DTV. The detection of lineage I virus in Colorado and California, and POWV-reactive antibodies in humans and animals in many parts of the U.S. and Canada highlights a much broader geographic range than previously appreciated (Fig 1.3). The lack of human cases in these parts may be due to tick density, alternative vector species, or host

preferences. For instance, in the southeastern U.S., immature stages of *I. scapularis* primarily feed on lizards as opposed to small rodents[118,119] which may not support POWV transmission to or between ticks[66]. Furthermore, *I. scapularis* in the Southeast have a shorter life cycle and tick population densities are also lower[120,121]. The absence of a smoking gun implicating a clear reservoir suggests non-viremic transmission may be an important route of POWV transmission. In this hypothesis, hosts act as tick aggregators, rather than reservoirs for virus to be transmitted horizontally between co-feeding ticks. Regardless, viremic transmission of POWV could be a significant component of the viral life cycle and has the potential to influence the circulation and pathogenicity of virus strains. Thus, viremic transmission is an important mechanism requiring further investigation.

1.8 The use of arthropods in vertebrate sampling and surveillance.

Hematophagous arthropods take small and frequent blood samples from a variety of human and animal hosts, resulting in a massive and untapped source of information without even touching a needle. The utility of using arthropods as a sample source is appreciated in three ways: (1) easy collection due to their host-seeking behavior and abundant populations, (2) feed frequently on a variety of vertebrate hosts, and (3) different vector species can be used to target various hosts based on known feeding preferences. Such a sample source could be utilized in several ways including virus surveillance, pathogen exposure, and biodiversity estimation[122]. Here, vector-enabled metagenomics (VEM) is used to describe the exploitation of arthropods to capture viral genetic diversity in animals, humans, or plants.

The ability to detect non-mosquito-borne viruses from mosquito bloodmeals has been demonstrated in both the lab[123–127] and the field[128–131]. A few of these studies have also utilized mosquito feeding behavior to facilitate blood collection from small or sensitive laboratory animals[123,127]. In the field, H5N1 avian influenza virus was detected from *Culex* bloodmeals collected from a poultry farm in Thailand[128]. Metagenomic sequencing on *Culex*, *Anopheles*, and *Armigeres* spp. mosquitoes in China revealed 3.6% of viral sequences were known vertebrate viruses, none of which are reported to be

transmitted by mosquitoes[129]. Similarly, non-vectored viruses that infect humans and animals were identified in mosquitoes from California[130]. Our group has also demonstrated the detection of vertebrate viral pathogens such as canine distemper and Epstein Barr viruses from the bloodmeals of mosquitoes collected in Liberia[125]. The validation of vertebrate virus detection from mosquito bloodmeals demonstrates potential application in disease surveillance.

Our group has tested the success of VEM for viral pathogen surveillance in the field, a technique Grubaugh et al. coined 'xenosurveillance'. In 2018, indoor resting blood-fed mosquitoes and blood samples from human participants were collected from 43 households in Liberia. Two human viruses were identified in both human blood and mosquito bloodmeals: GB virus C (non-pathogenic) and Hepatitis B virus[132]. These results demonstrate the ability for xenosurveillance to detect presently circulating viruses in humans and highlight potential to complement current surveillance strategies. Notably, *Anopheles* mosquitoes, which are highly anthropophilic, made up 80% of mosquitoes collected in West Africa[132] and likely contributed to the success of xenosurveillance in the detection of human viruses. Thus, the applicability of this technique in areas with less anthropophilic species (i.e. *Culex* and *Aedes* mosquitoes) should be addressed.

The ability to detect vertebrate antibodies from mosquito bloodmeals is also being evaluated as a surveillance tool to estimate pathogen exposure in humans, livestock, and wildlife. This technique has been successfully demonstrated in the laboratory by several groups[128,133–136], though only two studies have assessed antibody responses from wild-caught mosquitoes[128,136]. Both studies were successful is detecting virus-specific antibodies in mosquito blood-meals. Furthermore, Komar et al. used this technique in parallel with direct sampling of birds during a West Nile virus outbreak and found similar antibody prevalence between methods[136]. These studies highlight antibody detection from mosquito bloodmeals as a promising proxy method for virus exposure in humans and animals

Though mosquitoes have been most widely used for VEM to date, there have been a few studies which document vertebrate virus detection from other arthropods. Bitome-Esono et al. utilized the

generalized host-feeding approach of hematophagous flies, including tsetse, stomoxid, and tabanid species, to gather blood samples from wild vertebrates in the forests of Gabon. This method resulted in diverse haemosporidian parasites (i.e. malaria) identified in bloodmeals derived from 20 mammal, bird, and reptile hosts[137]. Non-hematophagous flies that feed on decomposing flesh or feces (known as carrion or blow flies) have also been used to assess mammal biodiversity in remote locations[138–142]. Similarly, blood-sucking leeches have also been used to assess mammal biodiversity in Vietnam[140]. H5N1 avian influenza[143] and New Castle disease viruses[144] have been detected in carrion flies, highlighting their potential to also be used for virus surveillance.

Vectored-enabled sampling has been demonstrated as a useful strategy for an array of applications and has potential to be applied to other arthropods including ticks, fleas, lice, batflies, midges, and bed bugs[122].

Goals of this dissertation

The overarching research goals of this dissertation were to (1) determine the scope of disease and tick transmission phenotypes for contemporary low-passage genetically and geographically diverse POWV isolates and (2) determine the feasibility and applicability xenosurveillance as a proxy for traditional surveillance in Guatemala. Other goals of this work included obtaining additional low-passage POWV isolates to use in experimental studies and establishing experimental tick methods in a biosafety level 3 laboratory at Colorado State University.

We approached the first goal from a culmination of field, *in vitro*, and *in vivo* studies. In chapter two, we reported DTV infection rates in ticks collected from 20 locations in the northeastern United States. From this effort, we obtained 14 low passage isolates for use in experimental studies. Ecological and evolutionary patterns of viral genetic diversity were described from genomic data generated from 84 field-collected DTV-positive ticks. In chapter three, we hypothesized that *in vivo* POWV phenotypes

would reflect the genetically diverse clades described in chapter one. We used 16 historical and contemporary POWV isolates from a broad geographic range to characterize replication and cytopathic phenotypes in cell culture. In chapter four, we hypothesized disease and tick transmission phenotypes would be similarly diverse *in vivo*. Five POWV isolates were used to describe pathogenesis in mice and viremic transmission to *I. scapularis* ticks.

Our second goal was building off previous studies which assessed the use of xenosurveillance in Liberia, where human-biting *Anopheles* mosquitoes are predominant. We hypothesized that xenosurveillance in Central America might be more complex due to the highly abundant and less anthropophilic *Culex* and *Aedes* mosquitoes. In chapter five, we conducted xenosurveillance in parallel with traditional surveillance techniques for 16 weeks in rural Guatemala. We then identified viruses present in mosquito bloodmeals and human blood samples. The host-feeding behavior was also determined for collected mosquitoes.

CHAPTER 2: PHYLODYNAMICS OF DEER TICK VIRUS IN NORTH AMERICA.

2.1 Introduction

Powassan virus (POWV) is an emerging tick-borne flavivirus endemic to North America and far eastern Russia. POWV can cause severe encephalitis leading to permanent neurological sequelae in 50% of patients and death in 10%[13,29]. Reported human cases in the United States (U.S.) have increased from twenty-six (1999 through 2009) to 186 (2010 through 2020)[14]. Furthermore, detection of POWV-neutralizing antibodies in Northeastern hunter-killed deer increased from 4% in 1979 to 91% in 2010[15].

POWV is the only North American member of the Flavivirus tick-borne encephalitis serogroup, first identified in 1958 in a patient with encephalitis in Powassan, Ontario, Canada[1]. Canonical lineage I POWV has been estimated to diverge from the European tick-borne encephalitis complex between 2000-6000 years ago, around the time the Bering Land Bridge between Alaska and Far Eastern Russia disappeared, effectively limiting migration between Russia and North America[145]. In 1995, a second lineage of the virus, deer tick virus (DTV), was identified in ticks in the northeast U.S.[8], and subsequently detected in Wisconsin two years later [102]. While lineage I POWV is typically found in nidicolous, host species-specific ticks such as *Ixodes cookei* and *I. marxi*, lineage II DTV is mainly found in human-biting *I. scapularis* ticks, thus posing a significant risk to humans[13]. However, *I. cookei* and *I. marxi* have been documented to feed on humans, albeit infrequently[146].

Given the rise of human cases and expansion of *I. scapularis* ticks and their associated pathogens, we sought to gain a better understanding of DTV emergence in North America. Here, we report DTV prevalence in ticks from a multi-state collection study in 2019 and isolation of diverse viruses in cell culture for in-depth studies. We present whole-genome, time-scaled phylogenic analyses of DTV in North America using 108 published and newly sequenced isolates that represent a broad geographic and temporal range.

2.2 Results

DTV detected in I. scapularis ticks collected in 2019. A total of 2,520 *I. scapularis* ticks were collected from twenty locations in the northeastern U.S. and Ontario, Canada (Fig. 2.1) in the spring and fall of 2019, the seasonal activity peaks of adult-stage *I. scapularis*. Though *Amblyomma americanum* and *Dermacentor variabilis* ticks were found, no other *Ixodes* species was observed. Because of the seasonal timing of surveys, only 11 *I. scapularis* nymphs were collected, all of which were negative for DTV. Eighteen DTV-positive ticks were detected in eight locations in New York, New Jersey, and Maine. Positive ticks ranged from 1.0 - 5.5% at sites where DTV was detected and significantly more female mice were DTV-positive (Fisher's exact test p=0.018; Table 2.1).

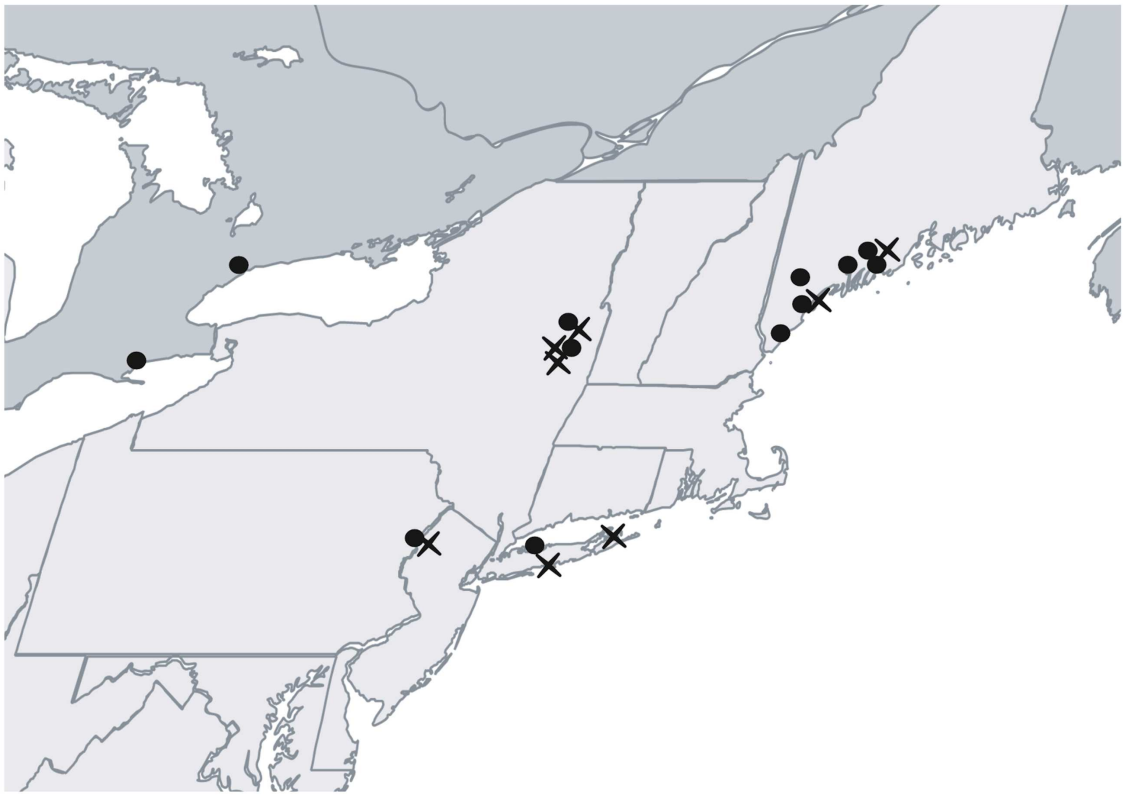

Figure 2.1. 2019 Spring tick collection sites. *I. scapularis* ticks were collected from twenty locations in Northeastern U.S (light gray) and Ontario, Canada (dark gray). Powassan positive locations are indicated by an X. Figure created with Biorender.com

Table 2.1. DTV prevalence in I. scapularis by collection location in 2019. For each location, the table lists the number of ticks collected, the number of DTV positive ticks by qRT-PCR, and, for sites with DTV positive ticks, the percent of DTV-positive ticks and 95% binomial confidence interval.

Location	# *I. scapularis* collected Total (ratio F/M)	# DTV positive: Total (F:M)	% DTV positive (95% CI)
East Stroudsburg, PA	19 (0.7)	0	
Hardwick, NJ	73 (0.9)	4 (3:1)	5.5 (1.5, 13.4)
Lloyd Harbor, NY	22 (1.4)	0	
Cedar Point, NY	71 (0.6)	1 (1:0)	1.4 (0.0, 7.6)
Connetquot, NY	372 (1.5)	4 (3:1)	1.1 (0.3, 2.7)
Saratoga Springs A, NY	101 (1.0)	2 (2:0)	2.0 (0.2, 7.0)
Stillwater, NY	100 (1.5)	0	
Saratoga Springs B, NY	99 (1.2)	2 (2:0)	2.0 (0.3, 7.1)
Saratoga Springs C, NY	124 (1.1)	0	
Saratoga Springs D, NY	60 (2.0)	1 (1:0)	1.7 (0.0, 8.9)
Wells, ME	148 (0.9)	0	
Cape Elizabeth A, ME	84 (2.5)	0	
Cape Elizabeth B, ME	304 (0.7)	3 (1:2)	1.0 (0.2, 2.9)
Standish, ME	113 (0.9)	0	
Newcastle, ME	141 (0.8)	0	
Thomaston, ME	98 (1.7)	0	
Thorndike, ME	12 (1.8)	0	
Rockland, ME	202 (1.2)	1 (1:0)	1.0 (0.0, 2.7)
Rouge Valley, ONTARIO	280 (1.1)	0	
Turkey Point, ONTARIO	96 (1.5)	0	
TOTAL	**2520 (1.1)**	**18 (14:4)**	**0.7 (0.4, 1.1)**
POSITIVE SITES	**1282 (1.1)**	**18 (14:4)**	**1.4 (0.8, 2.2)**

Virus population changes after isolation in BHK cells. Virus from sixteen of eighteen (88.9%) DTV-positive ticks were isolated in cell culture. Consensus full-length viral genomes were sequenced from fourteen tick homogenates and corresponding BHK-isolated virus. For twelve of the homogenate-isolate pairs, the consensus virus sequences were identical. Among the other two, isolate NJ19-48 differed by one single nucleotide polymorphism (SNP) in the 5' UTR, and isolate NY19-250 differed by one synonymous SNP in NS2A (Fig. 2.2).

A.

Isolate	Region	ΔNT	ΔAA	Frequency
NJ19-48	5'UTR	C22T	NCR	0.66
NJ19-250	ns2A	A3985C	R164R	0.71

AA, amino acid change; Frequency, frequency of allele in [tick]/[BHK] samples; NCR, non-coding region

B.

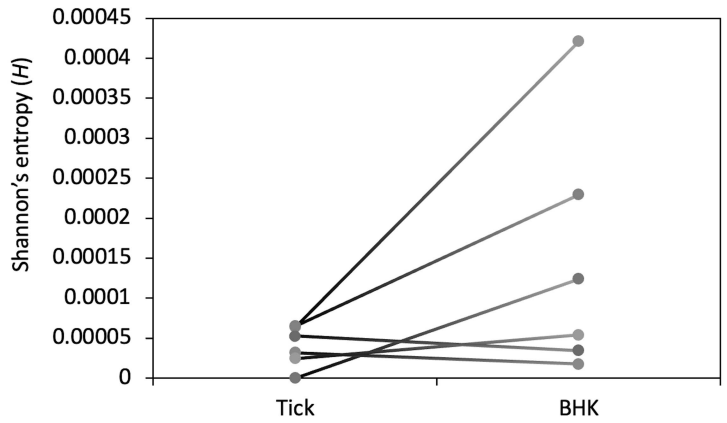

Figure 2.2. Comparison of DTV population from tick homogenate and virus isolated in cell culture. (A) Consensus level single nucleotide polymorphisms in DTV sequences after one passage in baby hamster kidney cells. (B) Average Shannon entropy for six paired samples, calculated based on iSNVs from two independent libraries.

High-depth sequencing was performed for six tick homogenates and corresponding BHK isolated virus to assess changes in intrahost single nucleotide variants (iSNVs) and population diversity (Table S3). We observed between two to four iSNVs per sample in tick homogenates and between five to forty-two iSNVs per sample in BHK-isolated virus. While the raw number of iSNVs (not accounting for sequencing depth) increased over one passage for each isolate, the allele frequencies remained mostly under 5% (Table S2.4 and Fig. S2.2). The average Shannon entropy increased after isolation in cell culture for three of the six isolates (Fig. 2.2), but not the others (two-tailed Wilcoxon signed-rank test, p=0.156).

Phylogenetic analysis. Our phylogenetic analysis of 108 POWV genome sequences recapitulated the known lineages I and II (DTV); all sixty-three sequences newly generated from ticks in this study belonged to DTV (Fig. 2.3). Our analysis also demonstrated the previously described DTV sublineages, one of which contains sequences from the northeast U.S. and the other of which contains sequences from the Midwest U.S. The average pairwise nucleotide difference was 99.4% between sequences in the northeast sublineage, 99.7% between sequences in the Midwest sub-lineage, and 93.6% between sequences from different sublineages. Most of the sequences newly generated in this study clustered with the expected sublineage based on their location of collection. Interestingly, however, a single isolate from New Jersey (NJ-H-56-2019) clustered within the Midwest sub-lineage and was 99.5% identical to the closest related sequence, WI_FA51240_2008. Sequences from three other samples collected at the same time in the same location (NJ-H-10-2019, NJ-H-39-2019, and NJ-H-48-2019) clustered with the northeast sublineage and had only 93.5% identity to NJ-H-56-2019.

The northeast sublineage included samples from multiple locations and years, allowing investigation of population dynamics at a finer scale. We observed clusters of sequences that were geographically restricted but reflected multiple sampling years (e.g. Maine 2018-2021; average pairwise nucleotide difference 99.9%). Other clusters contained closely-related sequences collected across multiple locations even within the same year (e.g. Maine – New York 2019; average pairwise nucleotide difference 99.8%). In Connetquot, New York, where *I. scapularis* ticks were abundant, three of four sequences clustered together with 99.9% similarity, while the remaining sequence clustered with Maine sequences (99.8% identity to Maine and 98.8% identity to sequences from the same site in New York) (Fig. 2.3).

Population dynamics. Time-scaled phylogenetic analysis of all ninety-one DTV samples using our best-fitting model, which included a strict molecular clock with exponential coalescent tree prior, indicated that sequences within the northeast sublineage shared a common ancestor approximately 138 years ago (95% HPD 88-192) (Fig. S2.3). The most ancestral of the northeast sublineage sequences were collected in Massachusetts in 2018. Our analysis indicated that the northeast lineage diverged from the Midwest

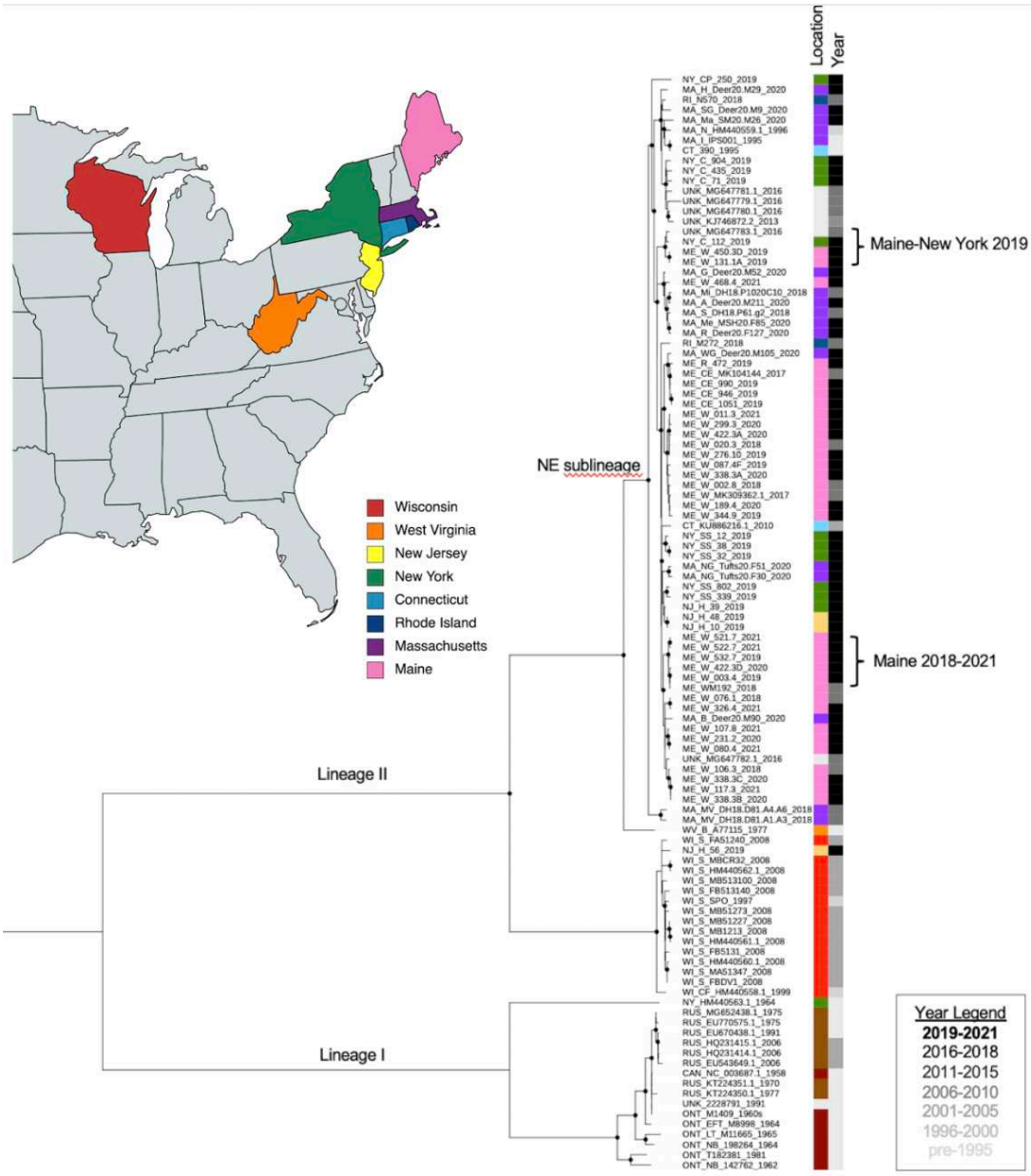

Figure 2.3: Maximum-likelihood phylogenetic tree of 108 Powassan virus genome sequences. Sequence names indicate location, unique identifier, and year. GenBank accession numbers are included for previously reported sequences. Circles indicated nodes with ultrafast bootstrap support of 99% or greater. The location strip plot indicates U.S. state (with colors matching the map and map legend) or Canada (maroon), Russia (brown), or unknown location (grey). The year strip plot is in greyscale as indicated by the year legend. Labeled branches indicate the two major lineages (I and II) and the northeast sublineage of lineage II. Specific

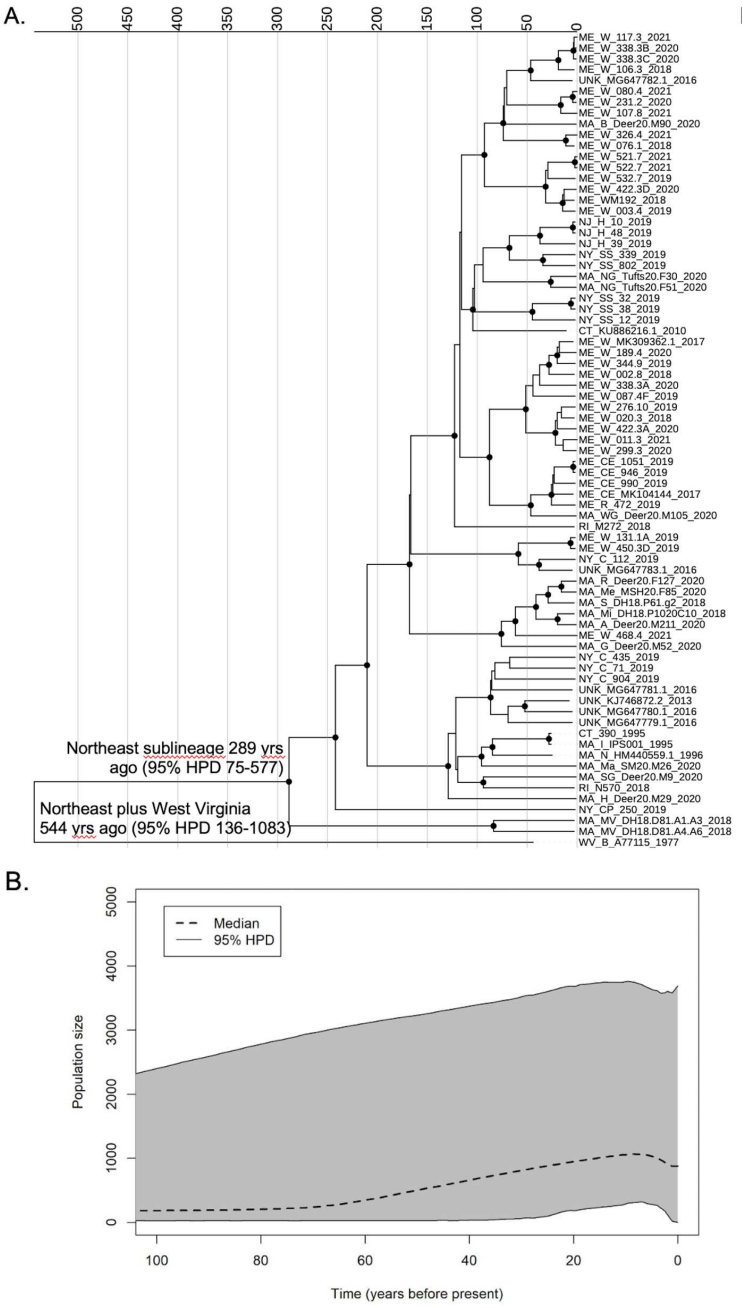

Figure 2.4: Time-scaled analysis of seventy-five Deer Tick Virus genome sequences from the northeast U.S. using a relaxed lognormal clock model and CEBS tree prior. (A) Maximum-clade credibility tree. Sequence names indicate location, unique identifier, and year. GenBank accession numbers are included for previously-reported sequences. Nodes with a posterior probability of 0.95 or higher are marked with circles. Nodes of interest are labeled with their tMRCA [95% HPD]. (B) Extended Bayesian skyline plot shows estimated population size over time since present.

sublineage approximately 1,184 years ago (95% HPD 770-1,658), and sequences within the Midwest sublineage shared a common ancestor approximately 87 years ago (95% HPD 59-119). The observed clock rate, 6.0 e-5, is somewhat higher than reported previously for NS5 alone, 3.9 e-5[147]. Clock rates and marginal likelihoods for models that include a coalescent or CEBS tree prior, as well as lognormal relaxed clock, are shown in Table S2.2.

Time-scaled phylogenetic analysis of the seventy-five DTV samples from the northeast U.S. was performed using two models with equal fit: a strict clock with exponential coalescent tree prior, and a lognormal relaxed clock with Coalescent Extended Bayesian Skyline (CEBS) tree prior. Both yielded similar clock rates (3.2 e-5 and 3.4 e-5, respectively, Table S2). CEBS analysis dated the MRCA of the northeast lineage to 289 years ago (95% HPD 75-577) (Fig. 2.4A) and inferred that there has been at least one change in the DTV population size in the northeast U.S. (median 2 changes, 95% HPD 1-3, excluding a constant population size). Plotting population size over time indicated growth over the last fifty years (Fig. 2.4B). The increase in population size was also supported by posterior estimates of the population growth rate in the exponential population model, which excluded 0 in the 95% HPD interval.

Altogether, our findings suggest that these DTV sequences from the northeast shared a common ancestor within the past several hundred years and support recent growth in the DTV population size.

2.3 Discussion

We collected, isolated, and sequenced DTV across a wide range of locations and years to increase understanding of the ecology and evolution of this emerging tick-borne flavivirus. We detected DTV in 1.0 to 5.5% of ticks screened, in line with previous rates found in Pennsylvania, Connecticut, Maine, and New York[16,103,109,110]. The highest DTV prevalence (5.5%) was found in Hardwick, New Jersey, though only seventy-three ticks were collected in this location. These prevalence data are much lower than recent reports of 11-67% in some Pennsylvania counties[18]. It should be noted that collection methods, confidence intervals and sample sizes were not reported for these counties, and previous tick surveys in

Pennsylvania found around 1% DTV-positive ticks[109,148], though this doesn't rule out the possibility that focal prevalence could be very high.

We detected significantly more adult female DTV-positive ticks than males, which has not been observed in other tick surveys[110,149]. The reasons for this are unclear at present but may be related to differences in viral tropisms of DTV between male and female adult *I. scapularis*. For example, tropism for female reproductive tissue, which would be required for efficient vertical transmission, might explain this difference. Alternatively, differences in the size and or cellular composition of midguts between males and females could alter infection success in ticks[150]. Thus, understanding flavivirus tissue tropism in both sexes is a critical gap in our knowledge of emerging tick-borne viruses.

We sequenced full viral genomes from eighty-four geographically and temporally diverse samples from ticks and low-passage cell cultures, contributing substantially to the available set of POWV and DTV sequences, and allowing us to perform detailed phylogenetic analyses. Our phylogenetic analysis supported the presence of two geographically separated DTV sublineages, consistent with prior reports[103,145,147]. Interestingly, a single sample from New Jersey (NJ-H-56-2019) clustered with the Midwest sublineage, suggesting that long-range dispersal of DTV-infected ticks on mammalian or avian hosts is likely, and highlighting the importance of further investigation of DTV in locations situated geographically between the Northeast and upper Midwest U.S. Finer-scale analysis of multiple tick collections in the Northeast from 2017-21 also supported geographic dispersal of closely related viruses over smaller distances, e.g. between sites in Maine and New York, Massachusetts and Maine, and New Jersey and New York. However, we also observed stable foci, in which DTV populations remained highly conserved over time in Maine and Massachusetts. The observation of stable foci in this study, which used an expanded sample set and full-genome sequencing, bolsters findings from prior studies that also identified stable foci of infection using partial sequences and fewer collection sites, which may have limited observations of intermingling between sites[99,103].

Time-scaled phylogenetic analysis of DTV sequences indicated that the Northeast and Midwest sublineages last shared a most recent common ancestor (MRCA) approximately 1,200 years ago. Our

results (time to MRCA (TMRCA) 1,184 years ago, 95% HPD 770-1,658) were consistent with results from an analysis of 26 full genome sequences in 2019 (TMRCA 1,160 years ago, 95% HPD 760-1,750)[145]. These recent analyses provide an update to prior studies which had available only partial genome sequences from a smaller number of samples [147]. While the Northeast and Midwest lineages diverged from one another over 1,000 years ago, the TMRCA of sequences within each sublineage are just within the last several hundred years. We estimated the TMRCA of the northeast lineage to be 289 years ago (95% HPD 75-577) when analyzing samples from the northeast only, and to be slightly more recent but within the same range (138 years ago, 95% HPD 88-192) when analyzing all DTV samples. This timing coincides with reforestation of the U.S. and booming populations of white-tailed deer, which allowed previously scattered relic populations *I. scapularis* to disseminate across eastern North America[21].

Our results suggest that there has been expansion of the DTV population over the last 50 years. Our inferences of population size must be interpreted cautiously given the wide 95% HPD and the fact that most of our samples were derived from the recent past. However, DTV population expansion would be consistent with population genetic studies of *I. scapularis* ticks and another pathogen it transmits, *Borrelia burgdorferi,* the spirochete that causes Lyme disease. Both *I. scapularis* and *B. burgdorferi* have experienced rapid population growth within the past 100 years[151–153]. Tick populations, including *I. scapularis,* have been increasing and expanding northward over the past century due to changes in landscape, host availability, and climate. Thus, there has been new detection or increased density of ticks and their associated pathogens in territories where little to none were found before[11]. Further expansion of ticks and tick-borne pathogens is predicted to occur with ongoing climate change[154], underscoring the importance of further work to understand POWV/DTV ecology, evolution, and pathogenesis with the ultimate goal of developing prevention, treatment, and mitigation strategies.

Our study highlights several additional directions of importance. Whereas prior studies of POWV/DTV pathogenesis relied upon a limited number of high-passage viruses, here, we obtained sixteen recent, low-passage isolates from a broad geographic range in the northeastern U.S. Successful

isolation in cell culture compared to the previous standard of using suckling mouse brain increases the feasibility of isolating virus for experimental studies. Importantly, we show that isolation in BHK cells does not significantly alter the virus population and rarely produces sequence changes on a consensus level. This observation permits us to conclude that these isolated strains are accurate representations of naturally circulating POWV, indicating their suitability for future studies.

In addition, our study emphasizes the importance of additional collection and sequencing of DTV isolates throughout a broader range of the U.S. While we observed geographic dispersal of DTV within the Northeast, additional sequences are needed to determine if this also occurs in the Midwest. Furthermore, sampling of sites between the northeastern and midwestern U.S. is important for a more comprehensive understanding of DTV dispersal across North America.

In conclusion, we confirm recent expansion of the DTV population in North America, with geographic patterns of evolution suggesting both geographic dispersal and the repeated establishment of stable foci of infection. These results contribute to our understanding of DTV evolution and ecology in North America.

2.4 Materials and Methods

Tick collection and screening. In the spring and fall of 2019, host-seeking *Ixodes scapularis* ticks were collected during surveys of vegetation using square meter white flannel drags [155]. Survey sites were selected based on guidance from the New York State Department of Health, Maine Health Institute for Research, and Tufts University. Ticks were kept alive in vented five-dram styrene vials at room temperature or 4°C with a paper towel moistened with water for up to five days before being moved to a 95% relative humidity chamber at 9°C until processed. Ticks were surface sterilized in 3% hydrogen peroxide and PBS for 20 seconds each. Ticks were then bead homogenized for two minutes at 24 hertz in 200µL PBS supplemented with 20% fetal bovine serum (FBS), 1% penicillin/streptomycin, 2.5mg/mL amphotericin B, and 50mg/mL gentamicin, then centrifuged at 10,000rcf for 5 minutes at 4°C.

Homogenates were pooled in groups of five and RNA was extracted using the Omega viral DNA/RNA kit on a King Fisher robotics platform. qRT-PCR was performed on homogenate pools using the following primers directed to the NS5 gene: GGCCATGACAGACACAACAGCGTTTG (forward) and GAGCGCTCTTCATCCACCAGGTTCC (reverse). Melt curves were used to verify true positives against background.

Virus isolation in BHK cells. Individual tick homogenates from RNA positive pools were used to attempt isolation in cell culture. Homogenate was incubated in close contact with baby hamster kidney (BHK) cells for 30 minutes to 1 hour before additional 2% FBS media was added to the flask. Virus infected cells were incubated until 20-50% cytopathic effect was observed (approximately four to five days post inoculation). Isolations were validated by plaque assay and qRT-PCR.

Whole genome sequencing and phylogenetic analysis. DTV genome sequencing was performed from RNA obtained from both tick homogenates and culture supernatants, as previously described [35] Briefly, samples underwent DNase (ArcticZymes), single-cycle cDNA synthesis using random primers and Superscript III (Invitrogen), library tagmentation and 16-cycle PCR amplification using Nextera XT (Illumina), and 150 bp paired-end sequencing using an Illumina MiSeq or NextSeq. Reads underwent reference-based assembly to generate a consensus DTV sequence from each sample, using viral-ngs v2.0.21('https://github.com/broadinstitute/viral-pipelines') and reference HM440559.1.

Full-length DTV sequences were generated from 18 RNA samples collected in this study, as well as 45 primary tick RNA samples provided by collaborators, which were collected between 2018-2021 in the northeast U.S. (Table S2.1). Full-length POWV and DTV sequences were also obtained from 21 culture isolates from ticks collected between 1977-2008 (Table S2.1). Sequencing and analysis methods were the same for field-collected ticks, ticks provided by collaborators, and culture supernatants.

These 84 newly generated sequences were aligned with 24 POWV and DTV reference sequences from GenBank, using MAFFT as implemented in Geneious (https://www.geneious.com). Focused

alignments were also made for just the DTV sequences (N=91) and just the DTV sequences from the northeast (N=75). ModelFinder implemented in IQ-TREE v1.6.12[157,158] was used to identify the best substitution model and gamma shape prior, and maximum likelihood (ML) trees were generated with 1,000 ultrafast bootstraps for each alignment. For each ML tree, root-to-tip analysis was performed using TempEst[159], with the best fitting root chosen using the correlation function. Moderate to strong support for a molecular clock was observed in all three trees, with a correlation coefficient 0.86 for all POWV, 0.63 for DTV alone, and 0.66 for the northeast sublineage of DTV (Fig. S2.1).

Time-scaled DTV phylogenies were constructed using BEAST2[160] with partitions for codon positions (1+2), codon position 3, and untranslated regions (Supplemental Data). Model testing was performed to identify the best fitting molecular clock and tree prior to assess population size change. We compared a strict molecular clock, a local random clock, and a relaxed lognormal clock. For all molecular clock models, the prior was set to 3.5E-5[147] with a uniform distribution and no upper or lower limits. For tree priors, we compared a constant coalescent population size (CC), the Coalescent Extended Bayesian Skyline (CEBS), and an exponential coalescent model (EC). The nested sampling method[161] was used to compare models with a sub-chain length of 20,000 and particle counts of 8 for the CC tree prior and 16 particles for CEBS and EC tree priors.

In our analysis of all DTV sequences (N=91), the marginal likelihoods of the strict clock models were higher than those of the lognormal models, with Bayes factor >2.2 (Table S2.2), providing support for the strict clock model[161,162]. Clock models were also compared using generalized stepping-stone sampling (GSS), which again provided support for a strict clock model (Bayes factor = 2.5). Among tree priors, we found that the exponential model was the best fit (Table S2.2).

We separately analyzed DTV sequences from the northeast sublineage (N=75) and identified two models of equally good fit. First, when using a GTR+G4 nucleotide substitution model (to be consistent with the analyses above), we found that a relaxed lognormal clock with CEBS tree prior was the fit best. However, using a TN93 nucleotide substitution model (as suggested by ModelFinder), a strict clock and

exponential growth model fit best. We did not separately analyze DTV sequences from the Midwest sub-lineage due to small sample number and limited time range of collection.

To assess possible change in the population size of the northeast DTV subpopulation, we used the CEBS model with the parameters described above, running the Markov chain Monte Carlo (MCMC) with 300 million steps. The log files were examined with Tracer v.1.7.2 and confirmed to have ESS values > 200 for all parameters[163]. The CEBS plot was visualized using custom R v4.1 scripts[164,165]. The maximum clade credibility tree was built from the files generated by the CEBS model, with 10% burn in, using TreeAnatator v2.6.6[160]. The median number of population changes was represented by the "sum(indicators.alltrees)" parameter.

Deep sequencing and analysis of passaged virus. 14 pairs of DTV-positive tick homogenates and corresponding cell culture-isolated virus were sequenced to assess DTV consensus sequence changes after isolation in cell culture. 6 of these pairs underwent successful deep sequencing of duplicate independent libraries for analysis of intrasample single nucleotide variants (iSNV). Trimmed, quality-filtered .bam files were generated using viral-ngs v2.0.21, and a merged .bam file was generated using samtools v1.10 (Li et al. 2009). Bam files were separated into respective R1 and R2 fastq files using samtools. Reads <25 bases in length and PCR duplicates were removed using fastp v0.23.2[166]. For each library, fastqs for both tick-derived and BHK-derived RNA were aligned to their respective tick-derived consensus sequence using bowtie2 v2.3.5.1[167] using the following parameters: --local -L 25 -N 1 --gbar 15 --rdg 5,1 --rfg 5,1 --score-min G,30,15 --mp 10. Output sam files were converted to sorted, indexed bam files using samtools, and iSNVs were called with VPhaser-2 v2.0 [168] with the following parameters: -ps 100 -ig 20 -dt 0 -a 0.001. Allele information for positions present in both libraries was extracted from the corresponding merged bam file. iSNVs were then filtered for those present at ≥1% allele frequency and indels were additionally filtered for those greater than two nucleotides in length to reduce spurious iSNV calls. Remaining iSNVs were manually inspected and any suspected spurious calls were removed. iSNVs were considered spurious if: 1) iSNV only occurred in one position across multiple reads (e.g. only at left-

most part of reads and never in the middle of reads); 2) iSNV only occurred in one mapping orientation; 3) iSNV only occurred in combinations with one another suggestive of processing artifact. Shannon's entropy was calculated as follows:

$$\frac{-\sum \quad frequency * ln\,(frequency)}{sequence\ length}$$

Normal distribution was assessed by Q-Q plot, and significance was assessed by Wilcoxon sign-rank test in SPSS. Associated amino acid changes were annotated using custom genome annotator excel files, and nucleotide positions were indexed to the HM440559.1 genome.

CHAPTER 3: PHENOTYPIC DIVERSITY OF DEER TICK VIRUS IN NORTH AMERICA

3.1 Introduction

Powassan virus (POWV) is an emerging tick-borne flavivirus that causes human neuroinvasive disease in North America. In the United States, reported cases have increased from 0.9 cases per year (1958-2007) to 16.7 cases per year (2008-2021)[13,14]. Though increased recognition and diagnostic capability have undoubtably played a part in this apparent increase, several observations indicate increased virus prevalence: elevated seroprevalence in deer[15], documented expansion of POWV-associated vectors[10,169], and reports of high tick infection rates[18,101]. Human cases of POWV largely occur in New England, and midwestern states such as Wisconsin and Minnesota. However, the geographic range of POWV is likely significantly broader: POWV has been detected in Colorado, California, Alaska, and New Mexico[96,97,170]. Moreover, the ecology of POWV and the determinants that lead to local emergence are poorly understood.

POWV is the sole North American member of the tick-borne encephalitis complex (Figs. 3.1A and C): a group of tick-borne flaviviruses with similar antigenic properties and vector associations[2]. Tick-borne encephalitis virus (TBEV) is broadly distributed throughout Europe and Asia and is divided into genetic subtypes linked to geography, vector species, and pathogenicity in humans. In far-eastern Russia and Asia, TBEV is linked to severe neurological disease resulting in permanent damage to the brain and spinal cord, and death in 20-30% of cases. In Siberia, TBEV causes more mild neurological disease associated with infrequent chronic infection. European TBEV generally causes biphasic febrile disease which can be mildly neurological in the second phase[23]. Case fatality rates for Siberian and European subtypes are between 6-8% and 1-2% respectively. These observations have led us to speculate that similar phenotypic diversity may exist among North American strains of POWV.

There are two genetic lineages of POWV that have 84.6% nucleotide identity and 95.1% amino acid identity (Figs. 3.1B and 3.2) and are indistinguishable by serology. Both virus lineages can cause disease in humans, but lineage II (deer tick virus; DTV) has been detected in humans more frequently due

to its association with the aggressively human biting tick *Ixodes scapularis*[31,32,171]. Clinical disease ranges from asymptomatic infection to severe neurological involvement, with 50% of patients developing permanent disorders and 11% succumbing to disease[13,29,31,38]. Although a range of clinical presentations is associated with POWV infection in people, the severity of both acute clinical disease and the high prevalence of neurological dysfunction among survivors are extremely concerning.

Figure 3.1. POWV isolates used. A) Maximum likelihood phylogenetic tree of all mammalian viruses of the *Flavivirus* tick-borne encephalitis complex. LIV=louping ill, TBEV= tick borne-encephalitis (Eu = Europe, Sib= Siberian, FE = far eastern), OHFV=Omsk hemorrhagic fever, KFDV=Kyasanur forest disease, POWV=Powassan, DTV=deer tick, KSIV=Karshi, RFV=royal farm, GGYV=Gadget Gully, KADV=Kadam, CFAV=cell fusing agent. B) Maximum likelihood of sixteen POWV and DTV isolates used in this study. C) Approximate locations of isolates in the U.S. and Canada. Dots may represent multiple isolates in proximity.

Relative % identity: low — high

		L1				L2 Northeast					L2 Midwest						
		LB	64-7062	M11665	1427-62	NFS9601	IPS001	ME19-1051	NY19-435	NY19-12	SPOB9901	FA5/12-40	MA5/13-47	MB5/12-73	FB5/13-140	MN19-61	MN20-CSF01
L1	LB		94.05	98.95	94.71	85.21	85.19	85.18	85.16	85.25	85.14	85.14	85.18	85.15	85.13	85.19	85.2
	64-7062	94.05		93.92	90.61	85.23	85.22	85.18	85.14	85.15	84.86	84.93	84.97	84.97	84.94	84.91	84.88
	M11665	98.95	93.92		94.22	85.01	84.97	84.99	84.98	85.03	84.9	84.88	84.95	84.93	84.93	84.95	84.92
	1427-62	94.71	90.61	94.22		82.55	82.54	82.55	82.47	82.53	82.41	82.52	82.56	82.52	82.53	82.49	82.54
L2 Northeast	NFS9601	85.21	85.23	85.01	82.55		99.76	99.22	99.59	99.31	93.7	93.74	93.74	93.75	93.7	93.89	93.72
	IPS001	85.19	85.22	84.97	82.54	99.76		99.23	99.61	99.32	93.75	93.79	93.79	93.79	93.75	93.94	93.75
	ME19-1051	85.18	85.18	84.99	82.55	99.22	99.23		99.2	99.6	93.65	93.7	93.7	93.71	93.67	93.83	93.66
	NY19-435	85.16	85.14	84.98	82.47	99.59	99.61	99.2		99.3	93.73	93.73	93.73	93.73	93.69	93.89	93.72
	NY19-12	85.25	85.15	85.03	82.53	99.31	99.32	99.6	99.3		93.74	93.77	93.77	93.77	93.74	93.91	93.74
L2 Midwest	SPOB9901	85.14	84.86	84.9	82.41	93.7	93.75	93.65	93.73	93.74		99.71	99.87	99.83	99.79	99.46	99.42
	FA5/12-40	85.14	84.93	84.88	82.52	93.74	93.79	93.7	93.73	93.77	99.71		99.75	99.71	99.69	99.51	99.47
	MA5/13-47	85.18	84.97	84.95	82.56	93.74	93.79	93.7	93.73	93.77	99.87	99.75		99.87	99.83	99.5	99.46
	MB5/12-73	85.15	84.97	84.93	82.52	93.75	93.79	93.71	93.73	93.77	99.83	99.71	99.87		99.8	99.47	99.42
	FB5/13-140	85.13	84.94	84.93	82.53	93.7	93.75	93.67	93.69	93.74	99.79	99.69	99.83	99.8		99.45	99.4
	MN19-61	85.19	84.91	84.95	82.49	93.89	93.94	93.83	93.89	93.91	99.46	99.51	99.5	99.47	99.45		99.39
	MN20-CSF01	85.2	84.88	84.92	82.54	93.72	93.75	93.66	93.72	93.74	99.42	99.47	99.46	99.42	99.4	99.39	

Fig 3.2. Nucleotide identity matrix for POWV isolates used in this study. Lower relative percent identity indicated by darker shading and higher percent identity indicated by light to no shading.

Phenotypic studies of POWV to date have almost exclusively used two highly passaged historical isolates: LB (lineage I) and SPO (lineage II). Therefore, we used 16 low-passage virus isolates collected from Canada, and Northeast and Midwest U.S. to assess phenotypic diversity of POWV *in vitro*. Using human neuroblastoma cells, we assessed replication and cytopathic effects to understand how individual POWV strains might differ in their pathogenic potential. Metagenomic sequencing was performed pre- and post- passage to identify single nucleotide variants (SNVs) that may be of medical importance. Briefly, we observed broad variation in replication and distinct cytopathic phenotypes on human neuronal cells. Though no causative genotypes were identified, two genetic changes were identified in multiple isolates post-culture and warrant further investigation. Our results provide clear evidence of significant phenotypic diversity in North American POWV and support the observation that naturally circulating viruses may have distinct propensities for perpetuation, transmission, and pathogenesis.

3.2 Results

POWV isolate characteristics. Sixteen POWV and DTV isolates were chosen as a representative sample set to assess replication phenotypes *in vitro*. These included four lineage I and twelve lineage II isolates (five from the Northeast clade, and seven from the Midwest clade). The lineage I isolates (1958-1965) derive from human, rodent, and tick sources from Ontario, Canada, and New York. The lineage II isolates (1995-2020) originate from five U.S. states and were mostly isolated from *I. scapularis* ticks. MN20-CSF01 was isolated from a human patient. Isolates were maintained at the lowest possible passage; however, many of the older isolates have been passaged multiple times through suckling mice (Table 3.1).

The 16 isolates used in this study have an overall nucleotide identity of 91.6% (97.0% amino acid identity). Lineage I isolates are the most dissimilar to each other with 94.4% identity, and at least 105 single nucleotide variants (SNVs) between them. Lineage II isolates are overall 96.5% identical: 99.4% among Northeast isolates and 99.6% among Midwest isolates. In the Midwest DTV group, SPOB9901 and MA5/13-47 are the most similar with 14 SNVs between them and a single amino acid difference in the NS5 RNA-dependent RNA polymerase (RDRP) at position 8819 (Figs. 3.1B and 3.2).

Table 3.1. POWV isolates used in this study. Virus isolates have been obtained either through collaborators or our own tick collections. All viruses have been grown up in BHK cells in our lab to create stocks used in this study. SM = suckling mice, V = Vero cells, B = BHK cells.

Label	Lineage	Location	Year	Source	Passage History	GenBank accession
LB	I	Powassan, Ontario	1958	human CSF	SM4V2B1	NC003687
1427-62	I	North Bay Ontario	1962	*I. marxi*	SM3V1B1	OP823405
64-7062	I	New York	1964	*Ixodes sp.*	SM6V2B1	HM440563
M11665	I	Laurier Township, Ontario	1965	*I. cookei*	SM2V1B1	OP823404
IPS001	II	Ipswitch, MA	1995	*I. scapularis*	SM1B2	OP823421
NFS9601	II	Nantucket, MA	1996	*I. scapularis*	SM1B2	HM440559
SPOB9901	II	Spooner, WI	1999	*I. scapularis*	SM1V2B1	OP823482
FB5/13-140	II	Spooner, WI site B	2008	*I. scapularis* F	B2	OP823484
MA5/13-47	II	Spooner, WI site A	2008	*I. scapularis* M	B2	OP823478
FA5/12-40	II	Spooner, WI site A	2008	*I. scapularis* F	B2	OP823475
MB5/12-73	II	Spooner, WI site B	2008	*I. scapularis* M	B2	OP823480
NY19-12	II	Saratoga Springs, NY	2019	*I. scapularis* F	B1	OP823461
NY19-435	II	Connetquot, NY	2019	*I. scapularis* M	B1	OP823469
ME19-1051	II	Rockland, ME	2019	*I. scapularis* M	B1	OP823442
MN19-61	II	St. Croix MN	2019	*I. scapularis*	B2	not yet published
MN20-CSF01	II	Northern MN	2020	human CSF	B2	not yet published

Virus replication and cytopathic effects in mammalian cells. Initial phenotypic analysis was performed on a subset of the isolates from Table 3.1. Two mammalian cells lines: baby hamster kidney (BHK-21, ATCC CCL-10), and human neuroblastoma (SH-SY5Y, ATCC CRL-2266) were used to assess replication phenotypes. A multiplicity of infection (MOI) of 0.01 was used to attain multi-step replication. In BHK-21 cells, viral loads in the supernatant peaked at three days post infection (dpi) and universal cell mortality was visually observed three to five dpi. Replication curves were uniform among DTV isolates, though variation was observed between lineage I isolates: LB and 64-7062, the most highly passaged isolates, peaked two dpi around 10^7 PFU/mL, while M11665 and 1427-62 peak three dpi around 10^6 PFU/mL (Fig 3.3A). In SH-SY5Y cells, LB, 64-7062, M11665 replicated similarly, peaking two dpi around 10^7-10^8 PFU/mL; however, delayed replication was observed for 1427-62 which peaks six dpi around 10^6 PFU/mL. DTV replication was significantly variable in SH-SY5Y cells with virus titer ranging from 10^2 to 10^6 PFU/mL two dpi. All DTV isolates peaked on six dpi with viral titers ranging from $10^{5.5}$ to 10^8 (Fig. 3.3B).

Variable CPE was visually noted during infection in SH-SY5Y cells, thus an MTT assay was used to measure cell viability nine dpi. FA5/12-40 and FB5/13-140 (lineage II Midwest) produced less CPE compared to the other isolates, though significance was only determined against the lineage I isolates

(p<0.01, Kruskal Wallis test). Lineage I isolates, MA5/13-47, and MB5/12-73, NFS9601, IPS001, and SPOB9901 resulted in 100% CPE (Fig. 3.3C).

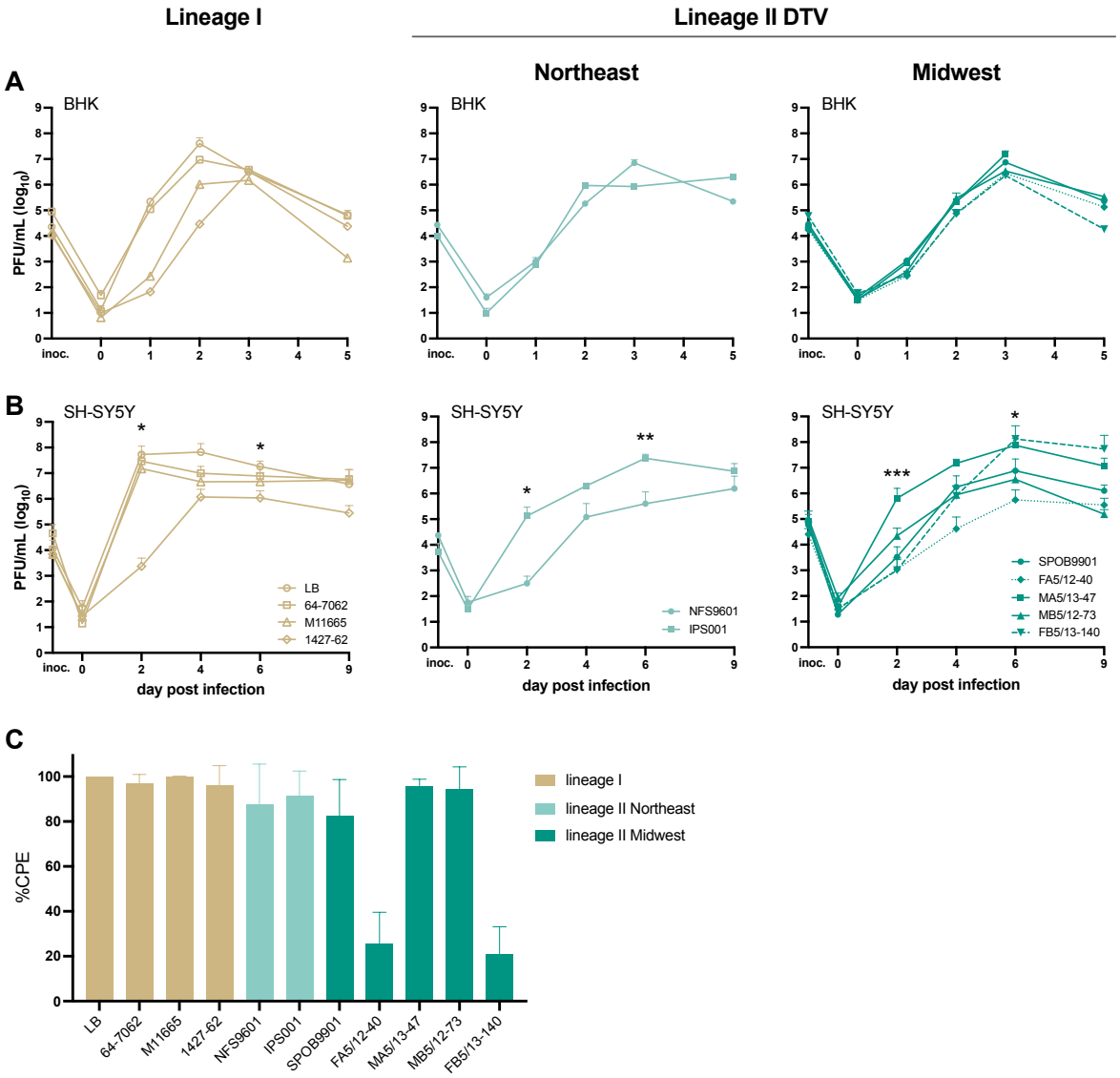

Figure 3.3. Replication and CPE phenotypes of POWV isolates 1958-2008. POWV is inoculated at an MOI of 0.01 in triplicate on A) BHK and B) SH-SY5Y for incubated up to 9 days at 37ºC. Replication curves are separated by genetic clade to appreciate the differences between closely related isolates. Data shown is from two replicate experiments. C) SH-SY5Y cells are inoculated (n=6 wells) with virus approximating an MOI of 0.01 and incubated for 9 days. Cells are stained with MTT, and absorbance is measured. Absorbances are background subtracted and normalized to uninfected control wells to calculate %CPE. Data shown is from two replicate experiments.

To bolster observations of *in vitro* phenotype, additional current low-passage isolates were obtained (those from 2019-2020), and replication and CPE assays were repeated in SH-SY5Y cells. Though the shape of the replication curve is different, significant variability was again observed between isolates. Highly variable replication was observed with peak viral titer ranging from $10^{4.5}$ to $10^{8.5}$ PFU/mL. Isolates from New York (NY19-435 and NY19-12) resulted in much lower titers than the isolates from Minnesota (MN19-61 and MN20-CSF01) and Maine (ME19-1051) (Fig 3.4A). All these isolates caused 100% CPE by nine dpi (Fig 3.4B).

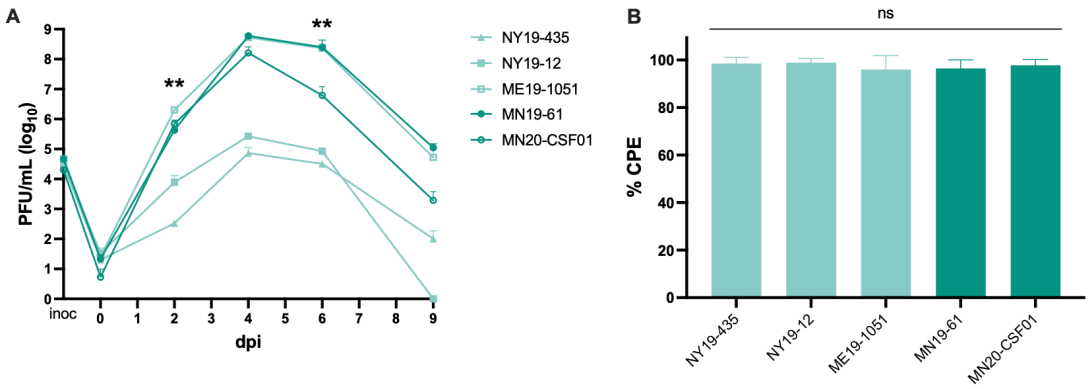

Figure 3.4. A) Replication and B) CPE of 2019-2020 DTV isolates on SH-SY5Y cells. Results are from a single experiment.

Potential genetic determinants of phenotype. Shotgun metagenomic sequencing was performed on RNA isolated from pre-infection 'input' POWV and after nine days replication in SH-SY5Y cells to identify intra-isolate SNVs that may be associated with *in vitro* phenotype and replication in neuronal cells. Isolates included in this experiment were LB, 64-7062, M11665, 1427-62, NFS9601, IPS001, MA5/13-47, MB5/12-73, and FB5/13-140. We first looked at consensus-level changes after a single passage in SH-SY5Y cells. Seven of eleven changes occurred in env protein, all of which are nonsynonymous. Four changes were identified in non-structural proteins, though three of four were synonymous changes in 1427-62. Interestingly, these changes start and end at the same approximate frequencies suggesting that they may be linked on the same virus genome. The only nonsynonymous change was identified in M11665 lineage I isolate in the NS3 protease protein. Two nonsynonymous SNVs in the envelope coding region (env) were identified in multiple isolates: G1096A was identified in lineage I isolates 1427-62 and

M11665, and A1868G was identified in lineage II isolates MA5/12 #47, SPOB9901, and IPS001. In most of these cases, this SNV was not found in the input, and resulted in substantial increase in frequency (Fig. 3.5A).

We next looked at changes in population complexity between input and nine dpi SH-SY5Y culture samples. All lineage I isolates started with higher complexity than lineage II isolates. All isolates, except for 1427-62 increased in complexity, though these changes were not significant (Fig. 3.5B).

A

Isolate	ΔNT*	Region	Type	ΔAA	Input Freq	9 DPI Freq
	G1096A	E	NS	E51K	0	78.4
	A1513G	E	NS	S190G	48.9	85.1
1427-62	C3675T	ns2A	S	V60V	40.3	79.7
	C4611T	ns3	S	D11D	41.1	81.4
	G8736A	ns5	S	K363K	42.7	82.4
64-7062	A1436G	E	NS	Q164R	0	61.7
M11665	G1096A	E	NS	E51K	0	61.7
	A5239G	ns3	NS	R221G	3.5	59.8
MA5/13-47	A1868G	E	NS	D308G	0	76.1
SPOB9901	A1868C/G	E	NS	D308A/G	0	43.1
IPS001	A1868G	E	NS	D308G	17.2	55.2

NT, nucleotide; **AA**, amino acid; **NS**, nonsynonymous; **S**, synonymous

*Indexed to HM440559

B

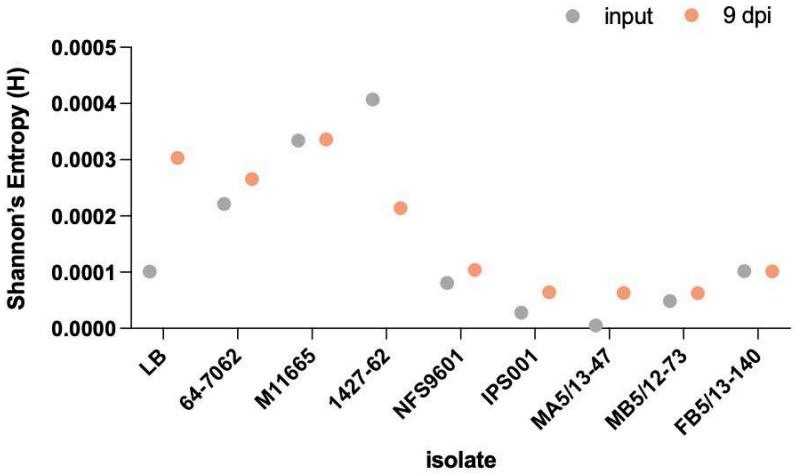

Figure 3.5. Intra-isolate genetic changes pre- and post- SH-SY5Y culture. A) All consensus level SNVs identified after a single passage in SH-SY5Y cells. B) Intra-isolate complexity pre- and post- SH-SY5Y culture, as measured by Shannon's entropy from merged biological replicate libraries. (Not significant by Wilcoxon signed rank test, two-tailed, p=0.13

3.3 Discussion

POWV has emerged in recent decades due to the expansion of deer ticks and increased recognition and diagnosis of disease in humans. However, the incidence of human disease, while increasing, lags far behind other areas where similar viruses (e.g. TBEV) have emerged. The reasons for this are unclear at present, but of significant interest due to the clinical severity of POWV disease in human beings and the ecological changes to the North American landscape that have facilitated the emergence of other tick-borne pathogens. In this work we sought to assess the overall hypothesis that the relative paucity of human cases may be due to reduced pathogenic potential of currently circulating isolates. Specifically, we measured *in vitro* replication, CPE in neuronal cells and assessed virus genetics during replication in cultured cells.

Sixteen viral isolates from three genetic clades were used in the present study. The represented lineage I isolates are more genetically dissimilar than the DTV isolates. DTV genetic subclades are tied to geographic location: Northeast and Midwest U.S. Many of the lineage I and II isolates are moderately to highly passaged; therefore, several current low-passage isolates from a broad geographic range were included in this study. The five DTV isolates from Spooner, WI present a unique opportunity to assess phenotype between isolates with close geographic and temporal characteristics. While SPO9901 was collected in 1999 and has been moderately passaged, it has similar consensus identity to the four low-passage isolates collected in 2008 (99.8%), indicating genetic stability of DTV in this area as previously described[99]. Despite the geographic proximity, they are genetically distinct, with 14-33 consensus differences among them. DTV isolates from 2019 originate from *I. scapularis* collected from four locations and represent both the Northeast and Midwest. Out of the 16 isolates evaluated in this study, two isolates originate from cerebral spinal fluid of patients with POWV disease. Together, these isolates represent a broad geographic and temporal range from all genetic clades, many of which are maintained with few passages in cell culture. Thus, the isolates included in this study are suitable to assess *in vitro* phenotypes.

SH-SY5Y cells are frequently used as *in vitro* disease model for encephalitic flaviviruses as they are neuronal cells originated from a bone-marrow-derived neuroblastoma. Here, we quantify virus replication and cytopathic effects in SH-SY5Y cells as a proxy for pathogenic potential in humans. BHK-21 cells are kidney-derived fibroblasts used extensively as general laboratory cells, highly permissive to flavivirus replication, and used here as a robust comparison of virus replication.

Isolates from all genetic clades were able to replicate to high titers in bone marrow-derived SH-SY5Y neuroblastoma cells, though significant variation was observed. At two dpi, over a 10,000-fold (lineage I, lineage II Northeast) and 1000-fold (lineage II Midwest) difference in viral titer was observed. Among DTV isolates, 10,000-fold differences were observed in peak viral titers at four or six dpi. Surprisingly, no correlation between replication phenotype and genetic clade, location, or originating source were observed. These observations clearly establish that POWV isolates possess extreme variation in their ability to replicate in neuronal cells.

Inspection of cell mortality nine dpi in human neuronal cells revealed virus strain-dependent differences in CPE. Most isolates resulted in 100% CPE on SH-SY5Y cells, apart from FB5/13-140 and FA5/12-40 (lineage II Midwest). Interestingly, FB5/13-140 and FA512-40 had both the highest and lowest peak viral titers (respectively) of the DTV Midwest isolates, indicating CPE phenotype did not correlate with increased replication. To determine whether any recent DTV isolates would be similarly unable to cause CPE, we repeated this experiment with five DTV isolates from 2019-2020. These isolates caused CPE in SH-SY5Y cells quite efficiently, suggesting that rarely, POWV strains cause minimal CPE in these cells. Collectively, these experiments document strain-dependent variation in the ability of POWV to cause CPE in a neuronal cell *in vitro* model. The significance of these data for human disease remains unclear at present.

Given the high passage history of some of the isolates used, enhanced replication could be due to adaptations to cell culture or suckling mice brain. Inoculation into the brains of suckling mice was (and sometimes still is) used to isolate POWV, though currently cell culture is used more frequently. For instance, lineage I isolates have been passaged multiple times in suckling mice and nearly all (excluding

1427-62) replicate similarly well in SH-SY5Y cells, despite having only 95.6% nucleotide identity. Thus, efficient replication could be due to adaption to neuronal cells. In contrast, the following observations demonstrate DTV phenotypes in SH-SY5Y cells are not a result of adaptation to cell culture: (1) uniform replication and CPE of DTV isolates in BHK cells, despite some being more highly passaged, and (2) high variation in SH-SY5Y cells between isolates with similar passage history. Most of the studies on POWV to date have used isolates LB (highly passaged) and SPO (moderately passaged) in experimental studies on transmission and disease. The present results demonstrate the importance of working with low-passage isolates for an accurate picture of POWV phenotypes.

Two nonsynonymous consensus changes were identified in post-SH-SY5Y culture samples that are shared between multiple isolates. Residue E51 and D308 in env were found in two lineage I and three lineage II isolates, respectively. Both residues resulted in increasing SNV frequency, in many cases going from 0% to over 60%, suggesting potential importance to neuronal cells. Interestingly, D308 lies on domain III in the protein binding motif and has been implicated for increased neuropathic potential in TBEV[172]. Residue E51 lies in domain II of the env protein, which is involved in protein dimerization and membrane fusion[172], though this residue has not been associated with neurovirulence. *In vitro* phenotype could not be linked to either SNV, thus additional studies are needed to determine the significance of these results.

In summary, our results demonstrate extensive *in vitro* phenotypic diversity present in POWV. Further investigation using *in vivo* models is needed to determine how these results may translate to disease in humans. Though no clear genetic determinants of *in vitro* phenotype were observed, there are a few key residues that warrant further investigation. Thus, the replication of POWV in human neuroblastoma cells and the ability of strains to cause CPE is highly variable and not currently attributable to a key set of viral genetic determinants.

3.4 Materials and Methods

Cells and viruses. BHK-21 (baby hamster kidney, ATCC CCL-10) cells were maintained in DMEM supplemented with 5% FBS and 1% Penicillin and Streptomycin. SH-SY5Y (human neuroblastoma, ATCC CRL-2286) cells were maintained in a 1:1 ratio of EMEM:DMEM F12 supplemented with 10% FBS and 1% Penicillin and Streptomycin. Cells were grown at 37°C with 5% CO^2. Cells were not maintained past passage 50. A table of the POWV isolates used in this study are in Table 3.1. All POWV stocks were grown up in BHK cells for three to six days, aliquoted with additional 20% FBS and stored at -80°C. Virus was tittered via plaque assay on BHK cells as described below.

Plaque assays. BHK cells were seeded to 90% confluency the day before in six-well cell culture plates. Samples were thawed rapidly and serially diluted in DMEM supplemented with 2% FBS and 1% Penicillin and Streptomycin. All media was removed from six-well plates before BHK cells were inoculated with 200µL of each dilution and incubated at RT on a rocker for one hour. Four milliliters of tragacanth/media overlay was added to each well and incubated at 37°C for five days. Cells were stained with crystal violet to visualize and count plaques.

Growth curves. BHK and SH-SY5Y cells were seeded in six-well cell culture plates the day before for ~70% confluency. One plate of each cell type was counted the day of to calculate the average cells per well. Virus was diluted to inoculate each cell type at a multiplicity of infection (MOI) of 0.01. Media was removed from each cell type, 200µL inoculum was added to the cells and incubated at RT on a rocker for one hour. Cells were washed three times with PBS and four milliliters of cell media with decreased FBS concentration of 2% was added to each well. The first time point (day 0) was taken immediately before plates are incubated at 37°C with 5% CO^2 for the remainder of the experiment. The remainder of the unused virus inoculum was used to immediately perform back titrations via plaque assay. For the remaining five to nine days, supernatant samples were collected from each well in 24-hour increments

and stored at -80°C. Plaque assays were performed as described above to measure infectious virus titer over time. Growth curves were performed in triplicate for both cell types. Growth curves were repeated for SH-SY5Y cells and data was combined for a total of six replicates per isolate. Tests for overall statistical significance were performed in GraphPad Software version 9.5.1 (San Diego, California) for two and six dpi timepoints in SH-SY5Y cells. Kruskal-Wallis test for statistical significance was performed for lineage I and lineage II Midwest. Mann-Whitney t-test was performed for lineage II northeast.

CPE assay. Cells were seeded to 70% confluency in 96-well cell culture plates. Viral stocks were diluted $1x10^3$ PFU/mL in DMEM supplemented with 2% FBS and 1% Pen/Strep. Diluted virus (50µL) was transferred to the cell culture plates and incubated for up to nine days. For each time point, 20µL of 5mg/mL MTT live cell stain was added to each well and incubated at 37°C for three hours. The media was removed, and cells were washed twice with PBS. 100µL of 1:2 DMSO:EtOH was added to solubilize the MTT crystals and incubated overnight in the dark at 4°C. Absorbance was measured at a wavelength of 490nm with background subtraction. Absorbance is normalized to negative control wells on each plate and calculated as a percent cytopathic effect (CPE). Kruskal Wallis test with Dunn's multiple comparisons was performed in GraphPad Software version 9.5.1 (San Diego, California).

Sequencing and iSNV analysis. POWV isolates (table 1) were grown in triplicate on SH-SY5Y cells for nine days. RNA was extracted from 50µL of clarified day nine and input supernatant using the Mag-Bind Viral DNA/RNA kit on a KingFisher Flex Purification System. POWV genome sequencing was performed on RNA as previously described[35] Briefly, samples underwent DNase (ArcticZymes), single-cycle cDNA synthesis using random primers and Superscript III (Invitrogen), library tagmentation and 16-cycle PCR amplification using Nextera XT (Illumina), and 150 bp paired-end sequencing using an Illumina MiSeq or NextSeq. Duplicate independent libraries underwent deep sequencing for analysis of

intrasample single nucleotide variants (iSNV). Trimmed, quality-filtered .bam files were generated using viral-ngs v2.0.21, and a merged .bam file was generated using samtools v1.10 (Li et al. 2009). Bam files were separated into respective R1 and R2 fastq files using samtools. Reads <25 bases in length and PCR duplicates were removed using fastp v0.23.2[166]. For each library, fastq files for both tick-derived and BHK-derived RNA were aligned to their respective tick-derived consensus sequence using bowtie2 v2.3.5.1[167] using the following parameters: --local -L 25 -N 1 --gbar 15 --rdg 5,1 --rfg 5,1 --score-min G,30,15 --mp 10. Output sam files were converted to sorted, indexed bam files using samtools, and iSNVs were called with VPhaser-2 v2.0[168] with the following parameters: -ps 100 -ig 20 -dt 0 -a 0.001. Allele information for positions present in both libraries was extracted from the corresponding merged bam file. iSNVs were then filtered for those present at ≥1% allele frequency and indels were additionally filtered for those greater than two nucleotides in length to reduce spurious iSNV calls. Remaining iSNVs were manually inspected and any suspected spurious calls were removed. iSNVs were considered spurious if: 1) iSNV only occurred in one position across multiple reads (e.g. only at left-most part of reads and never in the middle of reads); 2) iSNV only occurred in one mapping orientation; 3) iSNV only occurred in combinations with one another suggestive of processing artifact. Shannon's entropy was calculated as follows:

$$\frac{-\sum \quad frequency * ln\,(frequency)}{sequence\ length}$$

Normal distribution was assessed by Q-Q plot, and significance was assessed by Wilcoxon sign-rank test in SPSS version 28 (IBM Corp., Armonk, New York) Associated amino acid changes were annotated using custom genome annotator excel files, and nucleotide positions were indexed to the HM440559.1 genome.

CHAPTER 4: *IN VIVO* PHENOTYPES OF POWASSAN VIRUS

4.1 Introduction

In the United States, reported human cases have increased from 0.9 cases per year (1958-2007) to 16.7 cases per year (2008-2021)[14]. Increasing seropositivity in deer[15], recent reports of high infection rates in ticks[16–18], and human cases reported in states with no prior history of disease[14,17,19,20] highlight the changing epidemiology of this virus. POWV infection can result in severe neurological disease, resulting in permanent neurological disorders in 50% and death in 11% of reported cases[13,29]; however, evidence of asymptomatic or mild infections have been observed in serological surveys of people with no history of neurological disease[4,37,39]. Generalized febrile disease appears first, appreciated by fever, sore throat, drowsiness, and disorientation. If disease progresses to encephalitis or aseptic meningitis, patients may develop seizures, nausea, slow speech, and paralysis[30,173]. Though indistinguishable by serology, both virus lineages (POWV and DTV) can cause neurological disease in humans. Therefore, the true scope of disease and differences between lineages is not known.

Detection of POWV through serology, viral RNA, and virus isolation has provided evidence for a broad distribution through the United States and Canada[74,96,98,174,175], despite human cases almost exclusively occurring in Wisconsin, Minnesota, New England, and Ontario[14]. Despite serological evidence of widespread virus circulation and moderate prevalence in ticks, reported cases are still very low, and far less than the closely related tick-borne encephalitis virus in Europe and Asia, which results in over 10,000 human cases annually[22]. Though several factors are at play, it's not known how individual virus strains may be contributing to human cases.

In the present study, we use low-passage, geographic and temporally diverse viral isolates from all genetic clades to determine differences in tick transmission (viremic and transstadial) and disease in mice. We hypothesized strain-dependent differences in pathogenesis and tick transmission that make viruses less able to cause disease or be transmitted through the blood of the vertebrate host.

4.2 Results

POWV isolates used in this study. Eleven isolates were included in the initial study of POWV disease in mice. These isolates were chosen based on geographic and temporal origin, and passage history (Table 4.2). Five of these isolates were chosen for additional experiments to assess pathogenesis and transmission to ticks. A single lineage I isolate (M11665) and four lineage II isolates: two in the Northeast clade (NFS9601 and ME19-1051) and two in the Midwest clade (FA5/12-40 and NJ19-56). Notably NJ19-56 was collected in New Jersey, though clusters genetically with the Midwest isolates as discussed previously[114].

Morbidity and Mortality in C57BL/6 mice. Eleven POWV and DTV isolates were used to determine differences in morbidity and mortality. Four male and four female C57BL/6 mice were inoculated subcutaneously with 10^3 PFU and monitored for disease for up to 14 days or until euthanasia criteria were met. Notably, experimental infections of male and female mice were performed at separate times, though survival curves were combined to show overall mortality. While similar mortality rates (50-64%) were observed for mice inoculated with lineage II Midwest isolates, variable mortality was observed for

Table 4.1. Powassan virus isolates used in this study. SM= suckling mice, V=Vero cells, B=BHK cells, P=unknown passage *used for further investigation

Isolate ID	Lineage	location	year	source	passage history	GenBank accession
M11665*	I	Ontario	1965	*I. cookei*	P1SM1V1B1	OP823404
1427-62	I	Ontario	1962	*I. marxi*	SM3B1	OP823405
NFS9601*	II	Nantucket, MA	1996	*I. scapularis*	SM1B1	HM440559
ME19-1051*	II	Rockland, ME	2019	*I. scapularis*	B1	OP823442
NY19-12	II	Saratoga Springs, NY	2019	*I. scapularis*	B1	OP823461
NY19-435	II	Connetquot, NY	2019	*I. scapularis*	B1	OP823469
NY19-250	II	Cedar Pointe, NY	2019	*I. scapularis*	B1	OP823467
NY19-904	II	Connetquot, NY	2019	*I. scapularis*	B1	OP823471
FB5/13-140	II	Spooner, WI	2008	*I. scapularis*	B2	OP823484
FA5/12-40*	II	Spooner, WI	2008	*I. scapularis*	B2	OP823475
NJ19-56*	II	Hardwick, NJ	2019	*I. scapularis*	B1	OP823460

lineage I and lineage II Northeast-infected mice. Mice infected with lineage I isolates resulted in death for 25-63% of mice. Within the lineage II Northeast isolates, mortality ranged from 0-50%. (Fig 4.1) Isolates that resulted in mild disease include NFS9601, NY19-250, NY19-435, NY19-904, all of which originated from *I. scapularis* collected on Long Island, New York, and Nantucket, Massachusetts (Table 4.2).

Signs of generalized febrile disease such as ruffled fur and hunched poster were observed starting seven dpi. If disease progressed, neurological signs (tremors, slow and uncoordinated movement, paralysis) were usually observed the following day. For isolates M11665 and ME19-1051, 50-63% of mice were euthanized before the study end; however, disease was mild, and only a single ME19-1051-infected mouse progressed to hind-limb paralysis. Signs of febrile disease followed by paralysis were observed for both male and female NJ19-56-infected mice, resulting in 63% overall morbidity by 12 dpi. NFS9601-infected mice exhibited some weight loss starting nine dpi, though few signs of disease were observed (ruffled fur in two male mice), and all mice recovered by 12 dpi. All mice infected with FA5/12-40 exhibited similar patterns of weight loss, though no clinical signs of disease were observed for female mice. Ruffled fur or hunched posture was observed in all male FA5/12-40-infected mice, and two mice developed hind limb paralysis soon after; 75% of male mice were euthanized by 12 dpi, compared to 0% female mice. (Figs. 4.1B and C, S4.1, and S4.2)

To validate potential sex differences in disease for isolate FA5/12-40, the experiment was repeated with eight male and eight female mice. Similar weight loss and signs of neurological disease (ruffled fur, hunched posture, slow movement, loss of coordination, weakness, and paralysis) were observed for both sexes, and 65-75% of mice were euthanized by 14 dpi (Fig. S4.3) Notably, this validation study was performed by a separate institution than the above studies.

Pathogenesis in C57BL/6 mice. Pathogenesis over time was determined for five POWV isolates. Sixteen male C57BL/6 mice were subcutaneously injected with 10^3 PFU. Four mice per isolate were euthanized at three, six, nine, and twelve dpi, unless euthanasia criteria were reached. Virus was detected in the blood three dpi in 100% of mice but was not detected thereafter. Virus loads in the blood were approximately

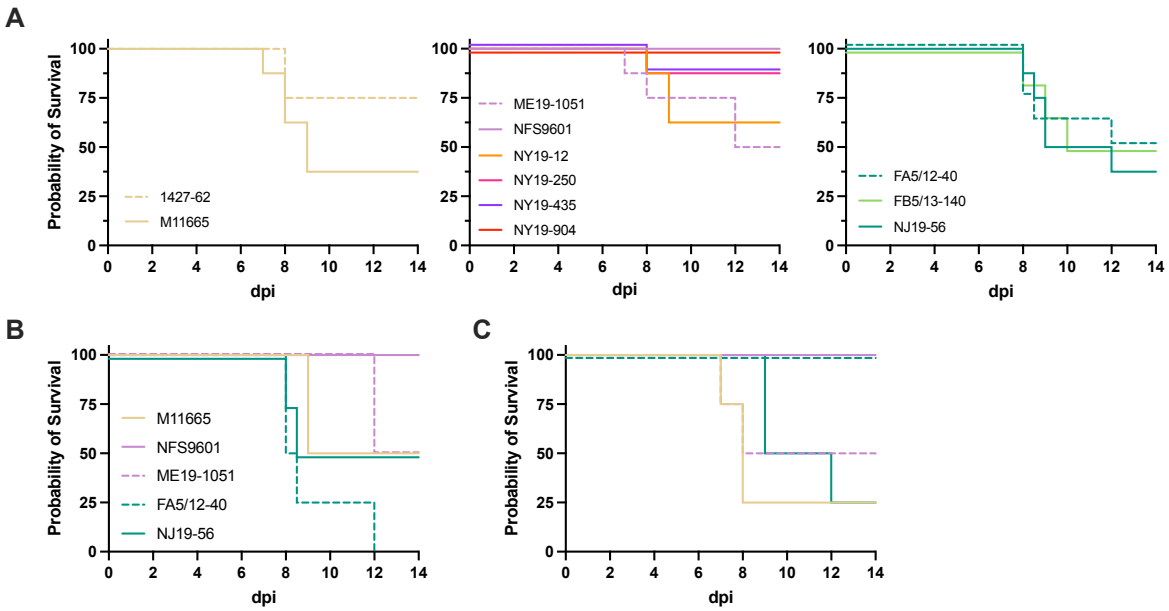

Figure 4.1. Morbidity of C57BL/6 mice inoculated with 11 POWV isolates. A) Survival curves are separated by genetic clade: lineage I (left), lineage II Northeast (middle), and lineage II Midwest (right). Data is combined results from n=4 female and n=4 male mice. Five isolates were broken up into survival of male (B) and female (C) mice.

10^2 PFU/mL, though many samples were at or below the limit of detection (Fig 4.2A). Viral RNA was detected in the spleens of most mice, except for M11665 which was not detected after three dpi. Viral titers in the spleen three dpi varied between isolates, with M11665 and ME19-1051 resulting in the highest viral loads (10^3-10^4 PFU/g) (Fig 4.2B). Viral RNA was detected in the brain starting six dpi for most isolates and in nearly 100% of all mice nine and twelve dpi. NJ19-56 was detected in the brain as early as three dpi and resulted in 100% mice with RNA-positive brains at six dpi. Viral loads in the brain nine dpi ranged from 10^4-$10^{5.5}$ PFU/g (Fig 4.2C).

Viremic transmission to ticks. Viremic transmission of POWV was assessed in *I. scapularis* ticks fed on BALB/c mice infected intraperitoneally with 10^3 PFU (Fig. 4.3A). Approximately 200 larvae were infested a day prior to infection (day 0) to better overlap peak viremia with blood-feeding. Three mice were infected per isolate on day one and replete larvae were collected as they detached, largely days three and four. Ten or approximately 20% of replete larvae per mouse were immediately homogenized and

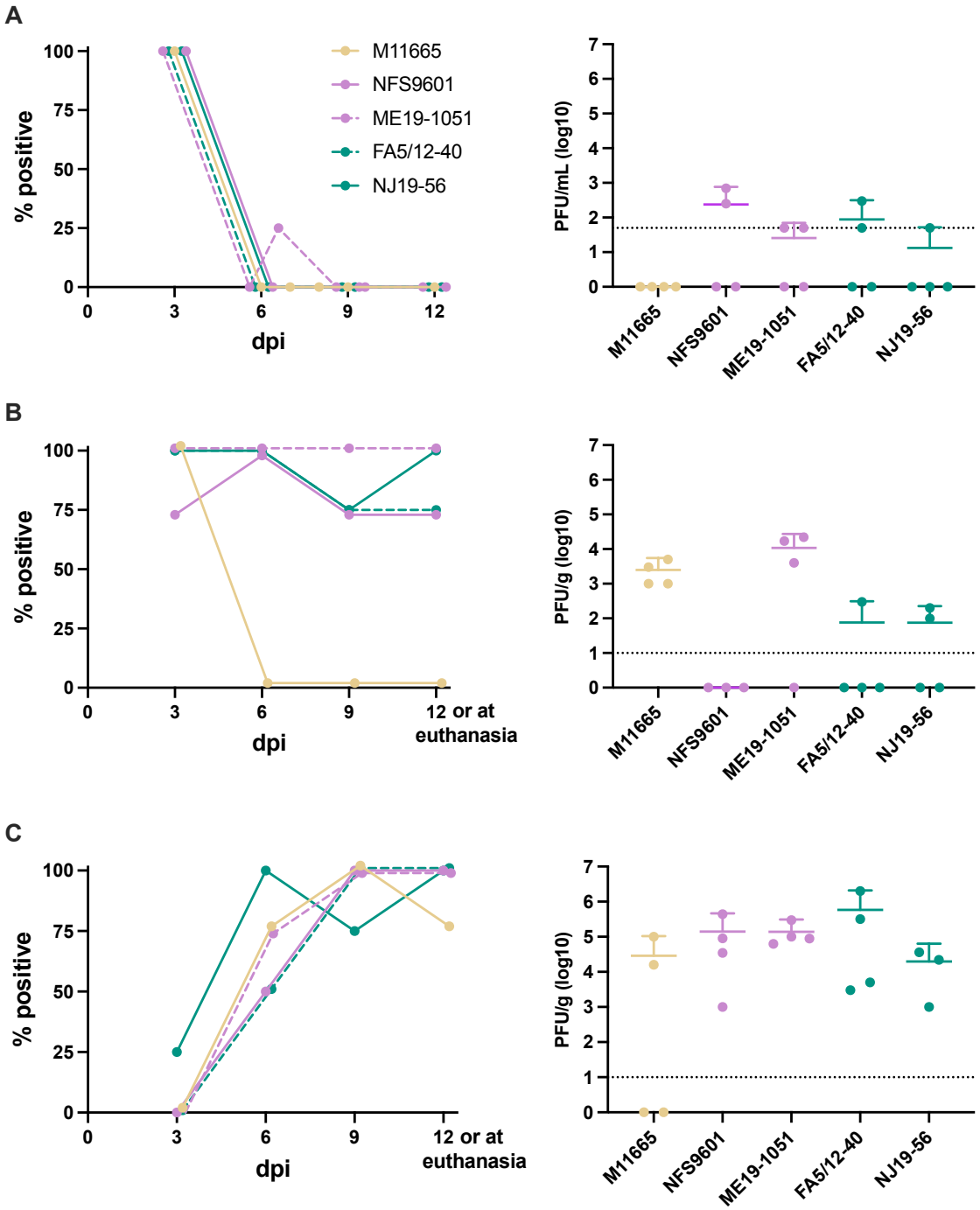

Figure 4.2. Pathogenesis of POWV in B6 mice. A) Percent POWV-positive mice based on viral RNA detection in the A) blood, B) spleen, and C) brain. Viral loads for A) blood and B) spleen were determined for 3 dpi samples. Viral loads for C) brain tissue was determine for 9 dpi samples. Lineage I isolates indicated in yellow. Lineage II Northeast isolates indicated in purple. Lineage II Midwest isolates indicated in teal.

used to determine rates of virus acquisition. 90.0% of ticks had detectable levels of viral RNA, and 10.0% had detectable virus. Remaining larvae were left to molt for eight weeks and nymphs were homogenized and screened for POWV. A median of 35 (range 10-78) nymphs were obtained per mouse. Blood was collected from all mice on day four, though viral RNA was not detected via qRT-PCR.

To bolster our sample size, the experiment was repeated at a lower inoculum (due to viral titers of our stocks) using only two isolates: ME19-1051 and NJ19-56 and six replicate mice per isolate. All replete larvae were allowed to molt for eight weeks prior to processing. A median of 54.5 (22-90) molted nymphs were obtained from each mouse. No statistical significance in viral titer or infection rate (IR) in nymphs was observed between studies (Table 4.1) and results from the combined experiments are discussed below.

Table 4.2. Statistical analysis between first and second viremic transmission experiments.

		exp. 1	exp. 2	test	p value
ME19 #1051	median PFU	370	610	Mann-Whitney t-test	0.1166
	mean proportion	11.33	11.9	t-test with Welch's correction	0.9007
NJ19 #56	median PFU	250	220	Mann-Whitney t-test	0.9243
	mean proportion	36.93	13.88	t-test with Welch's correction	0.0758

No significant difference in nymph IR was determined between POWV isolates (Kruskal-Wallis test). The overall IR averaged 14.7% (range 12.0-18.8) amongst all isolates. Greater IR variation was observed between ticks collected from individual host mice. For NJ19-56, tick IRs between host mice ranged from 4.0 to 47.4% (Fig. 4.3B). Some subtle trends in nymph viral loads were observed between isolates. M11665, NFS9601, and NJ19-56 resulted in an average $4x10^2$ PFU/tick, while ME19-1051 and FA5/12-40 average $1x10^3$ PFU/tick, though this difference is only significant compared to NJ19-56 (Kruskal-Wallis test with Dunn's multiple comparisons; Fig. 4.3C).

Artificial infection of ticks. To determine differences in the ability of isolates to infect the tick without host-dependent viremia, artificial infection using two DTV isolates (NJ19-56 and ME19-1051) was used. *I. scapularis* nymphs were immersed in 10^3 PFU/mL of DTV, fed on naive mice, and allowed to molt to

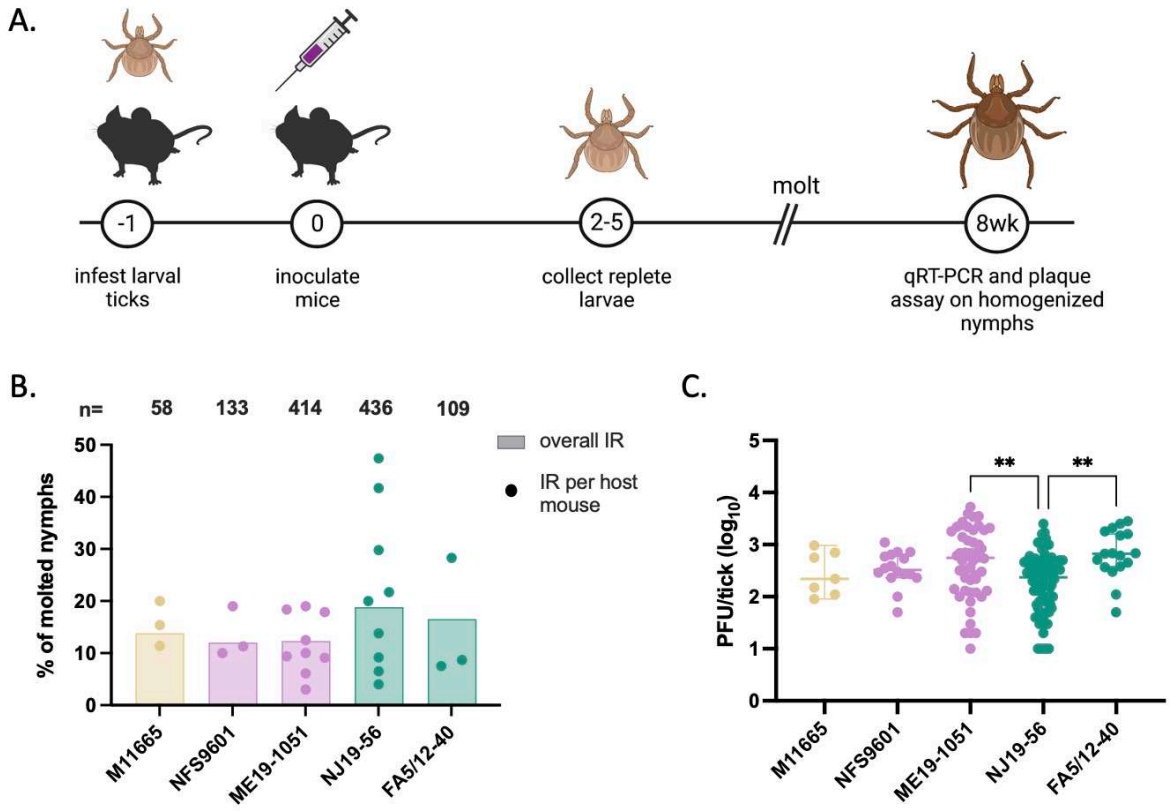

Figure 4.3. Viremic transmission to ticks. A) Methodology of viremic transmission experiments. B) Nymph infection rates per isolate. Colored bar represents overall IR, colored circles represent IR for nymphs fed on the same host mouse. Total n is listed at the top. Kruskal-Wallis test p=0.55 C) Viral load of all nymphs Kruskal-Wallis test **p<= 0.001

adults for eight weeks before processing (Fig. 4.4A). A subset of immersed, unfed nymphs was screened for DTV RNA by qRT-PCR four weeks post-immersion, though only one tick (2.6%) was found positive. Artificial infection of blood-fed nymphs resulted in 15.0-20.5% IR in adults with viral loads averaging $7.5x10^3$ PFU (4.4B and C). Differences between isolates (viral load and IR) were not significant (Kolmogorov-Smirnov test and chi square test respectively) and no differences were determined between male and female infected ticks.

Viremia in BALB/c mice. To assess differences in the ability to establish viremia in the vertebrate host, female BALB/C mice were infected with 10^3 PFU and three mice per isolate were euthanized one, two, and four days post infection (dpi) (Fig. 4.2A). Due to limits of virus detection in the blood, PFU

equivalents were calculated by extrapolation from qRT-PCR standard curves. Viral titers in the blood were highest one dpi around $8x10^2$ PFUeq/mL, dropping roughly ten-fold two dpi and only detected at low levels four dpi. Viral RNA was detected in the spleens of all mice one and two dpi, suggesting all mice from these time points were infected. In the blood, NJ19-56-infected mice demonstrated 100% infection, while virus was detected for two of three ME19-1051-infected mice one and two dpi. NJ19-56 resulted in somewhat higher viremia one dpi, though not statically significant. By four dpi, viral loads in the blood drop off: viral RNA was detected for only one NJ19-56-infected mouse. Virus is detected in the brain four dpi in all NJ19-56 mice and only one ME19-1051 mouse.

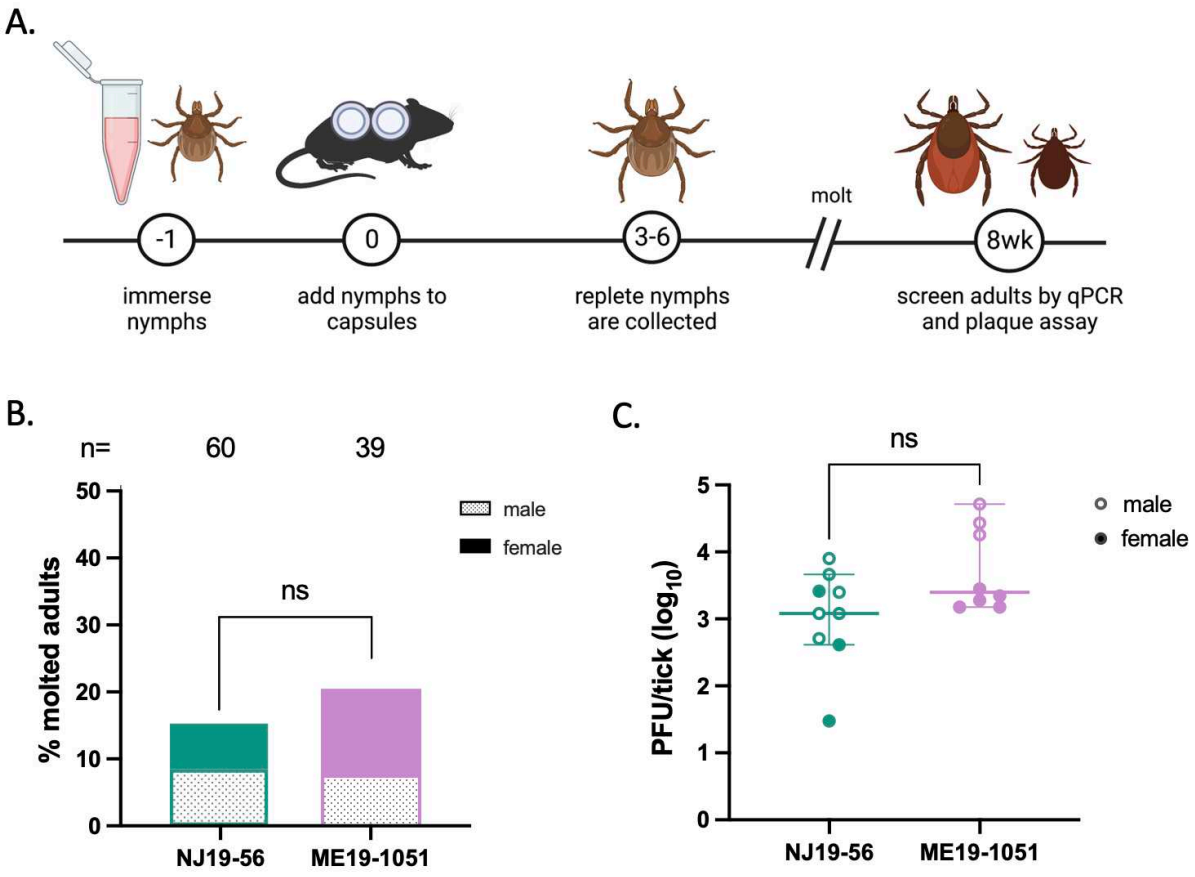

Figure 4.4. Artificial infection of ticks. A) Methodology of artificial infection. B) Adult male and female infection rates per isolate. Total n is listed at the top. Chi square test p= 0.48 C) Viral load of all nymphs Kolmogorov-Smirinov test p=0.56

4.3 Discussion

POWV is an emerging tick-borne virus in North America, which causes cases of human disease predominantly in the Northeast and Midwestern U.S. Though human cases are increasing in the U.S.[14], they are rare compared to reported cases of tick-borne encephalitis virus in Europe and Asia[22]. Thus, the contribution of individual strains to human cases and circulation in ticks is unknown. Genetically diverse

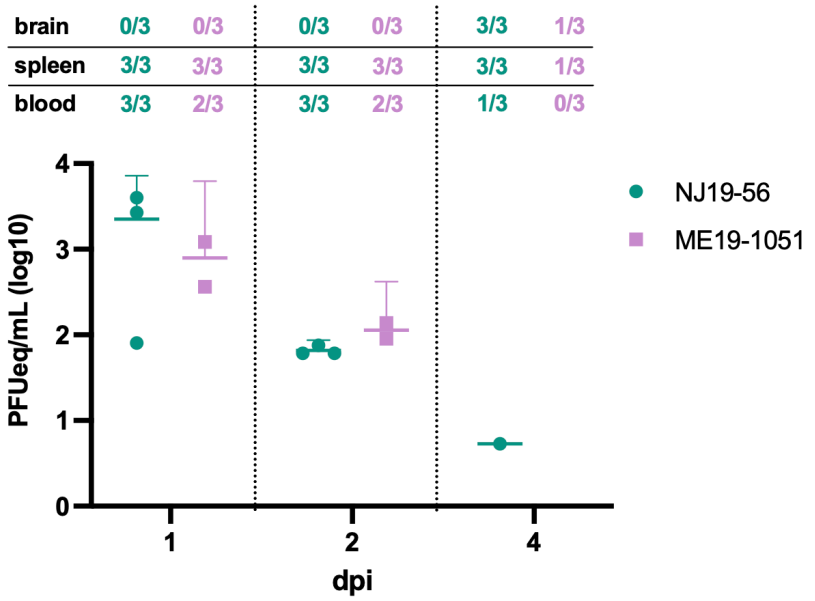

Figure 4.5. Viremia of DTV in BALB/c mice. Blood, brain, and spleen was samples from n=3 mice per isolate on days 1, 2, and 4 post infection. The number of positive mice for each sample type is indicated in the table above the graph.

POWV isolates of different geographic and temporal origin were used in the present study to determine differences in viremia in mice and transmission to *I. scapularis* ticks.

Eleven POWV isolates from a broad geographic and temporal range were used to determine differences in morbidity and mortality between isolates. Both POWV lineages were able to cause neurological disease in mice, although morbidity and mortality varied significantly, even between isolates of the same genetic clade. Mice infected with DTV Midwest strains universally caused severe disease with greater than 50% mortality. Several of these mice developed neurological signs of disease such as ataxia and paralysis. In contrast, mild disease was observed for mice infected with DTV Northeast

isolates, and only one mouse infected with virus from the Northeast subclade (ME19-1051) progressed to paralysis. Mice infected with isolates that originated from Long Island, New York and Nantucket, Massachusetts had almost no clinical signs of disease apart from weight loss, which most mice recovered from in a few days. Interesting, the first case of POWV disease was reported on Long Island in 2022[176], and no cases have thus far been identified on Nantucket. Thus, POWV infection encompasses variable disease outcomes in mice with potential links to location that warrant further investigation.

Five isolates were chosen to further assess pathogenic differences over time. Several differences between isolates were observed in the brain and spleen tissue of infected mice. Virus was detected in the spleens of most mice at all time points, except for M11665-infected mice, where virus was detected only three dpi. NJ19-56-infected mice demonstrated somewhat faster neuroinvasion, also observed in BALB/c mice, which could be linked to the severity of disease. Though some potentially significant strain-dependent differences in pathogenesis were observed, additional studies with greater sample size are needed to validate these results.

Given the observed variability in disease outcomes in mice, we sought to determine differences in the ability to infect ticks. *I. scapularis* ticks were infected via two methods: viremic transmission (feeding on an infected mouse) and artificial infection (via immersion). During viremic transmission, the virus establishes infection in the blood of the host animal and is ingested into the midgut of the engorging tick. Artificial infection removes the variable factor of host viremia; however, blood-feeding is still necessary to induce physiological changes in the tick that promote virus infection[59,177]. This effect was observed in our data as only 2.6% of un-fed nymphs were DTV-positive, compared to 17.8% of blood-fed molted nymphs. Therefore, the combination of viremic and artificial infection allows us to determine the impact of host viremia on infection rate (IR) and assess strain-dependent differences in the ability to infect ticks. Surprisingly, both methods resulted in comparable overall tick IRs 10-20%, similar to previously published data[78]; however tick IR was variable between individual host mice. Artificial infection resulted in somewhat higher viral loads per tick, though this did not seem to increase the likelihood of infection. Given these results, it seems infection acquired by blood-feeding on a live animal can result in variable IR

depending on the individual animal, but that overall infection rate is similar to artificial feeding when results from several animals are aggregated.

Despite significant genetic and ecological variability, the overall tick IR was also similar between isolates, regardless of infection method. This is surprising given the number of barriers a virus must overcome to (1) develop sufficient viremia in the host mouse, (2) establish infection in the tick, and 3) survive the histolysis and rearrangement of tissues that occurs during molting. Potential differences in host viremia were observed between two DTV isolates: ME19-1051 and NJ19-56. NJ19-56 infected mice had somewhat higher, sustained, and more consistent detection of virus in the blood, though these observations were subtle, and did not seem to affect the overall tick IR. Subtle, though statically significant differences were observed in tick viral loads between isolates, and this trend was repeated via artificial infection. The significance of this result is yet to be determined, though may impact viral maintenance or subsequent transmission. As ticks in this study were screened post-molt, all isolates were successfully transstadially transmitted (TST). Though only a small number of larvae were screened immediately post-repletion, the proportion that were virus-positive is similar to the IR in nymphs post-molt, indicating potentially low barriers to TST as previously described[77,78]. Together, these results suggest that mechanisms of POWV infection in *I. scapularis* are not POWV genotype-dependent and are highly conserved. Additional support for this result is given in the ability of POWV to replicate and be transmitted by many tick species including *Dermacentor variabilis*[74], *D. andersoni*[178], *Haemphysalis longicornus*[85], and five known *Ixodes sp.*[179].

We also assessed the infection rate and viral load of male and female ticks via artificial infection. Previously, our group reported significantly more female DTV-positive ticks collected form the Northeast U.S.[114]. Though we did not observe differences in the present data, our sample size is relatively small and could be impacted by the method of infection. Biological factors, such as the difference in sex organs and the size and function of the midgut and salivary glands[150] could influence virus replication and survival. Thus, additional work is needed to determine virus tropism in adult ticks.

There are several limitations and avenues for further investigation based on the described studies. First, many isolates were used to assess pathogenesis and sample size was limited to maintain feasibility. Therefore, the results from these data should be regarded with caution. Inbred laboratory mice were used for experimental tick studies because they produce high numbers of infected ticks to observe differences between isolates, however, they do not represent a natural host. Peromyscus mice are a potentially important host for POWV[8,116], but do not produce high viremia[50]. Thus, virus restriction in these hosts is more severe and may result in differential rates of virus transmission. Though TST was demonstrated, the efficiency of TST could not be determined. Furthermore, viral maintenance in nature may depend more highly on other routes of viral transmission in ticks, such as co-feeding transmission, which were not demonstrated in the present study. Finally, tick infection was determined in whole ticks, thus additional work is needed to determine differences in tissue tropism and oral transmission potential.

We determined strain-dependent differences in pathogenesis, with potential links to geographic location, and consistent rates of infected ticks between diverse viral isolates via viremic and artificial infection. These results demonstrate the presence of low-virulence strains in the U.S.. In addition, the present data highlights POWV as well adapted to survive within ticks, regardless of genotype.

4.4 Materials and Methods

Viruses and plaque assays. BHK cells were grown in DMEM supplemented with 10% FBS and 1% Penicillin/Streptomycin. L929 cells were grown in DMEM supplemented with 5% FBS and 1% Penicillin/Streptomycin. POWV isolates were grown up in BHK cells for 3-6 days and tittered via plaque assay on BHK cells.

Mice and ticks. C57BL/6 (strain #000664) and BALB/c (strain #000651) mice were obtained from Jackson Laboratories. Approval for animal protocols was obtained by the Colorado State University Institutional Animal Care and Use Committee, protocol 1257. Ticks were obtained from the Oklahoma State University tick rearing facility and kept at 24°C with 90-95% RH in glass humid chambers with ~ 2

inches of saturated potassium sulfate. Ticks were kept in 5-dram polystyrene vials with mesh sieve tops. Larval ticks were obtained by allowing replete adult female I. scapularis to oviposit. Eggs were separated into ~200 egg bunches in separate vials and allowed to hatch. Ticks were washed in 70% EtOH and PBS and moved into a clean vial and humid chamber every 3-5 weeks.

Nucleic acid extraction and qRT-PCR. 50µL sample was used for nucleic acid extraction using the Omega viral RNA/DNA kit on a King Fisher robotics platform. qRT-PCR was performed using the EXPRESS One-Step SYBR GreenER kit (Invitrogen) following manufacturer's instructions with 2µL sample volume with the following primers directed towards the NS5 gene: fw: GGCCATGACAGACACAACAGCGTT TG and POWV rv: GAGCGCTCTTCATCCACCAGGTTCC. Melt curves were used to confirm true POWV positives over background.

Morbidity and mortality studies. 8-week-old C57BL/6 mice were subcutaneously inoculated with $1x10^3$ PFU virus, n=4 per isolate housed in the same cage. Mice were weighed and scored daily and euthanized if they reached a clinical score of 3 or greater. Animal studies were approved by the IACUC review board under protocol 1257. Typical flavivirus scoring was used: (0) no signs, (1) ruffled fur, (2) hunched posture, (3) tremors, ataxia, weakness, (4) paralysis, (5) moribund. At euthanasia, blood, brain, kidney, and spleen was collected and frozen at -80C until processing. Morbidity and mortality studies of male and female mice for all isolates were performed at Tufts University veterinary campus in North Grafton, Massachusetts. Repeat study to assess sex-differences with FA5/12-40 was performed at Colorado State University in Fort Collins, CO. Tissue was weighed (g) and 10x volume tick diluent was added. Tissue was bead homogenized at 30 hertz for 2 minutes, spun at 10,000 rcf for 5 minutes, and used for RNA extraction and plaque assay.

Pathogenesis time course. 8-week-old male C57BL/6 mice were subcutaneously inoculated with $1x10^3$ PFU, n=16 mice per isolate. Mice were weighed and scored daily as described and euthanized if they met criteria as described above. n=4 mice per isolate were euthanized on 3, 6, 9, and 12 dpi. At euthanasia, blood, brain, kidney, and spleen were collected and processed as described above. Pathogenesis study was performed at Tufts University veterinary campus in North Grafton, Massachusetts.

Viremic transmission. Larval ticks (separated into vials with ~200 larvae) were used to infest 15-week-old female BALB/C mice. During infestation, mice were restrained in plastic restrainers and their tail was taped to prevent them from escaping. A single vial of larval *I. scapularis* were added to the nape and upper back of each mouse. The infested mouse was kept in the restrainer, loosely wrapped in paper towels and placed in secondary containment for 30 minutes. Mice were housed individually in wire-bottom cages with ~1/2 inch of water placed in the bottom during the study. The next day (day 1), mice were inoculated intraperitonially with $1x10^4$ or $1x10^3$ PFU. Cage water was changed daily. Blood was collected via retro-orbital bleed on day 4 post infestation. As larval ticks became replete, they were collected from the water, surface sterilized in 70% EtOH and PBS and homogenized immediately or moved into 5-dram vials to be held as described above until they molted to nymphs. Eight weeks post repletion, molted nymphs were bead homogenized in tick diluent (200µL PBS supplemented with 20% FBS, 1% Penicillin/streptomycin, 2.5ug/mL amphotericin B, 50ug/mL gentamicin) at 24Hz for 2 minutes. POWV infection was determined by qRT-PCR and plaque assay as described above.

Immersion infection method. Nymphal *I. scapularis* ticks were dehydrated overnight at 26°C at ~45% RH. Nymphs were immersed the next day (day -1) in 4mL of 1e3 PFU/mL POWV for 1 hour at 37C with light vortexing every ten minutes. Ticks were washed twice in PBS and moved into a ventilated tube to dry overnight. Foam capsules were made as previously described (CITE JOVE) with 20mm outer diameter and 12.5mm inner diameter. The backs of 10-week-old male BALB/C mice were closely shaved

and wiped with 70% EtOH. Two foam capsules were fixed on day -1 to each mouse with non-toxic leather adhesive (Tear Mender). One capsule was placed on the nape and the second was placed immediately posterior near the middle back. Capsule attachment was checked daily and patched with glue if needed. The next day (day 0), 15-20 immersed nymphs were added to capsules. Infested nymphs were checked daily and removed from the capsule when replete by cutting open the plastic capsule top and re-sealing with plastic stickers as previously described (CITE JOVE). Nymphs were left to molt in humid chambers as previously described. Two weeks after the start of molting, nymphs were homogenized as described above and screened via qRT-PCR and plaque assay.

Mouse viremia time course. 15-week-old BALB/C female mice were inoculated intraperitoneally with $1x10^4$ PFU. Three mice were euthanized for each isolate at days 1, 2, and 4. Brain, spleen and blood was collected. Brain and spleen tissue were homogenized in 10% weight/volume of tick diluent at 30Hz for 2minutes. RNA extraction and qRT-PCR was performed as described above. DTV infection was determined through qRT-PCR and plaque assay. PFU equivalents were determined through serial dilution of stock RNA via qPCR.

CHAPTER 5: EFFICIACY OF MOSQUITO-ENABLED XENOSURVEILLANCE IN GUATEMALA

5.1 Introduction

The ability to rapidly detect circulating pathogens in remote, resource-limited areas is inhibited by a lack of surveillance infrastructure. Rural populations with limited access to health care and biomedical support are frequently excluded from traditional surveillance methods due to extreme logistical complexities[180,181]. Noninvasive surveillance in these settings could have a significant impact by enabling early detection of viruses. Xenosurveillance is a novel surveillance approach that takes advantage of mosquito feeding behavior to identify blood-borne pathogens that may be circulating in human and animal hosts. This approach circumvents invasive blood sampling of individuals and results in an abundant sample source derived from both humans and animals. We therefore have proposed that xenosurveillance may be a useful method for disease surveillance in rural, resource-limited areas.

The detection of bacteria, viruses, and parasites from mosquito bloodmeals via membrane and animal blood feeding has been previously demonstrated[124,126,182]. Using field-caught blood-fed *Anopheles* mosquitoes from Liberia and Senegal, we previously detected non-mosquito-borne viruses such as canine distemper virus, Epstein-Barr virus, GB virus C, and Hepatitis B virus[132,182]. The utility of this approach in the American tropics, however, where the main human-biting mosquitoes are *Aedes* and *Culex*, not *Anopheles*, has not been addressed.

Accordingly, in the present study, we evaluated the utility of xenosurveillance in rural southwest Guatemala, where *Culex* and *Aedes* mosquitoes are highly abundant. We conducted xenosurveillance and human-directed biosurveillance in parallel to evaluate the logistical and technical feasibility to detect circulating blood-borne pathogens in humans over the course of a four-month study. We also determined the species composition of mosquitoes collected from within Guatemalan dwellings and their host feeding preferences.

5.2 Results

Study demographics and risk factors. Two communities in rural southwest Guatemala were targeted for participation in this study: Los Encuentros and Chiquirines. Of 37 households screened for participation, 32 (86.5%) were eligible, 20 (62.5%) were enrolled (10 from each village), and 19 (95.0%) completed the study. Households that were not enrolled either did not meet the enrollment requirements (13.5%) or declined to participate (32.4%). Of enrolled households, nearly all dwellings consisted of cement block structures without screened windows or doors. All households had open water wells or tanks on the property, and many had additional sources of standing water (potted plants, tires, natural water); 50.0% of households did not have a septic system (Table S3).

Households had a median of 4.5 people enrolled; 46.7% were under the age of 18 and 60.2% were female (Table 5.1). Animals were abundant in households (IQR 16-34 per household) and often found in and around the home. The most abundant animal were chickens (55% of all animals, excluding humans), though pigs, dogs, cats, and horses were also present (Table S4).

Table 5.1. Demographics and reported symptoms of study participants.

	Los Encuentros	Chiquirines	Total
Demographic characteristics			
Households, N	10	10	20
Median participants per household [IQR]	4.5 [3,6]	4.5 [4,6]	4.5 [3,6]
Participants, N	49	49	98
Children <18yo, N (%)	25 (51.0)	21 (42.9)	46 (46.9)
Female, N (%)	29 (59.2)	30 (61.2)	59 (60.2)
Median age [IQR]	17 [9,32]	19 [7,37]	18.5 [9,36]
Reported symptoms			
Episodes, N subjects (N households)	15 (10)	5 (5)	20 (15)
Fever, N (%)	13 (86.7)	4 (80.0)	17 (85.0)
Rash, N (%)	2 (13.3)	1 (20.0)	3 (15.0)
Body aches, N (%)	9 (60.0)	1 (20.0)	10 (50.0)

Symptomatic episodes and samples collected. During 16 weeks of observation, there were 15 symptomatic episodes, all of which included at least one report of fever, rash, or body aches. Seven of fifteen episodes reported more than one symptom, and symptoms were reported in multiple household

members for four episodes. Two households reported illness in two separate episodes, and a single household reported three instances of febrile illness. Most of the reported illness (15 of 20 reported episodes) occurred in Los Encuentros (Tables 5.1, 5.2). Including enrollment, 1,200 mosquitoes were collected during the study, 507 (42.3%; Fig. 5.1, Table 5.2) of which appeared to have taken a bloodmeal in the past 36 hours observed by a dark red/black bloated abdomen[183,184]. Indoor mosquitoes were most abundantly collected at the end of the rainy season (September-October) (Fig. 5.1); 488 of 517 (94.4%) blood-fed mosquito samples were speciated by PCR. *Culex, Aedes, Mansonia, Anopheles, and Psorophora* mosquitoes were collected, though *Culex pipiens* was by far the most abundant (60.9%) (Table 5.3).

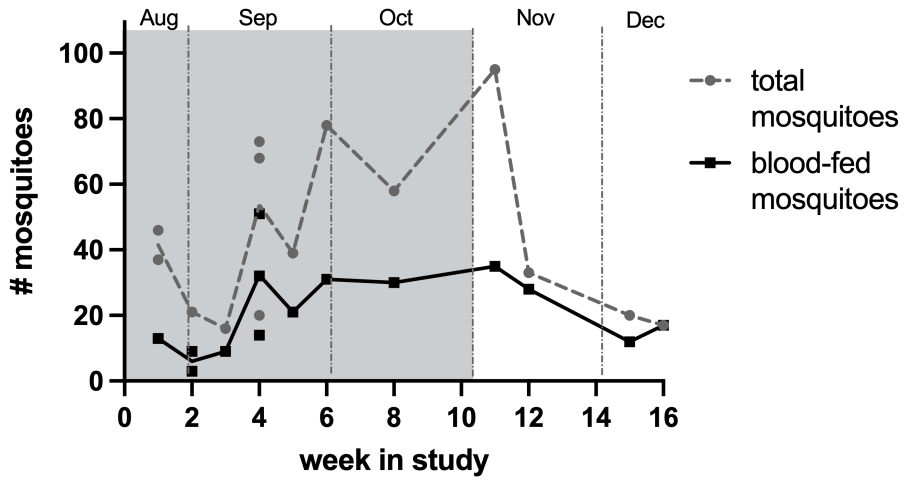

Figure 5.1. Total and blood-fed mosquitoes collected increases over rainy season. Total mosquitoes collected per household during symptomatic episodes over the 16-week study (gray dashed). Blood-fed mosquitoes collected per household (black solid). Rainy season indicated by shaded background.

Table 5.2. Symptoms reported in each household over 16 weeks. NR = not reported

Week	Village	Household ID	Subjects with fever	Subjects with rash	Subjects with body aches	Human subject blood samples taken	Blood-fed mosquitoes collected
enroll	Los Encuentros	all	NR	NR	NR	49	105
	Chiquirines	all	NR	NR	NR	49	84
1	Los Encuentros	1007	1			6	13
	Chiquirines	2013	1		1	5	13
2	Los Encuentros	1001	1			4	9
	Chiquirines	2002	1			7	3
3	Los Encuentros	1016	1		1	6	9
4	Los Encuentros	1019			1	6	51
	Chiquirines	2012		1		4	32
	Chiquirines	2014	1			2	14
5	Los Encuentros	1003	1		1	3	21
6	Los Encuentros	1002	2	1	1	7	31
7						0	0
8	Los Encuentros	1001	2		2	4	30
9						0	0
10						0	0
11	Los Encuentros	1019		1		6	35
12	Chiquirines	2002	1			4	28
13						0	0
14						0	0
15	Los Encuentros	1020	2		1	4	12
16	Los Encuentros	1019	3		2	5	17
TOTAL			17	3	10	171	507

Table 5.3. Mosquito species identified during course of study. 488 of 507 (96.3%) were able to be species-identified by COI sequencing.

	Los Encuentros	Chiquirines	Sum (% of identified)
Aedes aegypti	61	30	91 (18.6)
Aedes albopictus	2	1	3 (0.6)
Aedes taeniorhynchus	0	3	3 (0.6)
Anopheles sp.	0	2	2 (0.4)
Anopheles albimanus	3	5	8 (1.6)
Culex sp.	36	14	50 (10.2)
Culex nigripalpus	9	1	10 (2.0)
Culex pipiens	194	103	297 (60.9)
Mansonia dyari	11	9	20 (4.1)
Mansonia titilans	1	1	2 (0.4)
Psorophora ferox	2	0	2 (0.4)
Total identified	319	169	488

Mosquito abundance and bloodmeal identification. Five genera of mosquitoes were identified: *Culex, Aedes, Mansonia, Anopheles,* and *Psorophora. Culex* mosquitoes were most abundantly identified as *Cx. pipiens* though *Cx. nigripalpus* also were collected. *Aedes* mosquitoes included *Ae. aegypti, Ae. taeniorhynchus,* and *Ae. albopictus,* from highest to least abundant (Table S5.5). *Cx. pipiens* and *Ae. aegypti* were the most frequently collected species, accounting for 60.9% and 18.6% of identified mosquitoes respectively (Table 5.3). To identify mosquito bloodmeal sources, we used a previously described protocol to amplify and sequence vertebrate cytochrome oxidase 1 (CO1) sequences. We successfully amplified 464 of 488 (95.1%) total bloodmeal samples, indicated by the presence of a band corresponding to ~800 base pairs on an agarose gel. In total, 343 of 488 (70.3%) amplified samples were able to be host-identified. Unidentified samples were a result of poor sequencing results, indicating potential mixed hosts (i.e. mosquito feeding on multiple species). Of the 343 identified mosquito bloodmeal samples, our results demonstrate that humans and chickens were the most common sources of blood, accounting for 32.6% and 31.8% of identified bloodmeals respectively. All mosquito genera (excluding *Psorophora* which had no identified bloodmeals) fed upon humans. *Culex pipiens* fed most

abundantly on chickens and other avian hosts, while *Aedes aegypti* fed mainly upon humans (Fig. 5.2 and Table S5.5).

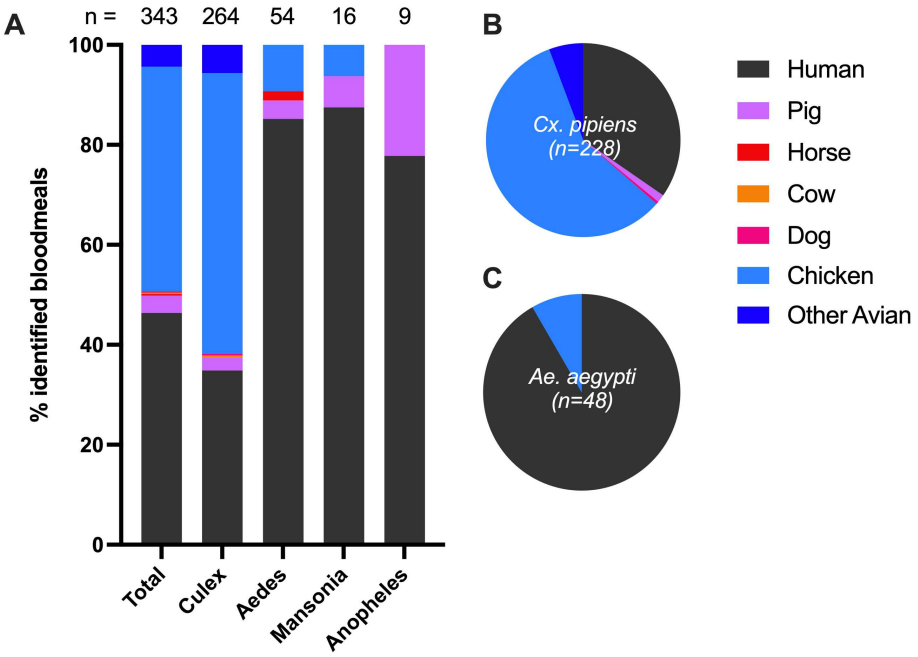

Figure 5.2. Many bloodmeals obtained from avian species due to large numbers of *Cx. pipiens*. Amplification and sequencing of the Cytochrome oxidase 1 gene was performed as described and blasted against the Barcode of Life database. A total of 343 of 488 (70.3%) species-identified mosquito samples were able to be traced to a single host source. A) Percent of mosquito bloodmeals identified as mammal or avian host sources for each mosquito species. B) Percent of all identified host sources *Cx pipiens* mosquito bloodmeals. C) Percent of all identified host sources of *Ae. aegypti* mosquito bloodmeals.

Virus identification in human and mosquito dried blood spots. Human and mosquito dried blood spots (hereto referred as H-DBS and M-DBS) collected during seven symptomatic episodes were used to identify viral agents using a shotgun metagenomic sequencing approach (Table S5.1). Retrospective bloodmeal analysis of the mosquitoes used for sequencing revealed 33.0% M-DBS derived from human hosts. To increase our sensitivity of detection using the SISPA method, all libraries underwent a high degree of amplification, thus even FTA and water control libraries produced reads from spurious sequence contaminants (Fig. 5.3A). No human or animal viruses were detected in any library except in HeLa cells, which are stably infected with human papilloma virus and act as a control for virus detection. Insect-specific viruses were detected in H-DBS, water, and FTA control libraries though did not exceed

27 identified reads. Thus, a threshold of 30 reads was used to identify viruses that were present above background. Many insect-specific viruses (ISVs) were detected at high levels in M-DBS (Figs. 5.3B and 5.3C). The most abundantly identified ISVs were Culex orthophasma virus (COPV; Phasmaviridae, previously known as Culex phasma-like virus[185]) and Hubei reo-like virus 7 (HRLV7; Reoviridae-like). Terena virus (TV; unclassified Bunyavirales-like) was also abundantly detected. However, upon validation of identified ISVs, we found 100% of reads identified as TV mapped to the COPV reference genome with 97.7% identity. We then discovered the S and M genes of TV are 99.1% and 99.3% identical to COPV, respectively. Reads identified as TV were therefore re-attributed to COPV. Pooled reads from M-DBS resulted in 98.6% identity (98.9% coverage) to the COPV reference genome (Table S2). qPCR for COPV was used to validate these results and screen the remaining M-DBS samples. Estimated prevalence for COPV was 24.6% [95% CI 18.0, 32.5] based on 60/67 positive pools (507 total samples)[186]. H-DBS were negative for COPV by qRT-PCR. During the time of our study, dengue virus 2 and 3 (DENV 2/3) were circulating in the region. However, DENV 2/3 was not detected in either H-DBS or M-DBS via shotgun metagenomic sequencing or qRT-PCR.

5.3 Discussion

The rise of global pandemics, coupled with the complexity and uncertainty associated with predicting pathogen emergence, emphasizes the need for minimally invasive, accessible, low-cost surveillance methods that are applicable under field conditions. We therefore evaluated xenosurveillance in rural Guatemala, a region that is of interest for three principal reasons. First, it is a region that has a high burden of infectious diseases with significant needs for and barriers to effective health surveillance[187]. Second, there is a high rate of human migration within and through the region, providing an important sentinel population for emerging infectious disease surveillance[187]. Finally, and perhaps most importantly, the region is quite different from those where we have previously conducted pilot studies of xenosurveillance, in that *Culex* and *Aedes* mosquitoes, which tend to be less anthropophilic

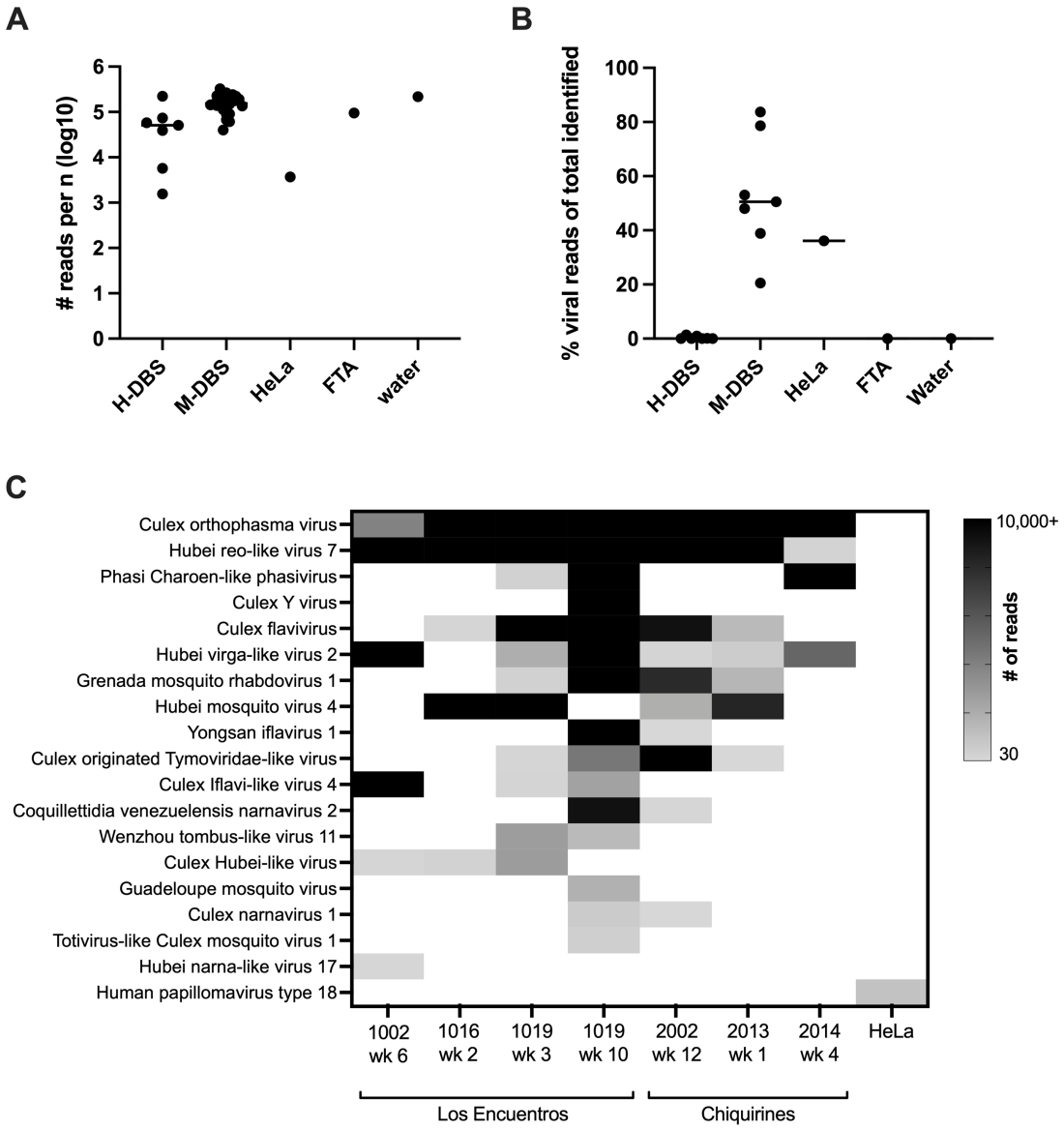

Figure 5.3. Shotgun metagenomic sequencing reveals many ISVs but no human viruses. Extracted DBS nucleic acid were pooled by volume according to household, collection time, and type (human or mosquito) in addition to water, FTA, and HeLa cell controls. Shotgun metagenomic sequencing libraries were created and obtained sequencing reads were run through a Taxonomic Assessment pipeline as described. Viral reads were tallied by unique taxonomic ID. A) Total number of reads obtained per n in sample for each library type. B) Proportion of identified reads aligning at the super-kingdom level to viruses. C) Virus read tallies (excluding phage) in mosquito libraries with a cutoff value of 30 hits.

compared to *Anopheles gambiae*, are the main mosquitoes that fed on humans indoors. Therefore, we sought to assess the extent to which xenosurveillance may be effective in this type of environment.

Twenty households were enrolled from two villages in rural southwest Guatemala that are a representative sample of households that is typical for the region where we conducted the study[187]. Nineteen (95%) households remained in the study for the full duration (16 weeks). A total of 98 people (average 4.5 people per household) participated in the study resulting in 171 H-DBS and 507 M-DBS. More females than males (60.2%), and slightly more adults than children (53%) participated as many of the men and children were at work or school during the day.

We collected and identified several mosquito genera, including *Culex, Aedes, Mansonia, Anopeheles*, and *Psorophora*. *Culex pipiens* were most abundant and fed mainly on birds, while *Ae. aegypti* fed mostly on humans. Thus, the feeding patterns of *Cx. pipiens* and *Ae. aegypti* at our site are typical for these species[188,189]. The disproportionate number of *Culex* samples skewed our blood samples towards those derived from birds, in contrast to our prior study in which *An. gambiae*[132] accounted for 80% of the collection and strongly prefer to feed on humans. These observations present challenges and opportunities for implementation of xenosurveillance in Latin America – more intensive sampling may be required to adequately capture human infection, but surveillance of domestic and peri-domestic animals may be enhanced.

Analysis of M and H-DBS revealed no human viruses present, in contrast to prior detection of human viruses (GB-virus C, Epstein-Barr virus and Hepatitis B virus) from *Anopheles* bloodmeals in Liberia[132,182]. There are many factors that likely contributed to the lack of human virus detection in the present study. First, the number of blood-fed mosquitoes was not sufficient for virus detection in humans. As previously described, the abundance of *Cx. pipiens* in this study limited the retrieval of human-sourced mosquito bloodmeals as the majority were derived from chickens and other birds. In addition, multiple samples are likely needed to adequately detect blood-borne viruses from any one individual[123], though the absence of viruses detected in H-DBS suggests circulating bloodborne viruses were not present at the

time of collection. Second, symptom surveillance was done once weekly resulting in samples that were not collected at the time of illness. We may therefore have missed critical windows where mosquitoes may have sampled circulating viremia[190]. Third, mosquitoes were not collected in the very early morning hours, which could limit collection of fresh bloodmeals from mosquitoes that fed overnight. However, stable detection of viral RNA from *Anopheles* mosquito bloodmeals over 12 hours post blood-feeding has been previously shown[124,126,182]. Viral RNA also has been detected from Culex and Aedes bloodmeals immediately post blood-feeding[123]. Although the stability of viral RNA over time in these vectors has not yet been shown, it seems reasonable to expect that it would be similar across mosquito genera. Finally, virus discovery was performed on a chosen subset of samples, and thus could result in missed human viruses. Collectively, these results suggest that efficient detection of human pathogens in this setting may require more frequent and abundant sampling or were not circulating at detectable levels.

Though no human viruses were detected, analysis of M-DBS revealed the presence of ISVs. The detection of ISVs was expected as excretion of the mosquito bloodmeal onto FTA cards is accompanied by mosquito tissues (e.g. the midgut) that may be infected by ISVs. ISVs have been described in xenosurveillance-based studies published previously[191] and provide an additional internal control for our ability to detect viral RNA by our sample processing and analysis procedures. We found several ISVs that were highly abundant in M-DBS, including COPV and HRLV7. TV was also identified, though upon further analysis, we found reads mapped solely to regions that were highly identical to COPV, thus we re-attributed TV-identified reads as COPV. COPV has been identified in a number of *Culex* mosquito collections in Australia[192], Brazil[193,194], and Grenada[192]. Similarly, HRLV7 has been described in both *Aedes* and *Culex* mosquitoes on three continents including this study[195,196]. There have been a few recent studies showing decreased vector competence and replication of pathogenic flaviviruses after cells or mosquitoes undergo primary infection with ISVs[197,198]. Despite the clear abundance of these ISVs around the world, there is currently comparatively little information on how they affect mosquito biology, arbovirus evolution, and pathogen transmission.

During this study, we identified several benefits and challenges in conducting xenosurveillance in Guatemala. We were successful in enrolling and maintaining a household cohort for this 4-month study. This was facilitated by The UC Center for Human Development, which has developed a good relationship with the surrounding communities. Notably, all household enrollments, interviews, sampling of blood and mosquitoes, and mosquito identification was performed by locally trained Guatemalan study nurses, highlighting the importance of developing local connections and expertise to conduct surveillance efficiently. We collected numerous blood-fed mosquitoes for this study using the Insectazooka, though mosquitoes were somewhat damaged, which makes species identification difficult and error-prone without extensive training and processing time. We were successful in detecting viral RNA from M-DBS, though more frequent sampling, or targeted detection of human pathogens, is needed.

In summary, xenosurveillance has some potential as a useful surveillance strategy in LMICs; however, mitigating the described challenges and maximizing the unique opportunities presented by the lack of host-specificity of most human-biting mosquitoes in Guatemala requires further work and development. In particular, the frequency of mosquito collection and feeding behavior (including the peak feeding times and host preferences) should be carefully considered. Building local capacity for beginning to end sample processing and analysis would ultimately benefit the application of this surveillance method. Technologies such as nanopore sequencing (Oxford Nanopore Technologies) and BioFire (BioFire Diagnostics) could be useful tools for on-site virus identification. We therefore foresee xenosurveillance being useful as a targeted approach in regions where zoonotic outbreaks are inevitable, and our evidence suggests that abundant and frequent sample sources are essential for early detection of circulating pathogens.

5.4 Materials and Methods

Study site. This study was performed through The Center for Human Development located in the coastal lowlands of southwestern Guatemala, approximately 20 km from the border with Chiapas, Mexico[187]. The

population in the region suffers from high levels of food insecurity, poverty, and poor access to health care, and diarrheal, respiratory, and other communicable diseases are frequent, especially in children[187,199]. Many households use pit latrines, which can flood during heavy rain and create ideal environments for mosquito breeding. Chickens, ducks, pigs, rats, dogs, and cats are common in households and have close contact with families.

Study design/enrollment. Twenty households from two villages, Los Encuentros and Chiquirines, adjacent to the Center for Human Development, were enrolled in August 2019. Requirements for enrollment included at least 3 animals in the household, and ability and willingness to consent. Once consent was obtained, capillary blood samples of all enrolled humans in addition to mosquito bloodmeals (described below) were collected at enrollment. We also collected epidemiologic data, including demographics, animals (indoor, outdoor, grazing), and risk factors for infection (water features, septic system, mosquito exposure, contact with animals, etc) through participant interviews. The study was approved by the Colorado Multiple Institutional Review Board (COMIRB) and the University del Valle de Guatemala (UVG) Ethics Committee. The local Community Advisory Board for Research agreed to the study. The protocols for blood extraction and animal handling were approved by the Colorado State University Institutional Animal Care and Use Committee (IACUC; Protocol #1091) and by the UVG IACUC (Protocol #I-2019).

Prospective Syndromic Surveillance. From August 22 to December 12, 2019, study nurses contacted (in person or over the phone if not home) enrolled households weekly to survey for the presence of fever, rash, or body aches in household members at any point over the week. If symptoms were present in any household member, human capillary blood and mosquito bloodmeals were collected at time of screening as described below. The study team was prepared to provide supportive medications to symptomatic household members and triage individuals to higher levels of care if they exhibited World Health Organization (WHO) danger signs[200]. However, no such danger signs were observed over the course of the study.

Sample Collection and Pre-processing. Human and mosquito samples were collected at enrollment and during symptomatic illness as described above. Mosquito bloodmeals: Local technicians were trained on mosquito collection, identification, and sample processing methods prior to the start of the study. Mosquitoes were collected using an InsectaZooka aspirator (BioQuip Products, Rancho Dominguez, California, USA) from the indoor areas of enrolled households, specifically targeting resting blood-fed mosquitoes on the walls and surfaces. Attempts to collect mosquitoes were usually made in the morning and placed in a -20°C freezer for at least two hours or overnight to ensure death and processed within 24 hours of collection. Blood-fed mosquitoes (female) were identified according to a simplified version of a previously published key for mosquitoes in Guatemala[201] and individual mosquito bloodmeals were expressed onto Whatman FTA cards. Forceps were dipped in ethanol and wiped clean between each mosquito. 50µL RNAlater® was added to each mosquito dried blood spot (M-DBS) at the end of each processing session. Human capillary blood: Blood was collected from all members of the household during enrollment and when a febrile illness occurred in the household. The subject's index finger was disinfected with an alcohol swab before using a sterile lancet to prick the finger. Blood was expressed from the finger and dabbed onto a labeled Whatman FTA card. 100µL RNA later was added to each human dried blood spot (H-DBS) by the end of the day. FTA cards were stored at -80°C until they were shipped (at room temperature) to Colorado State University where they were again stored at -80°C until further processing.

RNA/DNA extraction. H and M-DBS were removed using a Harris three-millimeter micro-puncher (GE Healthcare Life Sciences) and soaked in 70µL RNA rapid extract solution for 8-18 hours at 4°C. 50µL was subsequently used for nucleic acid extraction using the Mag-Bind Viral DNA/RNA kit with the King Fisher Flex Magnetic Particle Processor according to the manufacturer's protocol. Nucleic acid was eluted in 50µL nuclease-free water and stored at -80°C until processing.

Mosquito speciation and bloodmeal identification. Mosquito species were verified by PCR and sanger sequencing using primers directed against the cytochrome oxidase I gene as described previously[202]. To

identify the mosquito bloodmeal host source, Cytochrome Oxidase I (COI) DNA was PCR amplified with M13-tagged primers as previously described[203]. PCR products were separated on an agarose gel and the corresponding ~800bp piece was excised. DNA was purified using the Macherey Nagel DNA purification kit and Sanger sequenced with M13 primers. Obtained sequences were trimmed for quality and blasted against the Barcode of Life COI database[204] to identify the bloodmeal source. Samples with no visible band or poor-quality sequencing were re-run before being designated as 'No Match'.

Shotgun metagenomic sequencing library preparation. A subset of H and M-DBS were chosen to identify circulating viruses using shotgun metagenomic sequencing. Sample sets (all DBS from a household collection event) were chosen based on the week in study, number of symptomatic individuals, number of mosquito samples, and recurrent sampling events. DBS nucleic acid samples were pooled by volume according to time of collection, and household. A total of seven human and seven mosquito libraries were generated and sequenced along with water and a blank extracted FTA card as negative controls (Table S5.1). RNA extracted from HeLa cells was used as a positive control for virus detection. Solid Phase Reversible Immobilization (SPRI) bead clean-up was used between each step in the following library preparation procotol. Samples were DNAse-treated and rRNA-depleted using methods described previously[205]. Previously designed mosquito probes[205] were used on M-DBS and human probes (NEB) were used on H-DBS and HeLa cell RNA control. Water and FTA negative controls received both human and mosquito probes. The SISPA (sequence-independent, single primer amplification) method was used to generate and amplify cDNA as described previously[206]. Briefly, cDNA was created via the Superscript IV First-Strand Synthesis System (Invitrogen) following the standard protocol, except for the use of tagged random primers: CATAGTCGTACGTATACATC-(Nx12). Second strand synthesis was performed using a Klenow DNA polymerase I fragment (NEB). Primers aligning to the above tag were used to amplify dsDNA fragments and increase sensitivity of detection. Libraries approximately 300 base pairs in length were prepared using the Nextera XT DNA Sample Preparation kit (Illumina). Dual-indexed libraries were pooled together using DNA concentration measured with a Qubit Fluorometer

(ThermoFisher) and normalized for the number of individual samples included in each library. Size and quality of the pooled libraries were determined using the TapeStation high sensitivity DNA system (Agilent). A final concentration was determined via library quantification qPCR (NEB) and the pooled library was sent to Genomics and Microarray Core at the University of Colorado Denver Cancer Center for 2x150 paired-end sequencing on an Illumina NovaSeq6000 platform.

Shotgun metagenomic sequencing analysis. Shotgun metagenomic sequencing datasets were processed to identify and tally viral reads. An existing taxonomic identification pipeline was modified for use in this study[132,191,207]. Reads were quality assessed using FastQC[208]. Low quality, adapter, and SISPA sequences were removed using cutadapt tool version 1.14[209]. The CD-HIT-EST tool version 4.6.8 was used to remove PCR duplicates[210]. FastQC was again used to assess sequence quality post trimming and filtering. Human and mosquito bowtie indices were created to remove host reads using Bowtie version 2.2.9. The human index (GRCh38.p3) was used on H-DBS and HeLa cell libraries. The mosquito index was created using 4 mosquito genomes (*Ae. aegypti* GCF_002204515.2, *Ae. albopictus* GCA_006496715.1, *Anopheles darlingi* GCA_000211455.3, *C. pipiens* GCF_000209185.1) and was used to filter M-DBS libraries. No host filtering was done on water and FTA negative control libraries. The remaining reads were assembled using SPAdes genome assembler version 3.6.1[211]. Contigs and non-assembled reads were taxonomically assigned using the BLASTn alignment tool version 2.9.0+[212,213]. Taxonomic assignment was based on the highest alignment score and an E value less than 10^{-8}. If not able to be taxonomically assigned based on nucleotide sequence, DIAMOND version 0.9.30 was used to search reads against the NCBI nr database[214]. Identified viral sequences (excluding phage) were tallied according to NCBI taxonomic ID with a minimum cutoff of 30 hits. Taxonomic identifications were validated by re-blasting contigs (NCBI BLAST nucleotide) and mapping reads to indexed reference genomes using Bowtie vs 2.2.9 (Table S2).

Sample screening by qRT-PCR. H and M- DBS nucleic acid samples were pooled by volume (n=8 per pool) before screening. qPCR was run using the Express SuperMix Universal One Step system

(Invitrogen) on an Applied Biosystems Quant Studio machine according to manufacturer's instructions. The following primers and probes were used: DENV-2 primers as previously described[215], DENV-3 fw TGGCAACAGGTCCCTTTCTG, DENV-3 rev TGGCGTTGGATGCTAGTCTAAGA, COPV fw TGCAATCAAGAGCCATACAGACT, COPV rev TCGTCCACACTGGTACCCA. DENV-3 primer sequences were kindly provided by Dr. Laura St. Clair and Dr. Rushika Perrera (Colorado State University). DENV-2 and DENV-3 positive controls were provided by Dr. Irma Sanchez (Colorado State University). Melt curves were used to determine the validity of all amplified products.

CHAPTER 6: SUMMARY AND FUTURE CONSIDERATIONS

Powassan virus (POWV) is an emerging tick-borne flavivirus in North America. The contribution of individual strains to increasing human cases has not been described and the determination of POWV disease and tick transmission phenotypes have so far relied on few highly passaged and historical isolates. Therefore, strain-dependent differences in pathogenicity and transmission in ticks is sorely needed. Our first goal for this dissertation was to determine the scope of disease and tick transmission phenotypes for contemporary, low-passage, genetically and geographically diverse POWV isolates.

In our first study, we assessed the phylodynamics of deer tick virus (DTV) in the Northeast U.S. using whole-genome sequences from field-collected ticks and observed evidence of geographic dispersal and multiple stable foci of infection. We then estimated the effective population size over time using Coalescent Extended Bayesian Skyline and confirmed the expansion of deer tick virus in North America over the past 50 years. From field-collected *I. scapularis* ticks, we obtained 14 contemporary DTV isolates for use in experimental studies.

Our next studies began to characterize the scope of POWV pathogenicity *in vitro*. Specifically, we quantified the replication and cytopathic effects of 16 POWV and DTV isolates in human neuroblastoma cells. We observed extensive replication diversity between all genetic clades of POWV, and identified two isolates that are significantly less cytopathic to human neuronal cells. To identify potential genotypes determinants of phenotypes, we performed metagenomic sequencing pre- and post-culture. Although we could not determine genotypes responsible for the observed phenotypes, we did identify two genetic changes in the viral envelope coding region that each arose in multiple isolates post-culture, warranting further investigation. Overall, we concluded that replication and cytopathogenicity of POWV in human neuroblastoma cells is highly variable and not currently attributable to a key set of viral genetic determinants.

In building off our *in vitro* results, we sought to determine pathogenicity in mice and transmission to ticks. We first monitored morbidity and mortality in mice using eleven POWV and DTV isolates. We

found that both virus lineages resulted in neurological disease with varying severity and noted potential links to geographic location. In the second portion of our *in vivo* study, we investigated differences between isolates in their ability to infect *I. scapularis* ticks. We did this using two infection methods: viremic transmission (feeding on infected mice), and artificial infection (immersion). We observed similar tick infection rates across all five POWV isolates tested, regardless of infection method. Altogether, these results demonstrate the presence of low-virulence strains in the U.S. and suggest the ability of POWV to infect ticks may not be highly genotype dependent.

These data presented in this dissertation were obtained using 20 POWV and DTV isolates spanning over 62 years and 12 locations and sourced from tick and human samples. Although this approach was necessary to develop a better understanding of POWV ecology, pathogenicity, and tick transmission, the use of so many isolates limited our sample size and therefore, statistical power, especially given the variability in environmental isolates. Nevertheless, we observed many interesting trends between and among isolates that lead to many additional questions about POWV ecology in North America. Specifically, is there evidence of undetected human infections due to low-virulence strains in the coastal New York region? Is there a difference in the vertebrate host availability on Long Island and Nantucket that could potentially promote the evolution of less pathogenic strains, as described for TBEV[23]? Furthermore, the generation and use of clonal isolates would aid the determination of genotypes associated with specific phenotypes. Our laboratory is currently working on obtaining several consensus-derived DTV clones for future experimental studies.

The ability to infect ticks was demonstrated in the studies herein, however tissue-specific tropisms within the tick, and the ability to subsequently transmit to a naïve vertebrate host was not evaluated. Are some strains less able to infect and escape the salivary glands, leading to inefficient oral transmission? In general, barriers to infection and dissemination within the tick has been inadequately studied compared to mosquito-borne viruses. Our laboratory is currently working on generating a barcoded DTV, which contains engineered nonsynonymous diversity in a single 33-nucleotide region. This tool would enable

the exploration of virus population dynamics within the tick, as our lab and other have done with mosquito-borne viruses[216,217].

The second goal of this dissertation was to evaluate the use of xenosurveillance in Guatemala. Xenosurveillance takes advantage of mosquito feeding behavior to collect frequent and numerous blood samples to detect blood-borne pathogens in humans and animals. The utility of this approach has been demonstrated in Liberia, where anthropophilic *Anopheles gambiae* were the majority of collected mosquitoes. In Central America, less anthropophilic mosquitoes, such as *Aedes* and *Culex* species, are predominant. Therefore, we conducted xenosurveillance in parallel with traditional surveillance techniques for 16 weeks in rural Guatemala. We collected and identified several mosquito genera, among the most abundant were *Culex pipiens* and *Aedes aegypti.* As expected, less than half of mosquito bloodmeals were identified as human and many were sourced from chickens and other avian species. Using metagenomic sequencing, we identified viruses present in mosquito bloodmeals and human blood samples. Though no human viruses were detected, analysis of mosquito samples revealed the presence of many insect-specific viruses. The lack of host-specificity in Guatemalan mosquitoes requires further development on the applicability of this surveillance method in Central America. We therefore foresee xenosurveillance being useful as a targeted approach in regions where zoonotic outbreaks are inevitable. The use of xenosurveillance is currently still being evaluated in Guatemala. Specifically, this study has a longer duration and will include animal samples as well as human.

REFERENCES

1. McLean DM, Donohue WL. Powassan Virus: Isolation of Virus from a Fatal Case of Encephalitis. *Can Med Assoc J*. 1959;80(9):708. Accessed August 18, 2022. https://www.ncbi.nlm.nih.gov/pmc/articles/PMC1830849/
2. Calisher CH, Karabatsos N, Dalrymple JM, Shope RE, Porterfield JS, Westaway EG, Brandt WE. Antigenic relationships between flaviviruses as determined by cross-neutralization tests with polyclonal antisera. *J Gen Virol*. 1989;70(1):37-43. doi:10.1099/0022-1317-70-1-37
3. Mclean DM, Walker SJ, MacPherson LW, Scholton T, Ronald K, Wyllie JC, McQueen EJ. Powassan Virus: Investigations of Possible Natural Cycles of Infection. *J Infect Dis*. 1961;109.
4. Mclean DM, McQueen EJ, Petite HE, MacPherson LW, Scholton T, Ronald K. PowassanVirus: Field Investigations in Northern Ontario, 1959 to 1961. *Canad Med Ass J*. 1962;86.
5. Thomas LA, Kennedy RC, Eklund CM. Isolation of a virus closely related to POWV from Dermacentor andersoni collected along North Cache la Poudre River, CO. *Proc Soc Exp Biol Med*. 1960;104.
6. Mandl CW, Holzmann H, Kunz C, Heinz FX. Complete genomic sequencing of Powassan virus: Evaluation of genetic elements in tick-borne versus mosquito-borne flaviviruses. *Virology*. 1993;194:173-184.
7. Leonova GN, Kondratov IG, Ternovoi VA, Romanova E V., Protopopova E V., Chausov E V., Pavlenko E V., Ryabchikova EI, Belikov SI, Loktev VB. Characterization of Powassan viruses from Far Eastern Russia. *Arch Virol*. 2009;154(5):811-820. doi:10.1007/S00705-009-0376-Y
8. Telford SR, Armstrong PM, Katavolos P, Foppa I, Garcia AS, Wilson ML, Spielman A, Spielman A. A new tick-borne encephalitis-like virus infecting New England deer ticks, Ixodes dammini. *Emerg Infect Dis*. 1997;3(2):165-170. doi:10.3201/eid0302.970209
9. Beasley DWC, Suderman MT, Holbrook MR, Barrett ADT. Nucleotide sequencing and serological evidence that the recently recognized deer tick virus is a genotype of Powassan virus. *Virus Res*. 2001;79(1-2):81-89. doi:10.1016/S0168-1702(01)00330-6
10. Dennis DT, Nekomoto TS, Victor JC, Paul WS, Piesman J. Reported Distribution of Ixodes scapularis and Ixodes pacificus (Acari: Ixodidae) in the United States. *J Med Entomol*. 1998;35(5):629-638. doi:10.1093/jmedent/35.5.629
11. Eisen RJ, Eisen L. The Blacklegged Tick, Ixodes scapularis: An Increasing Public Health Concern. *Trends Parasitol*. 2018;34(4):295-309. doi:10.1016/J.PT.2017.12.006
12. Kuno G, Artsob H, Karabatsos N, Tsuchiya KR, Chang GJJ. *Genomic Sequencing of Deer Tick Virus and Phylogeny of Powassan-Related Viruses of North America*. Vol 65.; 2001. Accessed June 5, 2019. http://www.ajtmh.org/docserver/fulltext/14761645/65/5/11716135.pdf?expires=1559769670&id=id&accname=guest&checksum=9D4434C77C7C3B2F7857D078C6C8B073
13. Ebel GD. Update on Powassan Virus: Emergence of a North American Tick-Borne Flavivirus. *Annu Rev Entomol*. 2010;55(1):95-110. doi:10.1146/annurev-ento-112408-085446
14. *Powassan Virus*.; 2022. Accessed March 14, 2023. https://www.cdc.gov/powassan/statistics.html
15. Nofchissey RA, Deardorff ER, Blevins TM, Anishchenko M, Bosco-Lauth A, Berl E, Lubelczyk C, Mutebi JP, Brault AC, Ebel GD, Magnarelli LA. Seroprevalence of Powassan virus in New England deer, 1979-2010. *Am J Trop Med Hyg*. 2013;88(6):1159-1162. doi:10.4269/ajtmh.12-0586

16. Aliota MT, Dupuis Ii AP, Wilczek MP, Peters RJ, Ostfeld RS, Kramer LD. The Prevalence of Zoonotic Tick-Borne Pathogens in Ixodes Scapularis Collected in the Hudson Valley, New York State. *Vector-Borne Zoonotic Dis*. 2014;14(4). doi:10.1089/vbz.2013.1475

17. Smalley R, Zafar H, Land J, Samour A, Hance D, Brennan RE. Detection of Borrelia miyamotoi and Powassan Virus Lineage II (Deer Tick Virus) from Odocoileus virginianus Harvested Ixodes scapularis in Oklahoma. *Vector-Borne Zoonotic Dis*. 2022;22(4):209-216. doi:10.1089/vbz.2021.0057

18. Klinepeter K. *Powassan Virus Identified in Ticks*.; 2022. https://www.health.pa.gov/topics/Documents/HAN/2022-629-3-8-ADV-Powassan.pdf

19. Whitlow AM, Cumbie AN, Eastwood G. Pathogen prevalence in Amblyomma americanum and Ixodes scapularis ticks from central Appalachian Virginia, U.S.A. *J Vector Ecol*. 2022;47(1). doi:10.52707/1081-1710-47.1.51

20. Cumbie AN, Whitlow AM, Eastwood G. First Evidence of Powassan Virus (Flaviviridae) in Ixodes scapularis in Appalachian Virginia, USA. *Am J Trop Med Hyg*. 2021;106(3):905-908. doi:10.4269/ajtmh.21-0825

21. Sonenshine DE. Range Expansion of Tick Disease Vectors in North America: Implications for Spread of Tick-Borne Disease. *Int J Environ Res Public Health*. 2018;15(3). doi:10.3390/IJERPH15030478

22. Tick-borne encephalitis. Published 2023. https://www.who.int/health-topics/tick-borne-encephalitis

23. Gritsun T., Lashkevich V., Gould E. Tick-borne encephalitis. *Antiviral Res*. 2003;57(1-2):129-146. doi:10.1016/S0166-3542(02)00206-1

24. Bogovic P, Strle F. Tick-borne encephalitis: A review of epidemiology, clinical characteristics, and management. *World J Clin Cases WJCC*. 2015;3(5):430. doi:10.12998/WJCC.V3.I5.430

25. Kemenesi G, Bányai K. Tick-borne flaviviruses, with a focus on powassan virus. *Clin Microbiol Rev*. 2019;32(1). doi:10.1128/CMR.00106-17/ASSET/DC056300-2D1B-4DD2-AEEC-F1AE1B3F2625/ASSETS/GRAPHIC/ZCM0011926500006.JPEG

26. Goodman AG, Mihalca AD, Hirsch AJ, Bloom ME, Mlera L. The Role of Mammalian Reservoir Hosts in Tick-Borne Flavivirus Biology. *Front Cell Infect Microbiol*. 2018;8:298. doi:10.3389/fcimb.2018.00298

27. Gaunt MW, Sall AA, de Lamballerie X, Falconar AKI, Dzhivanian TI, Gould EA. Phylogenetic relationships of flaviviruses correlate with their epidemiology, disease association and biogeography. *J Gen Virol*. 2001;82(8):1867-1876. doi:10.1099/0022-1317-82-8-1867

28. Süss J. Tick-borne encephalitis 2010: Epidemiology, risk areas, and virus strains in Europe and Asia-An overview. *Ticks Tick Borne Dis*. 2011;2(1):2-15. doi:10.1016/j.ttbdis.2010.10.007

29. Krow-Lucal ER, Lindsey NP, Fischer M, Hills SL. Powassan Virus Disease in the United States, 2006–2016. *Vector-Borne Zoonotic Dis*. 2018;18(6):286-290. doi:10.1089/vbz.2017.2239

30. Smith R, Woodall JP, Whitney E, Deibel R, Gross MA, Smith V, Bast TF. Powassan Virus Infection. *Am J Dis Child*. 1974;127(5):691. doi:10.1001/archpedi.1974.02110240077010

31. Piantadosi A, Rubin DB, McQuillen DP, Hsu L, Lederer PA, Ashbaugh CD, Duffalo C, Duncan R, Thon J, Bhattacharyya S, Basgoz N, Feske SK, Lyons JL. Emerging Cases of Powassan Virus Encephalitis in New England: Clinical Presentation, Imaging, and Review of the Literature. *Clin Infect Dis*. 2016;62(6):707-713. doi:10.1093/CID/CIV1005

32. El Khoury MY, Camargo JF, White JL, Backenson BP, Dupuis II AP, Escuyer KL, Kramer L, St George K, Chatterjee D, Prusinski M, Wormser GP, Wong SJ, El Khoury M, Camargo J, Chatterjee D, Wormser G, White J, Backenson B, Dupuis AI, Escuyer K, Kramer L, St George K, Prusinski M, Wong S. Potential Role of Deer Tick Virus in Powassan Encephalitis Cases in Lyme Disease-endemic Areas of New York, USA. *Emerg Infect Dis • www.cdc.gov/eid •*. 2013;19(12). doi:10.3201/eid1912.130903

33. Ei Khoury MY, Camargo JF, Wormser GP. Changing epidemiology of Powassan encephalitis in North America suggests the emergence of the deer tick virus subtype. *Expert Rev Anti Infect Ther*. 2013;11(10):983-985. doi:10.1586/14787210.2013.837805

34. Tavakoli NP, Wang H, Dupuis M, Hull R, Ebel GD, Gilmore EJ, Faust PL. Fatal Case of Deer Tick Virus Encephalitis. *N Engl J Med*. 2009;360(20):2099-2107. doi:10.1056/nejmoa0806326

35. Normandin E, Solomon IH, Zamirpour S, Lemieux J, Freije CA, Mukerji SS, Tomkins-Tinch C, Park D, Sabeti PC, Piantadosi A. Powassan virus neuropathology and genomic diversity in patients with fatal encephalitis. *Open Forum Infect Dis*. Published online August 29, 2020. doi:10.1093/ofid/ofaa392

36. Cavanaugh CE, Muscat PL, Telford SR, Goethert H, Pendlebury W, Elias SP, Robich R, Welch M, Lubelczyk CB, Smith RP. Fatal deer tick virus infection in Maine. *Clin Infect Dis*. 2017;65(6):1043-1046. doi:10.1093/cid/cix435

37. McLean DM, MacPherson LW, Walker SJ, Funk G. Powassan Virus: Surveys of Human and Animal Sera. *Am J Public Heal Nations Heal*. 1960;50(10):1539-1544. doi:10.2105/ajph.50.10.1539

38. R D, S S, JP. W. Arboviruses in New York State: an attempt to determine the role of arboviruses in patients with viral encephalitis and meningitis. *Am J Trop Med Hyg*. 1979;28(3):577-582.

39. Frost HM, Schotthoefer AM, Thomm AM, Dupuis AP, Kehl SC, Kramer LD, Fritsche TR, Harrington YA, Knox KK. Serologic Evidence of Powassan Virus Infection in Patients with Suspected Lyme Disease. *Emerg Infect Dis*. 2017;23(8):1384. doi:10.3201/EID2308.161971

40. Vahey GM, Wilson N, McDonald E, Fitzpatrick K, Lehman J, Clark S, Lindell K, Pastula DM, Perez S, Rhodes H, Gould C V, Staples JE, Cervantes K, Martin SW. Seroprevalence of Powassan Virus Infection in an Area Experiencing a Cluster of Disease Cases — Sussex County, New Jersey, 2019. *Open Forum Infect Dis*. Published online January 17, 2022. doi:10.1093/OFID/OFAC023

41. Nemeth NM, Root JJ, Hartwig AE, Bowen RA, Bosco-Lauth AM. Powassan Virus Experimental Infections in Three Wild Mammal Species. *Am J Trop Med Hyg*. 2021;104(3):1048-1054. doi:10.4269/ajtmh.20-0105

42. Little PB, Thorsen J, Moore W, Weninger N. Powassan viral encephalitis: A review and experimental studies in the horse and rabbit. *Vet Pathol*. 1985;22(5):500-507. doi:10.1177/030098588502200510

43. Mlera L, Meade-White K, Saturday G, Scott D, Bloom ME. Modeling Powassan virus infection in Peromyscus leucopus, a natural host. *PLoS Negl Trop Dis*. 2017;11(1). doi:10.1371/JOURNAL.PNTD.0005346

44. Frolova MP, Isachkova LM, Shestopalova NM, Pogodina V V. Experimental encephalitis in monkeys caused by the Powassan virus. *Neurosci Behav Physiol*. 1985;15(1):62-69. doi:10.1007/BF01186452

45. Chernesky MA, Whittaker-Haines PJ. Dose-dependent viremia and the differential immunoglobulin response of hamsters to Powassan virus. *Can J Microbiol*. 1972;18(5):655-661.

doi:10.1139/m72-103

46. Holbrook MR, Aronson JF, Campbell GA, Jones S, Feldmann H, Barren ADT. An animal model for the tickborne flavivirus--Omsk hemorrhagic fever virus. *J Infect Dis*. 2005;191(1):100-108. doi:10.1086/426397

47. Kramer LD, Ebel GD. Short Report: Duration of Tick Attachment Required for Transmission of Powassan Virus By Deer Ticks. *Am J Trop Med Hyg*. 2004;71(3):268-271. doi:10.4269/ajtmh.2004.71.3.0700268

48. Hermance ME, Thangamani S. Tick Saliva Enhances Powassan Virus Transmission to the Host, Influencing Its Dissemination and the Course of Disease. *J Virol*. 2015;89(15):7852-7860. doi:10.1128/JVI.01056-15/FORMAT/EPUB

49. Hermance ME, Santos RI, Kelly BC, Valbuena G, Thangamani S. Immune cell targets of infection at the tick-skin interface during powassan virus transmission. *PLoS One*. 2016;11(5). doi:10.1371/journal.pone.0155889

50. Mlera L, Meade-White K, Saturday G, Scott D, Bloom ME. Modeling Powassan virus infection in Peromyscus leucopus, a natural host. doi:10.1371/journal.pntd.0005346

51. Santos RI, Hermance ME, Reynolds ES, Thangamani S. Salivary gland extract from the deer tick, Ixodes scapularis, facilitates neuroinvasion by Powassan virus in BALB/c mice. *Sci Reports 2021 111*. 2021;11(1):1-10. doi:10.1038/s41598-021-00021-2

52. Stone ET, Hassert M, Geerling E, Wagner C, Brien JD, Ebel GD, Hirsch AJ, German C, Smith JL, Pinto AK. Balanced T and B cell responses are required for immune protection against Powassan virus in virus-like particle vaccination. *Cell Rep*. 2022;38(7). doi:10.1016/J.CELREP.2022.110388

53. VanBlargan LA, Himansu S, Foreman BM, Ebel GD, Pierson TC, Diamond MS. An mRNA Vaccine Protects Mice against Multiple Tick-Transmitted Flavivirus Infections. *Cell Rep*. 2018;25(12):3382-3392.e3. doi:10.1016/j.celrep.2018.11.082

54. Scroggs SLP, Offerdahl DK, Stewart PE, Shaia C, Griffin AJ, Bloom ME. Of Murines and Humans : Modeling Persistent Powassan Disease. *MBio*. Published online 2023. doi:https://doi.org/10.1128/mbio.03606-22

55. Hermance ME, Hart CE, Esterly AT, Reynolds ES, Bhaskar JR, Thangamani S. Development of a small animal model for deer tick virus pathogenesis mimicking human clinical outcome. *PLoS Negl Trop Dis*. 2020;14(6):e0008359. doi:10.1371/JOURNAL.PNTD.0008359

56. PA N, M L. Tick-host interactions: saliva-activated transmission. *Parasitology*. 2004;129 Suppl(SUPPL.). doi:10.1017/S0031182004005633

57. Estrada A. Ticks as Vectors. *Encycl Parasitol*. 2016;34(1):2729-2729. doi:10.1007/978-3-662-43978-4_3182

58. Sonenshine DE. *Biology of Ticks*. 1st ed. Oxford University Press; 1992.

59. Maqbool M, Sajid MS, Saqib M, Anjum FR, Tayyab MH, Rizwan HM, Rashid MI, Rashid I, Iqbal A, Siddique RM, Shamim A, Hassan MA, Atif FA, Razzaq A, Zeeshan M, Hussain K, Nisar RHA, Tanveer A, Younas S, Kamran K, Rahman S ur. Potential Mechanisms of Transmission of Tick-Borne Viruses at the Virus-Tick Interface. *Front Microbiol*. 2022;13(May):1-20. doi:10.3389/fmicb.2022.846884

60. Gulia-Nuss M, Nuss AB, Meyer JM, Sonenshine DE, Roe RM, Waterhouse RM, Sattelle DB, De La Fuente J, Ribeiro JM, Megy K, Thimmapuram J, Miller JR, Walenz BP, Koren S, Hostetler JB, Thiagarajan M, Joardar VS, Hannick LI, Bidwell S, Hammond MP, Young S, Zeng Q, Abrudan JL, Almeida FC, Ayllón N, Bhide K, Bissinger BW, Bonzon-Kulichenko E, Buckingham SD,

Caffrey DR, Caimano MJ, Croset V, Driscoll T, Gilbert D, Gillespie JJ, Giraldo-Calderón GI, Grabowski JM, Jiang D, Khalil SMS, Kim D, Kocan KM, Koči J, Kuhn RJ, Kurtti TJ, Lees K, Lang EG, Kennedy RC, Kwon H, Perera R, Qi Y, Radolf JD, Sakamoto JM, Sánchez-Gracia A, Severo MS, Silverman N, Šimo L, Tojo M, Tornador C, Van Zee JP, Vázquez J, Vieira FG, Villar M, Wespiser AR, Yang Y, Zhu J, Arensburger P, Pietrantonio P V., Barker SC, Shao R, Zdobnov EM, Hauser F, Grimmelikhuijzen CJP, Park Y, Rozas J, Benton R, Pedra JHF, Nelson DR, Unger MF, Tubio JMC, Tu Z, Robertson HM, Shumway M, Sutton G, Wortman JR, Lawson D, Wikel SK, Nene VM, Fraser CM, Collins FH, Birren B, Nelson KE, Caler E, Hill CA. Genomic insights into the Ixodes scapularis tick vector of Lyme disease. *Nat Commun*. 2016;7(May 2015). doi:10.1038/ncomms10507

61. Vancová M, Bílý T, Šimo L, Touš J, Horodyský P, Růžek D, Novobilský A, Salát J, Strnad M, Sonenshine DE, Grubhoffer L, Nebesářová J. Three-dimensional reconstruction of the feeding apparatus of the tick Ixodes ricinus (Acari: Ixodidae): a new insight into the mechanism of blood-feeding. *Sci Rep*. 2020;10(1):1-7. doi:10.1038/s41598-019-56811-2

62. Karim S, Kumar D, Budachetri K. Recent advances in understanding tick and rickettsiae interactions. *Parasite Immunol*. 2021;43(5):1-11. doi:10.1111/pim.12830

63. Arthur DR. Tick Feeding and its Implications. *Adv Parasitol*. 1970;8(C):275-292. doi:10.1016/S0065-308X(08)60258-4

64. Grigor'eva L, Amosova L. Peritrophic matrix in the midgut of tick females of the genus Ixodes (Acari: Ixodidae). *Parazitologiia*. 2004;38(1):3-11.

65. Kitsou C, Foor SD, Dutta S, Bista S, Pal U. Tick gut barriers impacting tick–microbe interactions and pathogen persistence. *Mol Microbiol*. 2021;116(5):1241-1248. doi:10.1111/mmi.14822

66. Kocan KM, De La Fuente J, Coburn LA. Insights into the development of Ixodes scapularis: A resource for research on a medically important tick species. *Parasites and Vectors*. 2015;8(1):4-9. doi:10.1186/s13071-015-1185-7

67. Ko RC. Biology of Ixodes cookei Packard (Ixodidae) of groundhogs (Marmota monax Erxleben). *Can J Zool*. 1972;50(4):433-436. doi:10.1139/z72-061

68. Tick Lab. The University of Maine. Accessed February 12, 2023. https://extension.umaine.edu/ticks/maine-ticks/

69. Fogaça AC, Sousa G, Pavanelo DB, Esteves E, Martins LA, Urbanová V, Kopáček P, Daffre S. Tick Immune System: What Is Known, the Interconnections, the Gaps, and the Challenges. *Front Immunol*. 2021;12(March):1-23. doi:10.3389/fimmu.2021.628054

70. Nuttall PA, Jones LD, Labuda M, Kaufman WR. Adaptations of arboviruses to ticks. *J Med Entomol*. 1994;31(1):1-9. doi:10.1093/jmedent/31.1.1

71. Franz AWE, Kantor AM, Passarelli AL, Clem RJ. Tissue barriers to arbovirus infection in mosquitoes. *Viruses*. 2015;7(7):3741-3767. doi:10.3390/v7072795

72. Kazimírová M, Thangamani S, Bartíková P, Hermance M, Holíková V, Nuttall ŠI. Tick-Borne Viruses and Biological Processes at the Tick-Host-Virus Interface. 2017;7. doi:10.3389/fcimb.2017.00339

73. Piesman J. Dispersal of the Lyme disease spirochete Borrelia burgdorferi to salivary glands of feeding nymphal Ixodes scapularis (Acari: Ixodidae). *J Med Entomol*. 1995;32(4):519-521. doi:10.1093/jmedent/32.4.519

74. Chernesky MA, Mclean DM. Localization of Powassan virus in Dermacentor andersoni ticks by immunofluorescence. *Canada J Microbiol*. 1969;15:1399-1408. Accessed August 19, 2019.

www.nrcresearchpress.com

75. Chávez ASO, Shaw DK, Munderloh UG, Pedra JHF. Tick humoral responses: Marching to the beat of a different drummer. *Front Microbiol*. 2017;8(FEB):1-9. doi:10.3389/fmicb.2017.00223

76. Schnettler E, Tykalová H, Tykalová T, Watson M, Sharma M, Sterken MG, Obbard DJ, Lewis SH, Mcfarlane M, Bell-Sakyi L, Barry G, Weisheit S, Best SM, Kuhn RJ, Pijlman GP, Chase-Topping ME, Gould EA, Grubhoffer L, Fazakerley JK, Kohl A. Induction and suppression of tick cell antiviral RNAi responses by tick-borne flaviviruses. *Nucleic Acids Res*. 2014;42(14):9436-9446. doi:10.1093/nar/gku657

77. Grubaugh ND, Rückert C, Armstrong PM, Bransfield A, Anderson JF, Ebel GD, Brackney DE. Transmission bottlenecks and RNAi collectively influence tick-borne flavivirus evolution. *Virus Evol*. 2016;2(2). doi:10.1093/ve/vew033

78. Costero A, Grayson MA. Experimental transmission of Powassan virus (Flaviviridae) by Ixodes scapularis ticks (Acari: Ixodidae). *Am J Top Med Hygeine*. 1996;55(5):536-546.

79. Nuttall PA, Labuda M. Dynamics of infection in tick vectors and at the tick-host interface. *Adv Virus Res*. 2003;60:233-272.

80. Jones LD, Hodgson E, Nuttall PA. Enhancement of virus transmission by tick salivary glands. *J Gen Virol*. 1989;70(7):1895-1898. doi:10.1099/0022-1317-70-7-1895

81. Šimo L, Kazimirova M, Richardson J, Bonnet SI. The essential role of tick salivary glands and saliva in tick feeding and pathogen transmission. *Front Cell Infect Microbiol*. 2017;7(JUN):1-23. doi:10.3389/fcimb.2017.00281

82. Labuda M, Austyn JM, Zuffova E, Kozuch O, Fuchsberger N, Lysy J, Nuttall PA. Importance of localized skin infection in tick-borne encephalitis virus transmission. *Virology*. 1996;219(2):357-366. doi:10.1006/viro.1996.0261

83. Labuda M, Nuttall PA, Kozuch O, Eleckova E, Williams T, Zuffova E, Sabo A. Non-Viremic Transmission of Tick-Borne Encephalitis-Virus - a Mechanism for Arbovirus Survival in Nature. *Experientia*. 1993;49(9):802-805. doi:10.1007/BF01923553

84. Brackney DE, Armstrong PM. Transmission and evolution of tick-borne viruses. *Curr Opin Virol*. 2016;21:67-74. doi:10.1016/j.coviro.2016.08.005

85. Raney WR, Herslebs EJ, Langohr IM, Stone MC, Hermance ME. Horizontal and Vertical Transmission of Powassan Virus by the Invasive Asian Longhorned Tick, Haemaphysalis longicornis, Under Laboratory Conditions. *Front Cell Infect Microbiol*. 2022;12(July):1-14. doi:10.3389/fcimb.2022.923914

86. Danielová V, Holubová J, Pejčoch M, Daniel M. Potential significance of transovarial transmission in the circulation of tick-borne encephalitis virus. *Folia Parasitol (Praha)*. 2002;49(4):323-325. doi:10.14411/fp.2002.060

87. Turell MJ. Horizontal and Vertical Transmission of Viruses by Insect and Tick Vectors. In: *The Arboviruses*. 1st ed. CRC Press; 1988.

88. Rosà R, Pugliese A. Effects of tick population dynamics and host densities on the persistence of tick-borne infections. *Math Biosci*. 2007;208(1):216-240. doi:10.1016/j.mbs.2006.10.002

89. Mclean DM, Larke RPB. *Powassan and Silverwater Viruses: Ecology of Two Ontario Arboviruses*. Vol 88.; 1963. Accessed February 22, 2019. https://www.ncbi.nlm.nih.gov/pmc/articles/PMC1920964/pdf/canmedaj00980-0013.pdf

90. Whitney E, Jamnback H. The First Isolations of Powassan Virus in New York State. *Proc Soc Exp*

Biol Med. 1965;119(2):432-435.

91. Main AJ, Carey AB, Downs WG. POWASSAN VIRUS IN Ixodes cookei AND MUSTELIDAE IN NEW ENGLAND. *J Wildl Dis*. 1979;15(4):585-591. doi:10.7589/0090-3558-15.4.585

92. Mclean DM, Best JM, Mahalingam S, Chernesky MA, Wilson WE. Powassan Virus: Summer Infection Cycle, 1964. *Can Med Assoc J*. Published online 1964:1360-1362.

93. Smith K, Oesterle PT, Jardine CM, Dibernardo A, Huynh C, Lindsay R, Pearl DL, Bosco-Lauth AM, Nemeth NM. Powassan Virus and Other Arthropod-Borne Viruses in Wildlife and Ticks in Ontario, Canada. *Am J Trop Med Hyg*. 2018;99(2):458-465. doi:10.4269/ajtmh.18-0098

94. McLean DM, Cobb C, Gooderham SE, Smart CA, Wilson AG, Wilson WE. Powassan virus: persistence of virus activity during 1966. *Can Med Assoc J*. 1967;96(11):660-664.

95. Artsob H, Spence L, Surgeoner G, McCreadie J, Thorsen J, Th'ng C, Lampotang V. Isolation of Francisella Tularensis and Powassan Virus from Ticks (Acari: Ixodidae) in Ontario, Canada. *J Med Entomol*. 1984;21(2):165-168. doi:10.1093/JMEDENT/21.2.165

96. Johnson HN. Isolation of Powassan virus from a spotted skunk in California. *J Wildl Dis*. 1987;23(1):152-153. doi:10.7589/0090-3558-23.1.152

97. Deardorff ER, Nofchissey RA, Cook JA, Hope AG, Tsvetkova A, Talbot SL, Ebel GD. Powassan Virus in and New Mexico ,USA, and Russia, 2004–2007. *Emerg Infect Dis*. 2013;19(12):1-5.

98. Kettyls GD, Verrall VM, Wilton LD, Clapp JB, Clarke DA, Rublee JD. Arbovirus infections in man in British Columbia. *Can Med Assoc J*. 1972;106(11):1175-1179.

99. Brackney DE, Nofchissey RA, Fitzpatrick KA, Brown IK, Ebel GD. Short report: Stable prevalence of powassan virus in Ixodes scapularis in a Northern Wisconsin focus. *Am J Trop Med Hyg*. 2008;79(6):971-973.

100. Knox KK, Thomm AM, Harrington YA, Ketter E, Patitucci JM, Carrigan DR. Powassan/Deer Tick Virus and Borrelia Burgdorferi Infection in Wisconsin Tick Populations. *Vector-Borne Zoonotic Dis*. 2017;17(7):463-466. doi:10.1089/vbz.2016.2082

101. Campbell O, Krause PJ. The emergence of human Powassan virus infection in North America. *Ticks Tick Borne Dis*. 2020;11(6):101540. doi:10.1016/j.ttbdis.2020.101540

102. Ebel GD, Foppa I, Spielman A, Telford SR. A focus of deer tick virus transmission in the Northcentral United States. *Emerg Infect Dis*. 1999;5(4):570-574. doi:10.3201/eid0504.990423

103. Anderson JF, Armstrong PM. Prevalence and Genetic Characterization of Powassan Virus Strains Infecting Ixodes scapularis in Connecticut. *Am J Trop Med Hyg*. 2012;87(4):754-759. doi:10.4269/AJTMH.2012.12-0294

104. Grant-Klein RJ, Baldwin CD, Turell MJ, Rossi CA, Li F, Lovari R, Crowder CD, Matthews HE, Rounds MA, Eshoo MW, Blyn LB, Ecker DJ, Sampath R, Whitehouse CA. Rapid identification of vector-borne flaviviruses by mass spectrometry. *Mol Cell Probes*. 2010;24(4):219-228. doi:10.1016/j.mcp.2010.04.003

105. Tokarz R, Jain K, Bennett A, Briese T, Lipkin WI. Assessment of polymicrobial infections in ticks in New York state. *Vector-Borne Zoonotic Dis*. 2010;10(3):217-221. doi:10.1089/vbz.2009.0036

106. Sanchez-Vicente S, Tagliafierro T, Coleman JL, Benach JL, Tokarz R. Polymicrobial nature of tick-borne diseases. *MBio*. 2019;10(5):1-17. doi:10.1128/mBio.02055-19

107. Lange RE, Dupuis AP, Prusinski MA, Maffei JG, Koetzner CA, Ngo K, Backenson B, Oliver JA, Vogels CBF, Grubaugh ND, Kramer LD, Ciota AT. Identification and characterization of novel lineage 1 Powassan virus strains in New York State. *Emerg Microbes Infect*. 2023;12(1).

doi:10.1080/22221751.2022.2155585

108. Campagnolo ER, Tewari D, Farone TS, Livengood JL, Mason KL. Evidence of Powassan/deer tick virus in adult black-legged ticks (Ixodes scapularis) recovered from hunter-harvested white-tailed deer (Odocoileus virginianus) in Pennsylvania: A public health perspective. *Zoonoses Public Health*. 2018;65(5):589-594. doi:10.1111/ZPH.12476

109. Price KJ, Tewari D, Witmier BJ, Long J, Chroscinski MS, Livengood JL, Boyer CN, Dupuis AP, Kramer LD, Lind L. Prevalence and distribution of Powassan/deer tick virus in Pennsylvania. *Int J Acarol*. 2021;47(8):726-729. doi:10.1080/01647954.2021.2005141

110. Robich RM, Cosenza DS, Elias SP, Henderson EF, Lubelczyk CB, Welch M, Smith RP. Prevalence and Genetic Characterization of Deer Tick Virus (Powassan Virus, Lineage II) in Ixodes scapularis Ticks Collected in Maine. *Am J Trop Med Hyg*. 2019;101(2):467-471. doi:10.4269/AJTMH.19-0281

111. Johnson TL, Graham CB, Maes SE, Hojgaard A, Fleshman A, Boegler KA, Delory MJ, Slater KS, Karpathy SE, Bjork JK, Neitzel DF, Schiffman EK, Eisen RJ. Prevalence and distribution of seven human pathogens in host-seeking Ixodes scapularis (Acari: Ixodidae) nymphs in Minnesota, USA. *Ticks Tick Borne Dis*. 2018;9(6):1499-1507. doi:10.1016/j.ttbdis.2018.07.009

112. *2018 Vermont Survey for Tick-Borne Diseases*.; 2018.

113. Mueller S. An Assessment for the Presence of Powassan virus in Ixodes scapularis Nymphs from Locations in Virginia, Maryland, New Jersey, Pennsylvania, New York, and Connecticut. Published online 2013.

114. McMinn RJ, Langsjoen RM, Bombin A, Robich RM, Ojeda E, Normandin E, Goethert HK, Lubelczyk CB, Schneider E, Cosenza D, Meagher M, Prusinski MA, Sabeti PC, Smith RP, Telford S, Piantadosi A, Ebel GD. Phylodynamics of deer tick virus in North America. *Virus Evol*. Published online January 27, 2023. doi:10.1093/VE/VEAD008

115. Anderson JF. Ecology of Lyme disease. *Conn Med*. 1989;53(6):343-346.

116. Ebel GD, Campbell EN, Goethert HK, Spielman A, Telford SR. Enzootic transmission of deer tick virus in new England and Wisconsin sites. *Am J Trop Med Hyg*. 2000;63(1-2):36-42. doi:10.4269/ajtmh.2000.63.36

117. Goethert HK, Mather TN, Johnson RW, Telford SR. Incrimination of shrews as a reservoir for Powassan virus. *Commun Biol 2021 41*. 2021;4(1):1-8. doi:10.1038/s42003-021-02828-1

118. Apperson CS, Levine JF, Evans TL, Braswell A, Heller J. Relative utilization of reptiles and rodents as hosts by immature Ixodes scapularis (Acari: Ixodidae) in the coastal plain of North Carolina, USA. *Exp Appl Acarol*. 1993;17(10):719-731. doi:10.1007/BF00051830

119. De Jesus C, Bhosale C, Wilson K, White Z, Wisely SM. Reptile host associations of ixodes scapularis in florida and implications for borrelia spp. Ecology. *Pathogens*. 2021;10(8):6-8. doi:10.3390/pathogens10080999

120. Eisen RJ, Eisen L, Beard CB. County-Scale Distribution of *Ixodes scapularis* and *Ixodes pacificus* (Acari: Ixodidae) in the Continental United States. *J Med Entomol*. 2016;53(2):349-386. doi:10.1093/jme/tjv237

121. Keirans JE, Hutcheson HJ, Durden LA, Klompen JSH. Ixodes (Ixodes) scapularis (Acari: Ixodidae): Redescription of all Active Stages, Distribution, Hosts, Geographical Variation, and Medical and Veterinary Importance. *J Med Entomol*. 1996;33(3):297-318. doi:10.1093/jmedent/33.3.297

122. Brinkmann A, Nitsche A, Kohl C. Viral metagenomics on blood-feeding arthropods as a tool for

human disease surveillance. *Int J Mol Sci*. 2016;17(10). doi:10.3390/ijms17101743

123. Kading RC, Biggerstaff BJ, Young G, Komar N. Mosquitoes Used to Draw Blood for Arbovirus Viremia Determinations in Small Vertebrates. Adelman ZN, ed. *PLoS One*. 2014;9(6):e99342. doi:10.1371/journal.pone.0099342

124. Fauver JR, Gendernalik A, Weger-Lucarelli J, Grubaugh ND, Brackney DE, Foy BD, Ebel GD. The Use of Xenosurveillance to Detect Human Bacteria, Parasites, and Viruses in Mosquito Bloodmeals. *Am J Trop Med Hyg*. 2017;97(2):324-329. doi:10.4269/ajtmh.17-0063

125. Grubaugh ND, Sharma S, Krajacich BJ, Fakoli LS, Bolay FK, Diclaro JW, Johnson WE, Ebel GD, Foy BD, Brackney DE. Xenosurveillance: A Novel Mosquito-Based Approach for Examining the Human-Pathogen Landscape. *PLoS Negl Trop Dis*. 2015;9(3):e0003628. doi:10.1371/journal.pntd.0003628

126. Yang Y, Garver LS, Bingham KM, Hang J, Jochim RC, Davidson SA, Richardson JH, Jarman RG. Feasibility of using the mosquito blood meal for rapid and efficient human and animal virus surveillance and discovery. *Am J Trop Med Hyg*. 2015;93(6):1377-1382. doi:10.4269/ajtmh.15-0440

127. Yuill TM. Mosquitoes for drawing blood from small reptiles. *Trans R Soc Trop Med Hyg*. 1969;63(3):407-408. doi:10.1016/0035-9203(69)90019-4/2/63-3-407.PDF.GIF

128. Barbazan P, Thitithanyanont A, Missé D, Dubot A, Bosc P, Luangsri N, Gonzalez J-P, Kittayapong P. Detection of H5N1 Avian Influenza Virus from Mosquitoes Collected in an Infected Poultry Farm in Thailand. *VECTOR-BORNE ZOONOTIC Dis*. 2008;8(1). doi:10.1089/vbz.2007.0142

129. Shi C, Liu Y, Hu X, Xiong J, Zhang B, Yuan Z. A metagenomic survey of viral abundance and diversity in mosquitoes from hubei province. *PLoS One*. 2015;10(6):e0129845. doi:10.1371/journal.pone.0129845

130. Ng TFF, Willner DL, Lim YW, Schmieder R, Chau B, Nilsson C, Anthony S, Ruan Y, Rohwer F, Breitbart M. Broad surveys of DNA viral diversity obtained through viral metagenomics of mosquitoes. *PLoS One*. 2011;6(6). doi:10.1371/journal.pone.0020579

131. Ng TFF, Duffy S, Polston JE, Bixby E, Vallad GE, Breitbart M. Exploring the diversity of plant DNA viruses and their satellites using vector-enabled metagenomics on whiteflies. *PLoS One*. 2011;6(4):e19050. doi:10.1371/journal.pone.0019050

132. Fauver JR, Weger-Lucarelli J, Fakoli LS, Bolay K, Bolay FK, Diclaro JW, Brackney DE, Foy BD, Stenglein MD, Ebel GD. Xenosurveillance reflects traditional sampling techniques for the identification of human pathogens: A comparative study in West Africa. *PLoS Negl Trop Dis*. 2018;12(3). doi:10.1371/journal.pntd.0006348

133. Leighton BJ, Roitberg BD, Belton P, Lowenberger CA. *Host Antibodies in Mosquito Bloodmeals: A Potential Tool to Detect and Monitor Infectious Diseases in Wildlife*. Vol 45.; 2008. Accessed April 9, 2020. https://academic.oup.com/jme/article-abstract/45/3/470/906514

134. Gyawali N, Murphy AK, Hugo LE, Devine GJ. A micro-PRNT for the detection of Ross River virus antibodies in mosquito blood meals: A useful tool for inferring transmission pathways. *PLoS One*. 2020;15(7):e0229314. doi:10.1371/JOURNAL.PONE.0229314

135. Štefanić S, Grimm F, Mathis A, Winiger R, Verhulst NO. Xenosurveillance proof-of-principle: Detection of Toxoplasma gondii and SARS-CoV-2 antibodies in mosquito blood meals by (pan)-specific ELISAs. *Curr Res Parasitol Vector-Borne Dis*. 2022;2(December 2021):2-6. doi:10.1016/j.crpvbd.2022.100076

136. Komar N, Panella NA, Young GR, Basile AJ. Methods for detection of west nile virus antibodies in mosquito blood meals. *J Am Mosq Control Assoc*. 2015;31(1):1-6. doi:10.2987/14-6468R.1

137. Bitome-Essono PY, Ollomo B, Arnathau C, Durand P, Mokoudoum ND, Yacka-Mouele L, Okouga AP, Boundenga L, Mve-Ondo B, Obame-Nkoghe J, Mbehang-Nguema P, Njiokou F, Makanga B, Wattier R, Ayala D, Ayala FJ, Renaud F, Rougeron V, Bretagnolle F, Prugnolle F, Paupy C. Tracking zoonotic pathogens using blood-sucking flies as 'flying syringes'. *Elife*. 2017;6. doi:10.7554/eLife.22069

138. Calvignac-Spencer S, Leendertz FH, Gilbert MTP, Schubert G. An invertebrate stomach's view on vertebrate ecology. *BioEssays*. 2013;35(11):1004-1013. doi:10.1002/BIES.201300060

139. Calvignac-Spencer S, Merkel K, Kutzner N, Kühl H, Boesch C, Kappeler PM, Metzger S, Schubert G, Leendertz FH. Carrion fly-derived DNA as a tool for comprehensive and cost-effective assessment of mammalian biodiversity. *Mol Ecol*. 2013;22(4):915-924. doi:10.1111/mec.12183

140. Schnell IB, Thomsen PF, Wilkinson N, Rasmussen M, Jensen LRD, Willerslev E, Bertelsen MF, Gilbert MTP. Screening mammal biodiversity using DNA from leeches. *Curr Biol*. 2012;22(8). doi:10.1016/j.cub.2012.02.058

141. Schubert G, Stockhausen M, Hoffmann C, Merkel K, Vigilant L, Leendertz FH, Calvignac-Spencer S. Targeted detection of mammalian species using carrion fly-derived DNA. *Mol Ecol Resour*. 2015;15(2):285-294. doi:10.1111/1755-0998.12306

142. Bohmann K, Schnell IB, Gilbert MTP. When bugs reveal biodiversity. *Mol Ecol*. 2013;22(4):909-911. doi:10.1111/MEC.12221

143. Sawabe K, Hoshino K, Isawa H, Sasaki T, Hayashi T, Tsuda Y, Kurahashi H, Tanabayashi K, Hotta A, Saito T, Yamada A, Kobayashi M. Detection and isolation of highly pathogenic H5N1 avian influenza A viruses from blow flies collected in the vicinity of an infected poultry farm in Kyoto, Japan, 2004. *Am J Trop Med Hyg*. 2006;75(2):327-332. doi:10.4269/ajtmh.2006.75.327

144. Chakrabarti S, King DJ, Afonso C, Swayne D, Cardona CJ, Kuney DR, Gerry AC. Detection and isolation of exotic newcastle disease virus from field-collected flies. *J Med Entomol*. 2007;44(5):840-844. doi:10.1603/0022-2585(2007)44[840:DAIOEN]2.0.CO;2

145. Bondaryuk AN, Peretolchina TE, Romanova E V., Yudinceva A V., Andaev EI, Bukin YS. Phylogeography and Re-Evaluation of Evolutionary Rate of Powassan Virus Using Complete Genome Data. *Biology (Basel)*. 2021;10(12). doi:10.3390/BIOLOGY10121282

146. Rand PW, Lacombe EH, Dearborn R, Cahill B, Elias S, Lubelczyk CB, Beckett GA, Smith RP. Passive Surveillance in Maine, an Area Emergent for Tick-Borne Diseases. *J Med Entomol*. 2007;44(6):1118-1129. doi:10.1093/JMEDENT/44.6.1118

147. Pesko KN, Torres-Perez F, Hjelle BL, Ebel GD. Molecular epidemiology of Powassan virus in North America. *J Gen Virol*. 2010;91(Pt 11):2698-2705. doi:10.1099/vir.0.024232-0

148. Campagnolo ER, Tewari D, Farone TS, Livengood JL, Mason KL. Evidence of Powassan/deer tick virus in adult black-legged ticks (Ixodes scapularis) recovered from hunter-harvested white-tailed deer (Odocoileus virginianus) in Pennsylvania: A public health perspective. *Zoonoses Public Health*. 2018;65(5):589-594. doi:10.1111/zph.12476

149. Brackney DE, Brown IK, Nofchissey RA, Fitzpatrick KA, Gregory D. Homogeneity of Powassan Virus Populations in. 2011;402(2):366-371. doi:10.1016/j.virol.2010.03.035.HOMOGENEITY

150. Sonenshine DE. *Biology of Ticks*. Oxford University Press Inc.; 1991.

151. Khatchikian CE, Prusinski MA, Stone M, Backenson PB, Wang IN, Foley E, Seifert SN, Levy

MZ, Brisson D. Recent and rapid population growth and range expansion of the Lyme disease tick vector, Ixodes scapularis, in North America. *Evolution (N Y)*. 2015;69(7):1678-1689. doi:10.1111/evo.12690

152. Qiu WG, Dykhuizen DE, Acosta MS, Luft BJ. Geographic uniformity of the lyme disease spirochete (Borrelia burgdorferi) and its shared history with tick vector (Ixodes scapularis) in the Northeastern United States. *Genetics*. 2002;160(3):833-849. doi:10.1093/genetics/160.3.833

153. Xu G, Wielstra B, Rich SM. Northern and southern blacklegged (deer) ticks are genetically distinct with different histories and Lyme spirochete infection rates. *Sci Rep*. 2020;10(1):1-9. doi:10.1038/s41598-020-67259-0

154. Bouchard C, Dibernardo A, Koffi J, Wood H, Leighton PA, Lindsay LR. Increased risk of tick-borne diseases with climate and environmental changes. *Can Commun Dis Rep*. 2019;45(4):83-89. doi:10.14745/ccdr.v45i04a02

155. Salomon J, Hamer SA, Swei A. A Beginner's Guide to Collecting Questing Hard Ticks (Acari: Ixodidae): A Standardized Tick Dragging Protocol. *J Insect Sci*. 2020;20(6):1-8. doi:10.1093/jisesa/ieaa073

156. https://github.com/broadinstitute/viral-pipelines. Accessed November 21, 2022. https://github.com/broadinstitute/viral-pipelines

157. Kalyaanamoorthy S, Minh BQ, Wong TKF, Von Haeseler A, Jermiin LS. ModelFinder: fast model selection for accurate phylogenetic estimates. *Nat Methods 2017 146*. 2017;14(6):587-589. doi:10.1038/nmeth.4285

158. Nguyen LT, Schmidt HA, Von Haeseler A, Minh BQ. IQ-TREE: A Fast and Effective Stochastic Algorithm for Estimating Maximum-Likelihood Phylogenies. *Mol Biol Evol*. 2015;32(1):268-274. doi:10.1093/MOLBEV/MSU300

159. Rambaut A, Lam TT, Carvalho LM, Pybus OG. Exploring the temporal structure of heterochronous sequences using TempEst (formerly Path-O-Gen). *Virus Evol*. 2016;2(1). doi:10.1093/VE/VEW007

160. Bouckaert R, Heled J, Kühnert D, Vaughan T, Wu CH, Xie D, Suchard MA, Rambaut A, Drummond AJ. BEAST 2: a software platform for Bayesian evolutionary analysis. *PLoS Comput Biol*. 2014;10(4). doi:10.1371/JOURNAL.PCBI.1003537

161. Maturana P, Brewer BJ, Klaere S, Bouckaert R. Model selection and parameter inference in phylogenetics using Nested Sampling. *Syst Biol*. 2017;68(2):219-233. doi:10.1093/sysbio/syy050

162. Kass RE, Raftery AE. Bayes Factors. *J Am Stat Assoc*. 1995;90(430):773. doi:10.2307/2291091

163. Rambaut A, Drummond AJ, Xie D, Baele G, Suchard MA. Posterior Summarization in Bayesian Phylogenetics Using Tracer 1.7. *Syst Biol*. 2018;67(5):901-904. doi:10.1093/SYSBIO/SYY032

164. Heled J. Extended Bayesian skyline plot tutorial for BEAST 2. Published 2015. http://evomicsorg.wpengine.netdna-cdn.com/wp-content/uploads/2015/11/ebsp2-tut1.pdf

165. Team RC, R Foundation for Statistical Computing, Vienna A. R: a language and environment for statistical computing. Published online 2018. https://www.r-project.org/.

166. Chen S, Zhou Y, Chen Y, Gu J. fastp: an ultra-fast all-in-one FASTQ preprocessor. *Bioinformatics*. 2018;34(17):i884-i890. doi:10.1093/BIOINFORMATICS/BTY560

167. Langmead B, Salzberg SL. Fast gapped-read alignment with Bowtie 2. *Nat Methods*. 2012;9(4):357-359. doi:10.1038/nmeth.1923

168. Yang X, Charlebois P, Macalalad A, Henn MR, Zody MC. V-Phaser 2: Variant inference for viral

populations. *BMC Genomics*. 2013;14(1):1-10. doi:10.1186/1471-2164-14-674/TABLES/4

169. Eisen RJ, Eisen L, Beard CB. County-Scale Distribution of Ixodes scapularis and Ixodes pacificus (Acari: Ixodidae) in the Continental United States. doi:10.1093/jme/tjv237

170. Thomas LA, Kennedy RC, Eklund CM. Isolation of a Virus Closely Related to Powassan Virus from Dermacentor andersoni Collected along North Cache la Poudre River, Colo. *https://doi.org/103181/00379727-104-25836*. 1960;104(2):355-359. doi:10.3181/00379727-104-25836

171. Normandin E, Solomon IH, Zamirpour S, Lemieux J, Freije CA, Mukerji SS, Tomkins-Tinch C, Park D, Sabeti PC, Piantadosi A. Powassan Virus Neuropathology and Genomic Diversity in Patients With Fatal Encephalitis. *Open Forum Infect Dis*. 2020;7(10). doi:10.1093/OFID/OFAA392

172. Kellman EM, Offerdahl DK, Melik W, Bloom ME. Viral Determinants of Virulence in Tick-Borne Flaviviruses. doi:10.3390/v10060329

173. Piantadosi A, Rubin DB, Mcquillen DP, Hsu L, Lederer PA, Ashbaugh CD, Duffalo C, Duncan R, Thon J, Bhattacharyya S, Basgoz N, Feske SK, Lyons JL. Clinical Infectious Diseases Emerging Cases of Powassan Virus Encephalitis in New England: Clinical Presentation, Imaging, and Review of the Literature. Published online 2015. doi:10.1093/cid/civ1005

174. Deardorff ER, Nofchissey RA, Cook JA, Hope AG, Tsvetkova A, Talbot SL, Ebel GD. Powassan Virus in Mammals, Alaska and New Mexico, USA, and Russia, 2004–2007. *Emerg Infect Dis*. 2013;19(12):2012. doi:10.3201/EID1912.130319

175. Campbell O, Krause PJ. The emergence of human Powassan virus infection in North America. *Ticks Tick Borne Dis*. 2020;11(6):101540. doi:10.1016/J.TTBDIS.2020.101540

176. Bazer D, Orwitz M, Koroneos N, Syritsyna O, Wirkowski E. Powassan Encephalitis: A Case Report from Long Island, New York, USA (P18-1.002). *Neurology*. 2022;98(18 Supplement):1045. http://n.neurology.org/content/98/18_Supplement/1045.abstract

177. Godsey MS, Savage HM, Burkhalter KL, Bosco-Lauth AM, Delorey MJ. Transmission of Heartland Virus (Bunyaviridae: Phlebovirus) by Experimentally Infected Amblyomma americanum (Acari: Ixodidae). *J Med Entomol*. 2016;53(5):1226-1233. doi:10.1093/jme/tjw080

178. Thomas LA, Kennedy RC, Eklund CM. Isolation of a Virus Closely Related to Powassan Virus from Dermacentor andersoni Collected along North Cache la Poudre River, Colo. *Proc Soc Exp Biol Med*. 1960;104(2):355-359.

179. Hermance ME, Thangamani S. Powassan Virus: An Emerging Arbovirus of Public Health Concern in North America. *Vector Borne Zoonotic Dis*. 2017;17(7):453-462. doi:10.1089/vbz.2017.2110

180. Halliday JEB, Hampson K, Hanley N, Lembo T, Sharp JP, Haydon DT, Cleaveland S. Driving improvements in emerging disease surveillance through locally relevant capacity strengthening. *Science*. 2017;357(6347):146. doi:10.1126/SCIENCE.AAM8332

181. Jayatilleke K. Challenges in Implementing Surveillance Tools of High-Income Countries (HICs) in Low Middle Income Countries (LMICs). *Curr Treat Options Infect Dis 2020 123*. 2020;12(3):191-201. doi:10.1007/S40506-020-00229-2

182. Grubaugh ND, Sharma S, Krajacich BJ, Fakoli LS, Bolay FK, Diclaro JW, Johnson WE, Ebel GD, Foy BD, Brackney DE. Xenosurveillance: A Novel Mosquito-Based Approach for Examining the Human-Pathogen Landscape. *PLoS Negl Trop Dis*. 2015;9(3). doi:10.1371/journal.pntd.0003628

183. Gyawali N, Murphy AK, Hugo LE, Devine GJ. A micro-PRNT for the detection of Ross River

virus antibodies in mosquito blood meals: A useful tool for inferring transmission pathways. *PLoS One*. 2020;15(7 July):e0229314. doi:10.1371/journal.pone.0229314

184. Reeves LE, Gillett-Kaufman JL, Kawahara AY, Kaufman PE. Barcoding blood meals: New vertebrate-specific primer sets for assigning taxonomic identities to host DNA from mosquito blood meals. *PLoS Negl Trop Dis*. 2018;12(8):e0006767. doi:10.1371/journal.pntd.0006767

185. Abudurexiti A, Adkins S, Alioto D, Alkhovsky S V., Avšič-Županc T, Ballinger MJ, Bente DA, Beer M, Bergeron É, Blair CD, Briese T, Buchmeier MJ, Burt FJ, Calisher CH, Cháng C, Charrel RN, Choi IR, Clegg JCS, de la Torre JC, de Lamballerie X, Dèng F, Di Serio F, Digiaro M, Drebot MA, Duàn X, Ebihara H, Elbeaino T, Ergünay K, Fulhorst CF, Garrison AR, Gāo GF, Gonzalez JPJ, Groschup MH, Günther S, Haenni AL, Hall RA, Hepojoki J, Hewson R, Hú Z, Hughes HR, Jonson MG, Junglen S, Klempa B, Klingström J, Kòu C, Laenen L, Lambert AJ, Langevin SA, Liu D, Lukashevich IS, Luò T, Lǚ C, Maes P, de Souza WM, Marklewitz M, Martelli GP, Matsuno K, Mielke-Ehret N, Minutolo M, Mirazimi A, Moming A, Mühlbach HP, Naidu R, Navarro B, Nunes MRT, Palacios G, Papa A, Pauvolid-Corrêa A, Pawęska JT, Qiáo J, Radoshitzky SR, Resende RO, Romanowski V, Sall AA, Salvato MS, Sasaya T, Shěn S, Shí X, Shirako Y, Simmonds P, Sironi M, Song JW, Spengler JR, Stenglein MD, Sū Z, Sūn S, Táng S, Turina M, Wáng B, Wáng C, Wáng H, Wáng J, Wèi T, Whitfield AE, Zerbini FM, Zhāng J, Zhāng L, Zhāng Y, et al. Taxonomy of the order Bunyavirales: update 2019. *Arch Virol*. 2019;164(7):1949-1965. doi:10.1007/S00705-019-04253-6

186. Cowling DW, Gardner IA, Johnson WO. Comparison of methods for estimation of individual-level prevalence based on pooled samples. *Prev Vet Med*. 1999;39(3):211-225. doi:10.1016/S0167-5877(98)00131-7

187. Asturias EJ, Heinrichs G, Domek G, Brett J, Shick E, Cunningham M, Bull S, Celada M, Newman LS, Tenney L, Krisher L, Luna-Asturias C, McConnell K, Berman S. The Center for Human Development in Guatemala: An Innovative Model for Global Population Health. *Adv Pediatr*. 2016;63(1):357-387. doi:10.1016/j.yapd.2016.04.001

188. Barr AR, Brown AWA, Downs WG, Drummond RO, Furman DP, Holland GP, Hoogatraal H, Kanu R, Macdanald WW, Marchette NJ, Rabinovich J, Rageau J, Scanlon JE, Sonenshine DE, Tarasevich I, Traub R, Wharton RHCEY, Tempelis CH. REVIEW ARTICLE: Host-Feeding Patterns of Mosquitoes, with a Review of Advances in Analysis of Blood Meals by Serology. *J Med Entomol*. 1975;11(6):635-653. doi:10.1093/JMEDENT/11.6.635

189. Takken W, Verhulst NO. Host preferences of blood-feeding mosquitoes. *Annu Rev Entomol*. 2013;58:433-453. doi:10.1146/ANNUREV-ENTO-120811-153618

190. Guzman MG, Halstead SB, Artsob H, Buchy P, Farrar J, Gubler DJ, Hunsperger E, Kroeger A, Margolis HS, Martí-nez E, Nathan MB, Pelegrino JL, Simmons C, Yoksan S, Peeling RW. Dengue: a continuing global threat. *Nat Rev Microbiol 2010 812*. 2010;8(12):S7-S16. doi:10.1038/nrmicro2460

191. Fauver JR, Grubaugh ND, Krajacich BJ, Weger-Lucarelli J, Lakin SM, Fakoli LS, Bolay FK, Diclaro JW, Dabiré KR, Foy BD, Brackney DE, Ebel GD, Stenglein MD. West African Anopheles gambiae mosquitoes harbor a taxonomically diverse virome including new insect-specific flaviviruses, mononegaviruses, and totiviruses. *Virology*. 2016;498:288-299. doi:10.1016/j.virol.2016.07.031

192. Ramos-Nino ME, Fitzpatrick DM, Eckstrom KM, Tighe S, Hattaway LM, Hsueh AN, Stone DM, Dragon JA, Cheetham S. Metagenomic analysis of Aedes aegypti and Culex quinquefasciatus mosquitoes from Grenada, West Indies. *PLoS One*. 2020;15(4):e0231047. doi:10.1371/JOURNAL.PONE.0231047

193. da Silva Ferreira R, de Toni Aquino da Cruz LC, de Souza VJ, da Silva Neves NA, de Souza VC, Filho LCF, da Silva Lemos P, de Lima CPS, Naveca FG, Atanaka M, Nunes MRT, Slhessarenko RD. Insect-specific viruses and arboviruses in adult male culicids from Midwestern Brazil. *Infect Genet Evol*. 2020;85:104561. doi:10.1016/J.MEEGID.2020.104561

194. Pauvolid-Corrêa C, Solberg A, Couto-Lima O, Nogueira DM, Langevin RM, Komar S. Novel viruses isolated from mosquitoes in Pantanal, Brazil. *Genome Announc*. 2016;4(6):1195-1211. doi:10.1128/genomeA.01195-16

195. Ribeiro G de O, Monteiro FJC, Rego MO da S, Ribeiro ESD, de Castro DF, Caseiro MM, Marinho R dos SS, Komninakis SV, Witkin SS, Deng X, Delwart E, Sabino EC, da Costa AC, Leal É. Detection of RNA-Dependent RNA Polymerase of Hubei Reo-Like Virus 7 by Next-Generation Sequencing in Aedes aegypti and Culex quinquefasciatus Mosquitoes from Brazil. *Viruses*. 2019;11(2):147. doi:10.3390/V11020147

196. Vibin J, Chamings A, Collier F, Klaassen M, Nelson TM, Alexandersen S. Metagenomics detection and characterisation of viruses in faecal samples from Australian wild birds. *Sci Rep*. 2018;8(1):8686. doi:10.1038/S41598-018-26851-1

197. Vasilakis N, Tesh RB. Insect-specific viruses and their potential impact on arbovirus transmission. *Curr Opin Virol*. 2015;15:69-74. doi:10.1016/J.COVIRO.2015.08.007

198. Öhlund P, Lundén H, Blomström AL. Insect-specific virus evolution and potential effects on vector competence. *Virus Genes*. 2019;55(2):127. doi:10.1007/S11262-018-01629-9

199. Olson D, Lamb M, Lopez MR, Colborn K, Paniagua-Avila A, Zacarias A, Zambrano-Perilla R, Rodríguez-Castro SR, Cordon-Rosales C, Asturias EJ. Performance of a mobile phone app-based participatory syndromic surveillance system for acute febrile illness and acute gastroenteritis in rural Guatemala. *J Med Internet Res*. 2017;19(11). doi:10.2196/jmir.8041

200. Organization WH. *Handbook : IMCI Integrated Management of Childhood Illness*. World Health Organization; 2005. https://apps.who.int/iris/handle/10665/42939

201. Cark-Gil S, Darsie F. The Mosquitoes of Guatemala. Their Identification, Distribution and Bionomics, With Keys to Adult Females and Larvae in English and Spanish. *Mosq Syst*. 1983;15(3):151-284.

202. Hemmerter S, Šlapeta J, Van Den Hurk AF, Cooper RD, Whelan PI, Russell RC, Johansen CA, Beebe NW. A curious coincidence: mosquito biodiversity and the limits of the Japanese encephalitis virus in Australasia. *BMC Evol Biol*. 2007;7. doi:10.1186/1471-2148-7-100

203. Ivanova N V., Zemlak TS, Hanner RH, Hebert PDN. Universal primer cocktails for fish DNA barcoding. *Mol Ecol Notes*. 2007;7(4):544-548. doi:10.1111/j.1471-8286.2007.01748.x

204. Ratnasingham S, Hebert PDN. The Barcode of Life Data System. *Mol Ecol Notes*. 2007;7(April 2016):355-364. doi:10.1111/j.1471-8286.2006.01678.x

205. Fauver JR, Akter S, Morales AIO, Black WC, Rodriguez AD, Stenglein MD, Ebel GD, Weger-Lucarelli J. A reverse-transcription/RNase H based protocol for depletion of mosquito ribosomal RNA facilitates viral intrahost evolution analysis, transcriptomics and pathogen discovery. *Virology*. 2019;528:181-197. doi:10.1016/j.virol.2018.12.020

206. Chrzastek K, Lee D hun, Smith D, Sharma P, Suarez DL, Pantin-Jackwood M, Kapczynski DR. Use of Sequence-Independent, Single-Primer-Amplification (SISPA) for rapid detection, identification, and characterization of avian RNA viruses. *Virology*. 2017;509:159-166. doi:10.1016/j.virol.2017.06.019

207. Cross S, Kapuscinski M, Perino J, Maertens B, Weger-Lucarelli J, Ebel G, Stenglein M, Cross ST,

Kapuscinski ML, Perino J, Maertens BL, Weger-Lucarelli J, Ebel GD, Stenglein MD. Co-Infection Patterns in Individual Ixodes scapularis Ticks Reveal Associations between Viral, Eukaryotic and Bacterial Microorganisms. *Viruses*. 2018;10(7):388. doi:10.3390/v10070388

208. Babraham Bioinformatics - FastQC A Quality Control tool for High Throughput Sequence Data. Accessed June 16, 2021. https://www.bioinformatics.babraham.ac.uk/projects/fastqc/

209. Martin M. Cutadapt removes adapter sequences from high-throughput sequencing reads. *EMBnet.journal*. 2011;17(1):10. doi:10.14806/ej.17.1.200

210. Li W, Godzik A. Cd-hit: A fast program for clustering and comparing large sets of protein or nucleotide sequences. *Bioinformatics*. 2006;22(13):1658-1659. doi:10.1093/bioinformatics/btl158

211. Bankevich A, Nurk S, Antipov D, Gurevich AA, Dvorkin M, Kulikov AS, Lesin VM, Nikolenko SI, Pham S, Prjibelski AD, Pyshkin A V., Sirotkin A V., Vyahhi N, Tesler G, Alekseyev MA, Pevzner PA. SPAdes: A new genome assembly algorithm and its applications to single-cell sequencing. *J Comput Biol*. 2012;19(5):455-477. doi:10.1089/cmb.2012.0021

212. Camacho C, Coulouris G, Avagyan V, Ma N, Papadopoulos J, Bealer K, Madden TL. BLAST+: Architecture and applications. *BMC Bioinformatics*. 2009;10(1):1-9. doi:10.1186/1471-2105-10-421

213. Altschul SF, Gish W, Miller W, Myers EW, Lipman DJ. Basic local alignment search tool. *J Mol Biol*. 1990;215(3):403-410. doi:10.1016/S0022-2836(05)80360-2

214. Buchfink B, Xie C, Huson DH. Fast and sensitive protein alignment using DIAMOND. *Nat Methods*. 2014;12(1):59-60. doi:10.1038/nmeth.3176

215. Laue T, Emmerich P, Schmitz H. Detection of dengue virus RNA in patients after primary or secondary dengue infection by using the TaqMan automated amplification system. *J Clin Microbiol*. 1999;37(8):2543-2547. doi:10.1128/JCM.37.8.2543-2547.1999

216. Weger-Lucarelli J, Garcia SM, Rückert C, Byas A, O'Connor SL, Aliota MT, Friedrich TC, O'Connor DH, Ebel GD. Using barcoded Zika virus to assess virus population structure in vitro and in Aedes aegypti mosquitoes. *Virology*. 2018;521:138-148. doi:10.1016/j.virol.2018.06.004

217. Aliota MT, Dudley DM, Newman CM, Weger-Lucarelli J, Stewart LM, Koenig MR, Breitbach ME, Weiler AM, Semler MR, Barry GL, Zarbock KR, Haj AK, Moriarty R V., Mohns MS, Mohr EL, Venturi V, Schultz-Darken N, Peterson E, Newton W, Schotzko ML, Simmons HA, Mejia A, Hayes JM, Capuano S, Davenport MP, Friedrich TC, Ebel GD, O'Connor SL, O'Connor DH. Molecularly barcoded Zika virus libraries to probe in vivo evolutionary dynamics. *PLoS Pathog*. 2018;14(3):1-25. doi:10.1371/journal.ppat.1006964

APPENDIX A: ADDITIONAL ACADEMIC ACCOMPLISHMENTS

During my first-year rotation in Dr. Sue VandeWoude's lab, I worked with Dr. Eric Gagne to project to determine the capability of extracting and sequencing viral DNA from puma teeth and obtaining sufficient sequence data to assess ecological patterns based on phylogenetic structuring. Specifically, I was involved in performing PCR and extracting amplified bands of feline foamy virus and feline immunodeficiency virus from puma tooth samples. Gratefully, my work was rewarded with co-authorship on a manuscript titled "Viral Sequences Recovered from Puma Tooth DNA Reconstruct Statewide Viral Phylogenies." in the journal *Frontiers of Ecology and Evolution* in 2021.

Also in my first year in 2017, I submitted a proposal for the Graduate Research Fellowship Program with the National Science Foundation. The proposal was centered around the genetic ecology and evolution of feline immunodeficiency virus in pumas. I was very proud to receive excellent reviews, however the proposal was still not funded.

In 2019, after passing my preliminary exams, I submitted a new proposal for the Ruth Kirschstein Predoctoral Fellowship Award with the National Institutes of Health. The proposal was written on my proposed thesis project and received outstanding reviews. It ended up scoring in the top 5% of applications and successfully funded the remaining years of my Ph.D. work.

In 2021, I was offered an internship with Dr. May Chu at the University of Colorado Anschutz. I spent five months working with Dr. Chu and another public health student, Mattie Cassaday, to organize a virtual international forum on Zika Diagnostics. The forum included panelists and speakers from UNICEF, WHO, USAID, local governments, and industry leaders to speak on funding, developing, and producing, and utilizing Zika virus diagnostics. The forum brought together over 100 participants from 30 countries in industry, government, and academia. I also had the opportunity to help write the following meeting report which was published on the UNICEF website.

A)

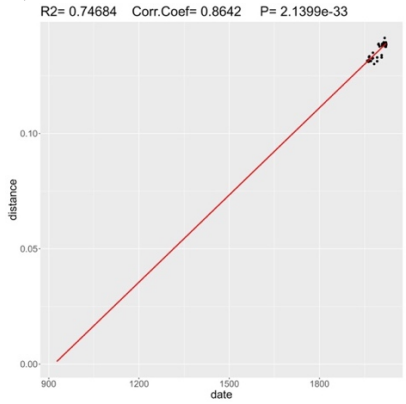

B)

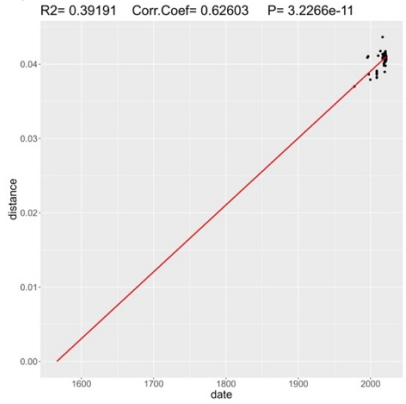

C)

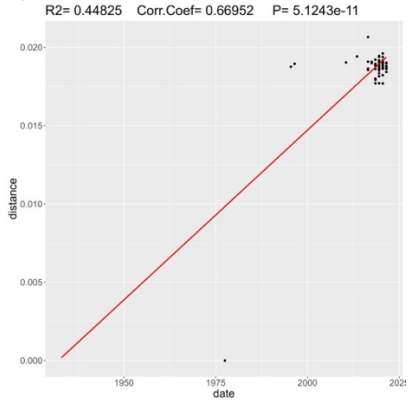

Figure S2.1. Root-to-tip analysis of A) all 108 POWV sequences; B) 91 DTV sequences, and C) 75 DTV sequences from the northeast U.S. alone. The slope for each plot is: 1.26E-4 (A), 9.00E-5 (B), and 2.17E-4 (C).

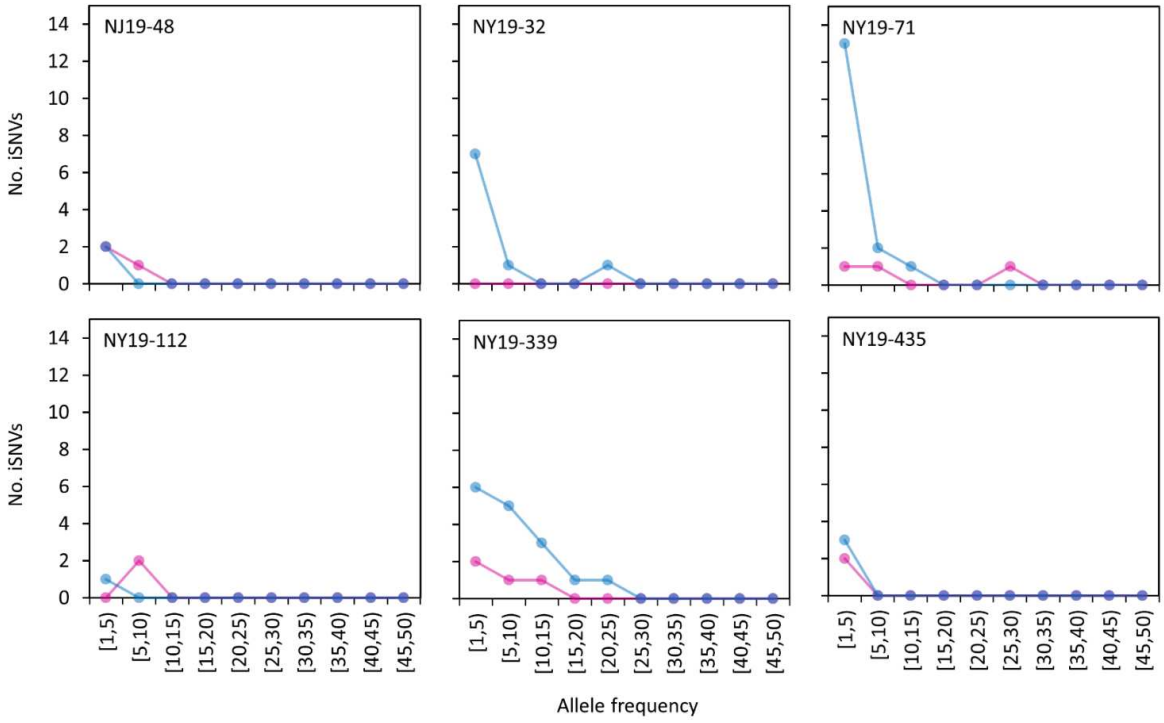

Figure S2.2. Distribution of iSNV allele frequencies between primary tick isolates (pink) and single passage BHK (blue).

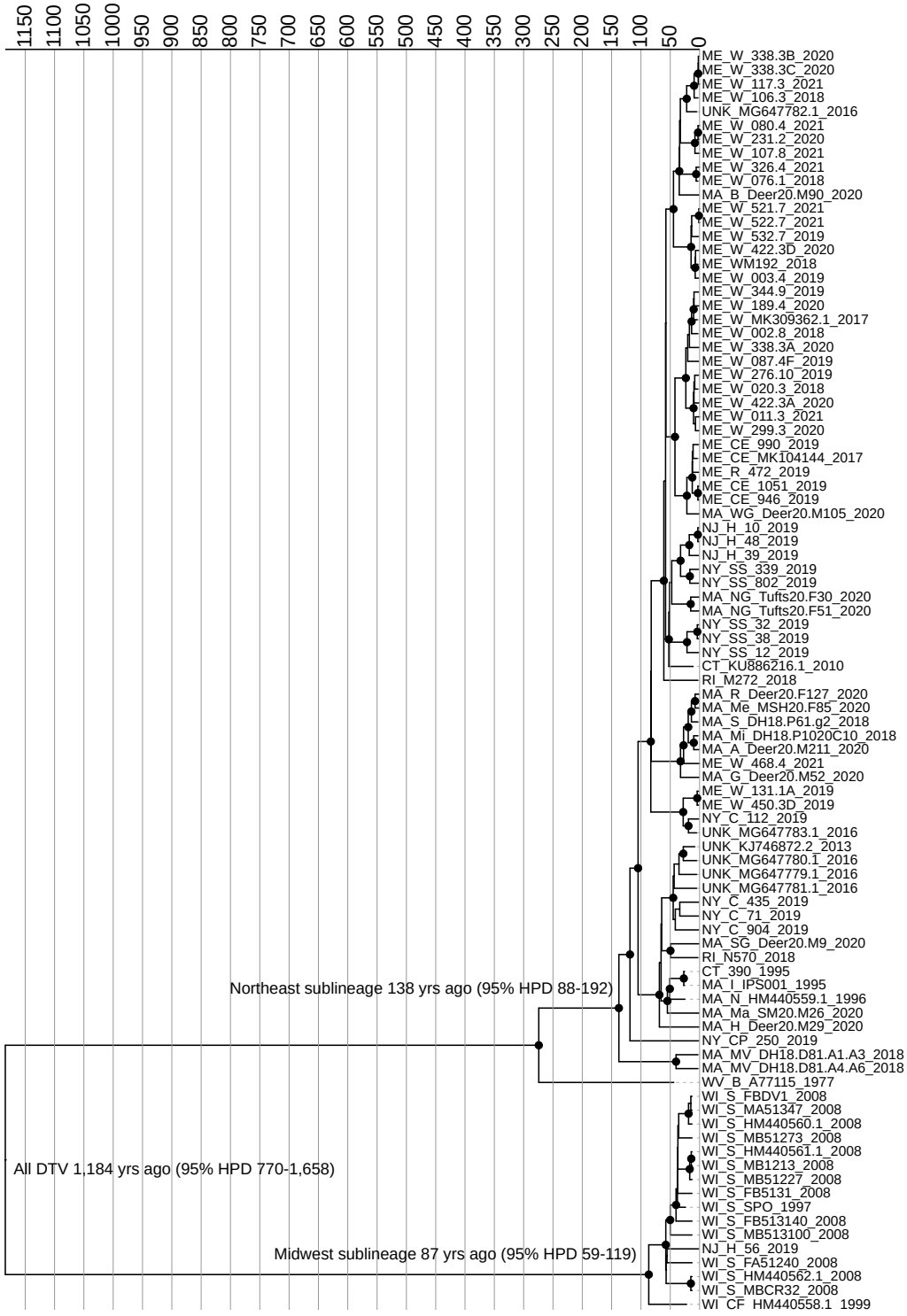

Figure S2.3: Maximum-clade credibility tree of ninety-one Deer Tick Virus genome sequences using a strict clock model and exponential coalescent tree prior. Sequence names indicate location, unique identifier, and year. GenBank accession numbers are included for previously-reported sequences. Nodes with a posterior probability of 0.95 or higher are marked with circles.

Table S2.1. Sample information and sequencing metrics. For each sample newly sequenced in this study, the table lists collection date (or year if only year is available), collection location, and passage history. SM: suckling mouse, B: BHK, V: Vero.

Sample	Collection Date	Location	Passage history	Total Reads	Genome Coverage	Depth
CT_390_1995	1995	Connecticut	SM1B3V1	10,694,347	100%	11,663
MA_A_Deer20.M211_2020	2020	Arena, MA	0	1,990,630	100%	415
MA_B_Deer20.M90_2020	2020	Bowdoinham, MA	0	987,547	100%	136
MA_G_Deer20.M52_2020	2020	Glenburn, MA	0	2,191,421	100%	366
MA_H_Deer20.M29_2020	2020	Harvard, MA	0	1,077,300	100%	246
MA_I_IPS001_1995	1995	Ipswich, MA	SM1B2	12,237,645	100%	33,819
MA_Ma_SM20.M26_2020	2020	Marshfield, MA	0	134,806	99%	24
MA_Me_MSH20.F85_2020	2020	Medfield, MA	0	1,118,040	100%	84
MA_Mi_DH18.P1020C10_2018	2018	Millis, MA	0	339,653	99%	65
MA_MV_DH18.D81.A1.A3_2018	2018	Martha's Vineyard, MA	0	317,769	99%	141
MA_MV_DH18.D81.A4.A6_2018	2018	Martha's Vineyard, MA	0	139,231	98%	97
MA_NG_Tufts20.F30_2020	2020	North Grafton, MA	0	2,134,002	97%	35
MA_NG_Tufts20.F51_2020	2020	North Grafton, MA	0	2,104,096	100%	1,064
MA_R_Deer20.F127_2020	2020	Rochester, MA	0	2,183,464	99%	38
MA_S_DH18.P61.g2_2018	2018	Sherborn, MA	0	381,416	99%	184
MA_SG_Deer20.M9_2020	2020	South Grafton, MA	0	242,640	100%	246
MA_WG_Deer20.M105_2020	2020	West Gray, MA	0	3,501,882	100%	3,397
ME_CE_1051_2019	2019-10-30	Jordan Rd, Cape Elizabeth, ME	0	787,495	100%	2,493
ME_CE_946_2019	2019-10-30	Jordan Rd, Cape Elizabeth, ME	0	803,651	100%	2,195
ME_CE_990_2019	2019-10-30	Jordan Rd, Cape Elizabeth, ME	0	834,072	100%	2,356
ME_R_472_2019	2019-05-16	Oyster River Bog, Rockland, ME	0	104,496,691	98%	25
ME_W_002.8_2018	2018-09-27	Wells, ME	0	16,489,328	98%	61
ME_W_003.4_2019	2019-09-24	Wells, ME	0	5,659,209	99%	194

ME_W_011.3_2021	2021-04-15	Wells, ME	0	1,596,657	99%	651
ME_W_020.3_2018	2018-06-07	Wells, ME	0	15,528,025	99%	169
ME_W_076.1_2018	2018-10-19	Wells, ME	0	7,477,408	99%	3,928
ME_W_080.4_2021	2021-04-07	Wells, ME	0	1,517,187	99%	206
ME_W_087.4F_2019	2019-10-09	Wells, ME	0	7,276,742	98%	293
ME_W_106.3_2018	2018-10-25	Wells, ME	0	12,677,074	99%	643
ME_W_107.8_2021	2021-04-07	Wells, ME	0	1,491,703	99%	52
ME_W_117.3_2021	2021-04-23	Wells, ME	0	1,563,502	99%	60
ME_W_131.1A_2019	2019-10-16	Wells, ME	0	13,676,536	99%	893
ME_W_189.4_2020	2020-10-15	Wells, ME	0	38,213,127	99%	138
ME_W_231.2_2020	2020-10-22	Wells, ME	0	28,086,588	99%	180
ME_W_276.10_2019	2019-10-16	Wells, ME	0	5,043,928	99%	457
ME_W_299.3_2020	2020-10-08	Wells, ME	0	34,309,318	99%	291
ME_W_326.4_2021	2021-10-07	Wells, ME	0	1,328,936	98%	93
ME_W_338.3A_2020	2020-10-20	Wells, ME	0	35,296,095	99%	127
ME_W_338.3B_2020	2020-10-20	Wells, ME	0	33,601,388	99%	342
ME_W_338.3C_2020	2020-10-20	Wells, ME	0	17,549,357	100%	242
ME_W_344.9_2019	2019-06-28	Wells, ME	0	10,484,269	99%	210
ME_W_422.3A_2020	2020-11-05	Wells, ME	0	27,423,922	99%	118
ME_W_422.3D_2020	2020-11-05	Wells, ME	0	30,026,014	99%	222
ME_W_450.3D_2019	2019-10-25	Wells, ME	0	7,807,053	99%	140
ME_W_468.4_2021	2021-10-28	Wells, ME	0	1,365,482	96%	24
ME_W_521.7_2021	2021-11-04	Wells, ME	0	1,395,931	96%	18
ME_W_522.7_2021	2021-11-04	Wells, ME	0	1,125,952	99%	360
ME_W_532.7_2019	2019-10-25	Wells, ME	0	13,672,685	99%	827
ME_WM192_2018	2018	Wells, ME	0	449,817	99%	455
NJ_H_10_2019	2019-05-04	Millbrook Flatbrook Rd, Hardwick, NJ	0	32,106,046	100%	609

NJ_H_39_2019	2019-05-04	Millbrook Flatbrook Rd, Hardwick, NJ	0	21,699,338	99%	52
NJ_H_48_2019	2019-05-04	Millbrook Flatbrook Rd, Hardwick, NJ	0	36,911,784	100%	628
NJ_H_56_2019	2019-05-04	Millbrook Flatbrook Rd, Hardwick, NJ	0	33,157,057	99%	30
NY_C_112_2019	2019-05-02	Connetquot, NY	0	591,415	100%	1,100
NY_C_435_2019	2019-05-02	Connetquot, NY	0	765,182	100%	950
NY_C_71_2019	2019-05-02	Connetquot, NY	0	342,482	100%	371
NY_C_904_2019	2019-05-02	Connetquot, NY	0	823,715	99%	11
NY_CP_250_2019	2019-05-01	Cedar Pointe, NY	0	178,126	100%	642
NY_SS_12_2019	2019-05-07	Saratoga Springs, NY	0	729,095	98%	42
NY_SS_32_2019	2019-05-06	Saratoga Springs, NY	0	356,883	99%	130
NY_SS_339_2019	2019-05-06	Saratoga Springs, NY	0	329,651	100%	308
NY_SS_38_2019	2019-05-06	Saratoga Springs, NY	0	797,322	98%	58
NY_SS_802_2019	2019-05-06	Saratoga Springs, NY	0	448,489	100%	491
ONT_EFT_M8998_1964	1964	E. Ferris township, Ontario	P1SM1V1B1	2,151,720	100%	4,512
ONT_LT_M11665_1965	1965	Laurier Township, Ontario	P1SM1V1B1	3,617,759	100%	4,187
ONT_M1409_1960s	1960	Ontario	P4SM1B1	1,667,415	100%	3,996
ONT_NB_142762_1962	1962	North Bay, Ontario	SM3B1	1,909,287	100%	2,329
ONT_NB_198264_1964	1964	North Bay Ontario	P2V1B1	2,022,844	100%	3,110
ONT_T182381_1981	1981	Ontario	P1SM1V1B1	1,595,983	100%	3,527
RI_M272_2018	2018	"Trust", RI	0	413,638	97%	26
RI_N570_2018	2018	"Crew", RI	0	383,067	98%	67
UNK_2228791_1991	1991	Unknown	P9SM1B1	1,578,334	100%	3,410
WI_S_FA51240_2008	2008-05-12	Spooner, WI	B2	10,173,056	100%	34,756
WI_S_FB5131_2008	2008-05-13	Spooner, WI	B2	13,149,650	100%	11,700
WI_S_FB513140_2008	2008-05-13	Spooner, WI	B2	1,291,261	99%	1,413

WI_S_FBDV1_2008	2008-05-12	Spooner, WI	B2	7,546,905	100%	24,009
WI_S_MA51347_2008	2008-05-13	Spooner, WI	B2	8,146,474	100%	10,983
WI_S_MB1213_2008	2008-05-13	Spooner, WI	B2	3,431,284	100%	5,351
WI_S_MB51227_2008	2008-05-12	Spooner, WI	B2	1,642,358	100%	13,966
WI_S_MB51273_2008	2008-05-12	Spooner, WI	B2	2,102,424	100%	4,973
WI_S_MB513100_2008	2008-05-13	Spooner, WI	B2	1,419,789	100%	12,279
WI_S_MBCR32_2008	2008	Spooner, WI	B2	8,451,442	100%	31,104
WI_S_SPO_1997	1997	Spooner, WI	M1V2B2	1,859,908	100%	4,921
WV_B_A77115_1977	1977	Braxton Co, West Virginia	SM3B1	1,420,756	100%	10,622

Table S2.2. Model testing results. Best-fitting models for each analysis are in bold. CEBS: Coalescent Extended Bayesian Skyline; NS: Nested Sampling

Substitution Model	Clock Model	Tree Prior	Mean Clock Rate	Clock Rate 95% HPD Interval	Growth Rate	NS Marginal Likelihood	NS Standard Deviation
All DTV							
GTR+G	Strict	Constant Coalescent	5.8 E-05	3.6 E-5, 8.2 E-5		-26964.5	7.9
GTR+G	Lognormal	Constant Coalescent	7.6 E-05	4.6 E-5, 1.1 E-4		-26996.0	8.1
GTR+G	Strict	CEBS	5.2 E-05	2.6 E-5, 7.7 E-5		-26978.6	5.4
GTR+G	Lognormal	CEBS	6.7 E-05	3.4 E-5, 1.0 E-4		-27014.1	6.0
GTR+G	**Strict**	**Exponential Coalescent**	**6.0 E-05**	**4.0 E-5, 8.4 E-5**	**4.1 E-04**	**-26963.7**	**5.7**
GTR+G	Lognormal	Exponential Coalescent	8.1 E-05	4.9 E-5, 1.2 E-4	1.1 E-03	-26991.0	5.7
Northeast DTV							
TN93	Strict	Constant Coalescent	3.4 E-05	1.2 E-5, 5.4 E-5		-27543.9	5.3
TN93	Lognormal	Constant Coalescent	4.3 E-05	1.7 E-5, 7.2 E-5		-23080.3	4.9
TN93	Strict	CEBS	2.7 E-05	4.1 E-6, 4.9 E-5		-23075.3	5.1
TN93	Lognormal	CEBS	3.4 E-05	6.5 E-6, 6.4 E-5		-23089	4.9
TN93	**Strict**	**Exponential Coalescent**	**3.2 E-05**	1.2 E-5, 5.3 E-5	**1.0 E-2**	**-23074.1**	**5**
TN93	Lognormal	Exponential Coalescent	4.2 E-05	1.5 E-5, 7.1 E-5	1.5 E-2	-23089.7	5.2
GTR+G	Strict	CEBS	2.7 E-05	4.2 E-6, 5.0 E-5		-23099.4	5.4
GTR+G	**Lognormal**	**CEBS**	**3.4 E-05**	5.6 E-6, 6.3 E-5		**-23074.5**	**5.2**
GTR+G	Strict	Exponential Coalescent		Did not converge			
GTR+G	Lognormal	Exponential Coalescent	5.7 E-05	3.2 E-5, 8.7 E-5	1.7 E-2	-23080.7	5.3

Table S2.3. Sequencing metrics of tick and BHK-isolated viruses.

Isolate	Source	Library	Raw Reads	Mapped	AvgNTDep
NJ19-48	Tick	L1	73823568	845198	7365
NJ19-48	Tick	L2	2960608	60028	656
NJ19-48	BHK	L1	3477206	1669071	20640
NJ19-48	BHK	L2	5201464	2259573	28311
NY19-32	Tick	L1	713766	20667	242
NY19-32	Tick	L2	871478	11250	133
NY19-32	BHK	L1	2584880	958812	11490
NY19-32	BHK	L2	2448432	802692	9779
NY19-71	Tick	L1	684964	17485	214
NY19-71	Tick	L2	4399272	36425	437
NY19-71	BHK	L1	2519946	322520	3817
NY19-71	BHK	L2	3249430	360460	4487
NY19-339	Tick	L1	1575562	8870	116
NY19-339	Tick	L2	11164156	30305	385
NY19-339	BHK	L1	1919628	896407	10958
NY19-339	BHK	L2	3658396	1443035	17675
NY19-435	Tick	L1	1530364	72229	886
NY19-435	Tick	L2	3009250	87284	1040
NY19-435	BHK	L1	2218344	1006819	12333
NY19-435	BHK	L2	3188920	1171682	14189

Table S2.4. Confirmed iSNVs found in duplicate sequencing libraries.

Isolate	Source	NT	NT-Index	Con	Variant	AF*	Type	Subtype	Region	ΔAA
NJ19-48	Tick	451	462	C	T	3.19	Sub	NS	prM	H24Y
NJ19-48	Tick	706	717	A	G	9.28	Sub	NS	prM	R109G
NJ19-48	Tick	2543	2554	A	G	2.94	Sub	NS	ns1	D40G
NJ19-48	BHK	2543	2554	A	G	3.21	Sub	NS	ns1	D40G
NJ19-48	BHK	5169	5180	T	C	1.47	Sub	S	ns3	P201P
NJ19-48	BHK	7443	7454	C	T	1.54	Sub	S	ns4B	N188N
NJ19-48	BHK	9009	9020	G	A	1.15	Sub	S	ns5	K458K
NJ19-48	BHK	9105	9116	A	G	2.23	Sub	S	ns5	L490L
NY19-112	Tick	715	717	A	G	6.00	Sub	NS	prM	R109G
NY19-112	Tick	10372	10374	T	C	6.07	Sub	NCR	3'UTR	NCR
NY19-112	BHK	9093	9095	T	C	1.22	Sub	S	ns5	R483R
NY19-112	BHK	10372	10374	T	C	4.32	Sub	NCR	3'UTR	NCR
NY19-32	BHK	1123	1147	C	T	1.34	Sub	NS	E	T68M
NY19-32	BHK	2010	2034	A	G	2.04	Sub	NS	E	T364A
NY19-32	BHK	3152	3176	C	T	2.17	Sub	S	ns1	V247V
NY19-32	BHK	3435	3459	T	A	3.94	Sub	NS	ns1	S342T
NY19-32	BHK	5704	5728	A	G	23.02	Sub	NS	ns3	Q384R
NY19-32	BHK	6054	6078	A	G	2.03	Sub	NS	ns3	I501V
NY19-32	BHK	7442	7466	G	A	4.97	Sub	S	ns4B	A192A
NY19-32	BHK	7550	7574	G	A	2.70	Sub	S	ns4B	L228L
NY19-32	BHK	7801	7825	C	T	4.61	Sub	NS	ns5	A60V
NY19-32	BHK	8963	8987	A	G	6.71	Sub	S	ns5	Q447Q
NY19-339	Tick	698	717	A	G	5.27	Sub	NS	prM	R109G
NY19-339	Tick	3031	3050	C	T	4.25	Sub	S	ns1	S205S
NY19-339	Tick	6595	6614	A	G	11.11	Sub	S	ns4A	V57V

NY19-339	Tick	7417	7436	G	A	4.89	Sub	NS	ns4B	M182I
NY19-339	BHK	857	876	A	G	1.02	Sub	NS	prM	M162V
NY19-339	BHK	1308	1327	T	C	12.85	Sub	NS	E	V128A
NY19-339	BHK	1333	1352	A	G	7.78	Sub	S	E	K136K
NY19-339	BHK	1492	1511	A	G	1.62	Sub	S	E	A189A
NY19-339	BHK	1493	1512	A	G	1.94	Sub	NS	E	S190G
NY19-339	BHK	1524	1543	T	C	5.77	Sub	NS	E	M200T
NY19-339	BHK	1596	1615	C	T	1.12	Sub	NS	E	A224V
NY19-339	BHK	1672	1691	A	G	13.01	Sub	S	E	A249A
NY19-339	BHK	2119	2138	T	C	1.03	Sub	S	E	S398S
NY19-339	BHK	2203	2222	A	G	1.20	Sub	S	E	S426S
NY19-339	BHK	3031	3050	C	T	15.05	Sub	S	ns1	S205S
NY19-339	BHK	3125	3144	G	A	1.32	Sub	NS	ns1	G237R
NY19-339	BHK	3148	3167	T	C	1.95	Sub	S	ns1	F244F
NY19-339	BHK	3272	3291	A	G	1.46	Sub	NS	ns1	S286G
NY19-339	BHK	3324	3343	C	A	2.32	Sub	NS	ns1	T303N
NY19-339	BHK	3846	3865	A	G	9.71	Sub	NS	ns2A	N124S
NY19-339	BHK	4664	4683	C	A	1.04	Sub	NS	ns3	H36N
NY19-339	BHK	5140	5159	C	T	4.01	Sub	S	ns3	I194I
NY19-339	BHK	5284	5303	A	G	1.51	Sub	S	ns3	Q242Q
NY19-339	BHK	5434	5453	A	G	1.61	Sub	S	ns3	E292E
NY19-339	BHK	6007	6026	T	C	7.68	Sub	S	ns3	D483D
NY19-339	BHK	6460	6479	A	G	2.22	Sub	S	ns4A	V12V
NY19-339	BHK	6595	6614	A	G	23.40	Sub	S	ns4A	V57V
NY19-339	BHK	6689	6708	G	A	1.26	Sub	NS	ns4A	V89M
NY19-339	BHK	6856	6875	A	C	2.09	Sub	S	2K	I18I
NY19-339	BHK	6916	6935	C	T	3.87	Sub	S	ns4B	G15G
NY19-339	BHK	7362	7381	A	G	1.35	Sub	NS	ns4B	K164R

NY19-339	BHK	7417	7436	G	A	13.42	Sub	NS	ns4B	M182I
NY19-339	BHK	7483	7502	T	G	1.19	Sub	S	ns4B	A204A
NY19-339	BHK	7616	7635	G	A	1.84	Sub	NS	ns4B	G249R
NY19-339	BHK	8442	8461	A	G	1.98	Sub	NS	ns5	K272R
NY19-339	BHK	8607	8626	A	G	6.02	Sub	NS	ns5	K327R
NY19-339	BHK	9043	9062	C	T	1.32	Sub	S	ns5	S472S
NY19-339	BHK	9097	9116	A	G	1.08	Sub	S	ns5	L490L
NY19-339	BHK	9175	9194	T	G	1.23	Sub	S	ns5	L516L
NY19-339	BHK	9924	9943	A	G	1.49	Sub	NS	ns5	N766S
NY19-339	BHK	10027	10046	G	A	1.95	Sub	S	ns5	A800A
NY19-339	BHK	10372	10391	C	T	1.49	Sub	NCR	3'UTR	NCR
NY19-339	BHK	10401	10420	G	A	1.22	Sub	NCR	3'UTR	NCR
NY19-339	BHK	10465	10484	T	C	1.02	Sub	NCR	3'UTR	NCR
NY19-339	BHK	10474	10493	C	T	1.77	Sub	NCR	3'UTR	NCR
NY19-339	BHK	10528	10547	C	T	1.06	Sub	NCR	3'UTR	NCR
NY19-435	Tick	715	717	A	G	3.40	Sub	NS	prM	R109G
NY19-435	Tick	7682	7684	A	G	4.93	Sub	NS	ns5	K13R
NY19-435	BHK	2090	2092	T	C	2.34	Sub	NS	E	I383T
NY19-435	BHK	4182	4184	A	G	1.07	Sub	S	ns2A	R230R
NY19-435	BHK	5388	5390	T	C	1.22	Sub	S	ns3	T271T
NY19-435	BHK	7173	7175	G	A	1.15	Sub	S	ns4B	V95V
NY19-435	BHK	7682	7684	A	G	3.78	Sub	NS	ns5	K13R
NY19-435	BHK	7701	7703	C	T	1.15	Sub	S	ns5	C19C
NY19-435	BHK	7800	7802	T	C	1.18	Sub	S	ns5	G52G
NY19-435	BHK	8510	8512	A	T	1.24	Sub	NS	ns5	Y289F
NY19-435	BHK	8624	8626	A	G	1.51	Sub	NS	ns5	K327R
NY19-71	Tick	3052	3054	C	T	8.95	Sub	NS	ns1	R207W
NY19-71	Tick	5805	5807	C	T	27.72	Sub	S	ns3	D410D

NY19-71	Tick	7682	7684	A	G	3.89	Sub	NS	ns5	K13R
NY19-71	BHK	850	852	G	A	3.04	Sub	NS	prM	A154T
NY19-71	BHK	913	915	C	T	3.33	Sub	S	prM	L175L
NY19-71	BHK	1183	1185	A	G	2.72	Sub	NS	E	T81A
NY19-71	BHK	1533	1535	T	A	3.07	Sub	S	E	T197T
NY19-71	BHK	1712	1714	T	C	6.42	Sub	NS	E	L257P
NY19-71	BHK	2254	2256	G	A	5.49	Sub	NS	E	V438I
NY19-71	BHK	2869	2871	C	T	2.06	Sub	NS	ns1	P146S
NY19-71	BHK	3052	3054	C	T	2.13	Sub	NS	ns1	R207W
NY19-71	BHK	4014	4016	A	G	2.50	Sub	NS	ns2A	I174M
NY19-71	BHK	4588	4590	T	C	1.32	Sub	NS	ns3	F5L
NY19-71	BHK	4644	4646	C	T	2.98	Sub	S	ns3	G23G
NY19-71	BHK	5063	5065	A	T	1.11	Sub	NS	ns3	Y163F
NY19-71	BHK	5123	5125	T	C	1.50	Sub	NS	ns3	I183T
NY19-71	BHK	5340	5342	C	T	3.72	Sub	S	ns3	N255N
NY19-71	BHK	5382	5384	C	T	1.87	Sub	S	ns3	H269H
NY19-71	BHK	5805	5807	C	T	12.55	Sub	S	ns3	D410D
NY19-71	BHK	6703	6705	G	A	4.36	Sub	NS	ns4A	V88M
NY19-71	BHK	6939	6941	C	T	2.34	Sub	S	ns4B	F17F
NY19-71	BHK	7341	7343	T	C	1.57	Sub	S	ns4B	D151D
NY19-71	BHK	8624	8626	A	G	2.67	Sub	NS	ns5	K327R
NY19-71	BHK	9366	9368	T	C	1.10	Sub	S	ns5	Y574Y
NY19-71	BHK	9513	9515	C	T	1.70	Sub	S	ns5	R623R
NY19-71	BHK	9999	10001	C	T	3.43	Sub	S	ns5	P785P

NT, nucleotide; NT-index, nucleotide indexed to reference genome; Con, consensus; AF, allele frequency; ΔAA, amino acid change.
*For tick isolates, based on frequency in merged library, for BHK based on average frequency across three replicates.

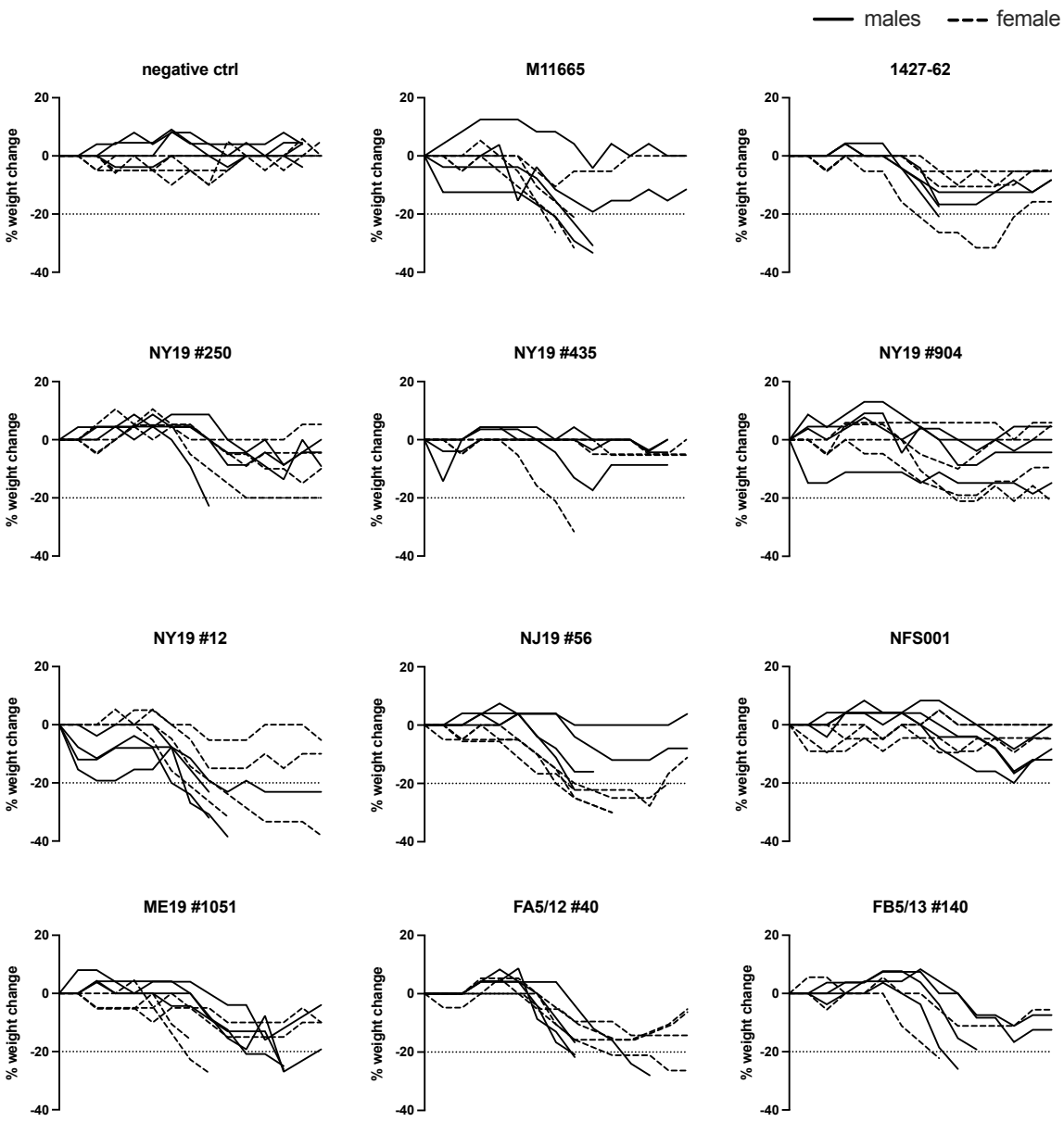

Figure S4.1. Percent weight change for male and female C57BL/6 mice inoculated with POWV or DTV isolates.

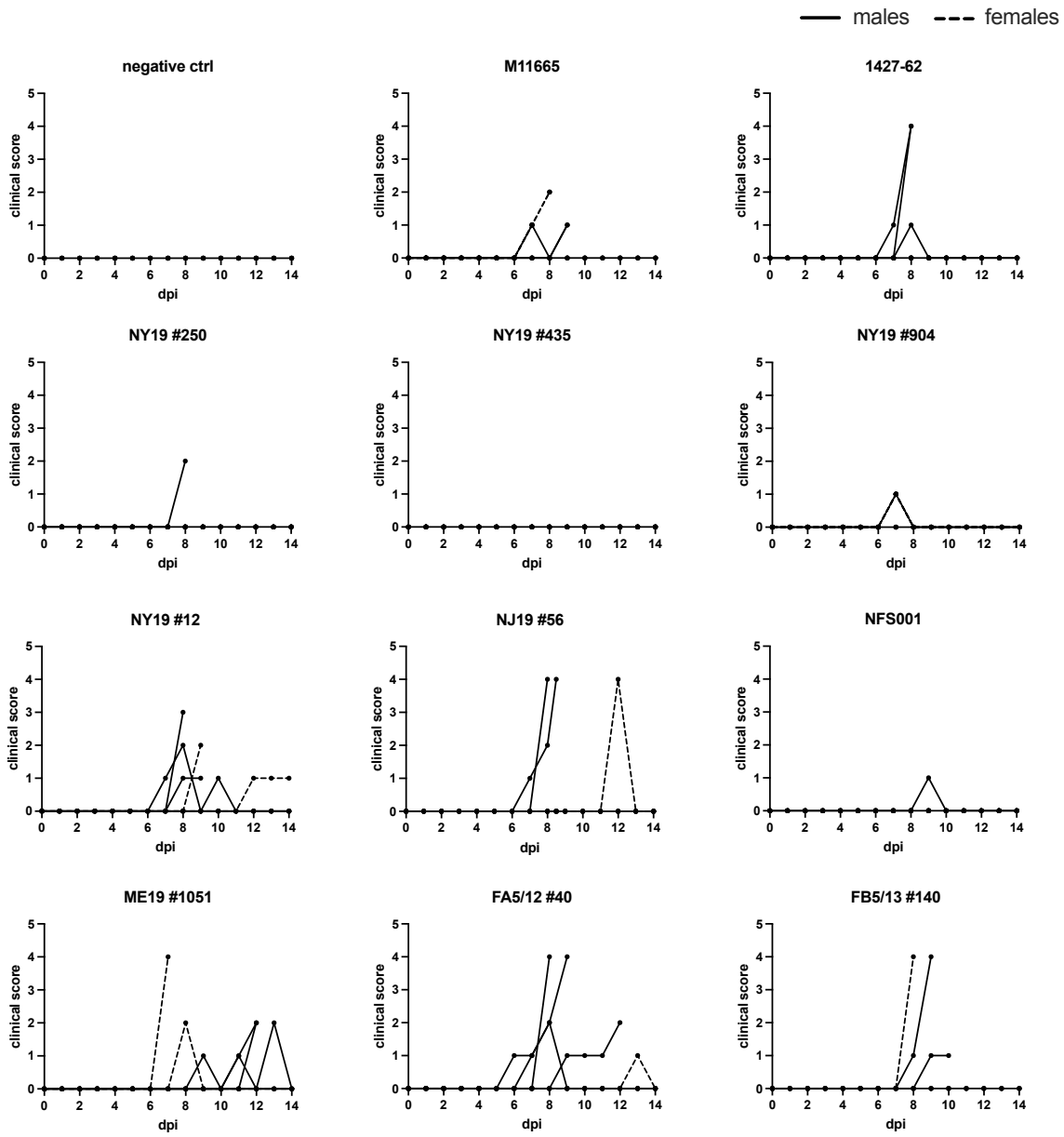

Figure S4.1. Clinical scores for male and female C57BL/6 mice inoculated with POWV or DTV isolates.

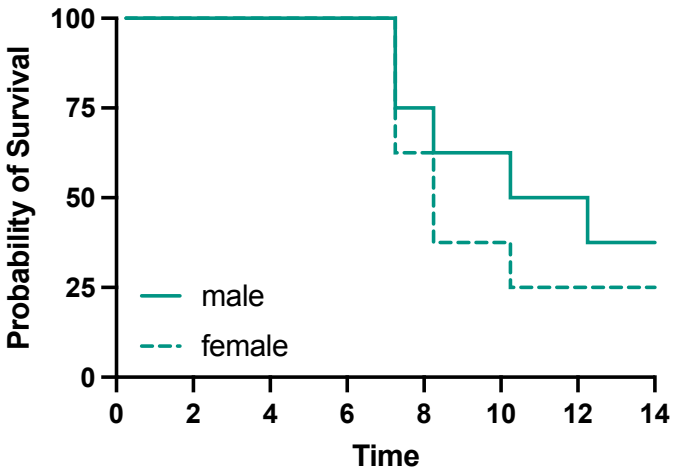

Figure S4.3. Validation of sex differences for DTV isolate FA5/12-40. Eight male and eight female mice were inoculated subcutaneously with 1e3 PFU Powassan virus and monitored for 14 days post infection. Weights and clinical scores were recorded daily. Mice were euthanized if they exhibited signs of neurological disease (ataxia, paralysis) or lost greater than 20% of their body weight.

Table S5.1. Metagenomic shotgun sequencing reads pre- and post- processing.

library type	village	household	week	n in sample	starting reads	reads post trimming	reads post host filtering	final reads/sample	%reads after trimming	% trimmed reads after filtering
human	Chiquirines	2002	12	4	2520214	613772	295139	73784.75	24.35	48.09
mosquito	Chiquirines	2002	12	28	19607041	9430716	5228255	186723.39	48.10	55.44
human	Chiquirines	2013	1	5	51091968	2256570	1117652	223530.40	4.42	49.53
mosquito	Chiquirines	2013	1	13	11164683	4463504	2197622	169047.85	39.98	49.24
human	Chiquirines	2014	4	4	2977902	90483	6248	1562.00	3.04	6.91
mosquito	Chiquirines	2014	4	14	10523552	1852666	1007962	71997.29	17.60	54.41
human	Los Encuentros	1002	6	7	3593351	618889	355082	50726.00	17.22	57.37
mosquito	Los Encuentros	1002	6	31	20653974	6564342	4330199	139683.84	31.78	65.97
human	Los Encuentros	1016	2	6	3209223	463913	347609	57934.83	14.46	74.93
mosquito	Los Encuentros	1016	2	9	4911169	1609229	1142141	126904.56	32.77	70.97
human	Los Encuentros	1019	3	7	5117911	45888	40228	5746.86	0.90	87.67
mosquito	Los Encuentros	1019	3	51	17591039	7133004	6206331	121692.76	40.55	87.01
human	Los Encuentros	1019	10	7	6073426	718598	274051	39150.14	11.83	38.14
mosquito	Los Encuentros	1019	10	35	23458047	9481068	6736275	192465.00	40.42	71.05
water control				1	917217	218336	218336	218336.00	23.80	100.00
FTA control				3	1425736	285732	285732	95244.00	20.04	100.00
HeLa control				1	520536	430899	3676	3676.00	82.78	0.85

Table S5.2. Coverage and Identity of ISVs.

ISV	ref genebank #	coverage	% identity
Culex phasma-like virus (Culex orthophasma virus)	NC_055214.1, NC_055213.1, NC_055215.1	97.2	97.6
Terena virus	KT966492, KT966493, KT966494	40.7	97.7
Hubei reo-like virus 7	KX884635.1 (RdRp gene)	98.9	98.6
Grenada mosquito rhabdovirus 1	MG385079.1	93.7	98.8
Culex flavivirus	AB262759.2	79.7	99.2
Hubei virga-like virus 2	MW435011.1	77.7	98.9
Culex originated Tymoviridae-like virus	MH188018.1	61.6	98.9
Hubei mosquito virus 4	KX883008.1	26.4	97.4
Phasi Charoen-like phasivirus	MN866293.1, MN866262.1, MN866241.1	89.4	98.9
Culex Iflavi-like virus 4	NC_040832.1	7.7	98.1
Culex Hubei-like virus	MH188025.1	29.3	99.2
Culex narnavirus 1	MW434207.1	96	98.3
Yongsan iflavirus 1	MW699047.1	45	98
Coquillettidia venezuelensis narnavirus 2	MK285334.1	45.8	98.4
Wenzhou tombus-like virus 11	KX883008.1	12.9	90.2
Culex Y virus	JQ659254.1, JQ659255.1	82.6	97.9
Guadeloupe mosquito virus	MN053805.1, MN053806.1	75.8	99
Culex Iflavi-like virus 1	NC_040646.1	2.5	96.6
Human papillomavirus type 18	NC_001357.1	20	99.5
Totivirus-like Culex mosquito virus 1	MH188048.1	1.9	95.1
Hubei narna-like virus 17	KX883536.1	9.4	87.3

Table S5.3. Household enrollment and risk factors.

household ID	total adults living in house	adults not enrolled	Why did adults not enroll?	total children in house	children not enrolled	Why did children not enroll?	Building material
1001	4	2	work	2			cement blocks
1002	7	3	work	7			cement blocks
1003	3			0			cement blocks
1007	4	3	work	3			cement blocks
1008	8	1	work	2			cement blocks
1015	2	1	work	2	1	not at the house during the day	cement blocks
1016	3			3			cement blocks
1018	2	1	work	3	1	school	cement blocks
1019	4			5			cement blocks
1020	3			3	2	refused	cement blocks
2001	4			1			cement blocks
2002	5	3	work	5			cement blocks
2003	3			0			cement blocks
2004	4			3			cement blocks
2008	3			0			cement blocks
2010	3			4			cement blocks
2012	4	3	refused	1			cement blocks
2013	2			3			cement blocks
2014	2	1	work	3			madera
2017	2			1			Plywood

Table S5.3 (continued).

household ID	screened windows/ doors?	potted plants?	water well?	septic tank?	tires?	capless water tank	natural water on property or nearby?	fumigated in the last year?
1001	No	No	Yes	No	Yes	Yes	No	No
1002	No	Yes	Yes	No	Yes	Yes	Yes	No
1003	No	Yes	No	No	Yes	Yes	Yes	No
1007	No	Yes	No	Yes	Yes	Yes	No	No
1008	Yes	Yes	Yes	Yes	No	Yes	No	No
1015	No	Yes	Yes	No	Yes	Yes	Yes	Yes
1016	No	Yes	Yes	Yes	No	No	No	No
1018	No	Yes	No	Yes	No	Yes	Yes	Yes
1019	No	Yes	Yes	No	No	No	No	No
1020	No	Yes	Yes	No	Yes	No	No	No
2001	Yes	Yes	Yes	Yes	No	Yes	Yes	Yes
2002	No	Yes	Yes	No	No	Yes	No	Yes
2003	No	Yes	Yes	Yes	No	Yes	No	Yes
2004	No	Yes	Yes	Yes	Yes	No	No	No
2008	No	No	No	Yes	No	Yes	No	Yes
2010	No	No	Yes	Yes	No	No	Yes	No
2012	No	No	Yes	No	Yes	Yes	No	No
2013	No	Yes	Yes	No	Yes	Yes	No	No
2014	No	No	Yes	No	No	Yes	No	No
2017	No	Yes	Yes	Yes	Yes	No	Yes	Yes

Table S5.4. Household animals.

	Household ID	Chickens	Ducks	Rats	Pigs	Dogs	Cats	Turkey	other birds	Cows	Rabbit	Total
Los Encuentros	1001	10	0	6	1	4	0	0	0	0	0	21
	1002	2	1	3	1	3	1	0	0	0	0	11
	1003	22	73	0	0	5	0	0	0	0	0	100
	1007	45	0	5	7	2	0	0	8	0	0	67
	1008	25	0	0	1	1	3	3	0	0	0	33
	1015	1	0	4	1	0	3	0	0	0	0	9
	1016	20	0	6	0	3	0	0	0	0	0	29
	1018	30	3	0	2	2	0	0	0	0	0	37
	1019	20	0	0	0	3	1	0	0	0	0	24
	1020	3	0	0	2	0	0	0	0	0	0	5
Chiquirines	2001	10	10	0	1	1	2	2	0	0	0	26
	2002	9	1	5	12	1	0	0	0	0	0	28
	2003	9	0	1	0	0	1	0	0	0	1	12
	2004	1	0	0	0	1	1	0	0	0	0	3
	2008	6	0	10	6	3	4	0	1	0	0	30
	2010	22	0	2	0	0	0	0	0	0	0	24
	2012	8	5	2	2	1	0	0	0	0	0	18
	2013	50	1	3	1	3	1	6	0	0	0	65
	2014	6	0	10	1	0	0	0	0	0	0	17
	2017	30	0	0	4	4	2	1	0	0	0	41
	Total	329	94	57	42	37	19	12	9	0	1	600

Table S5.5. Bloodmeal Identification.

		Mammals				
	total	***Homo sapiens* (human)**	***Sus scrofa* (pig)**	***Equus caballus* (horse)**	***Canis lupus* (dog)**	***Bos taurus* (cow)**
Aedes aegypti	91	44	0	0	0	0
Aedes albopictus	3	2	0	0	0	0
Aedes taeniorhynchus	3	0	2	1	0	0
Anopheles albimanus	8	5	2	0	0	0
Anopheles sp.	2	2	0	0	0	0
Culex nigripalpus	10	1	0	0	0	1
Culex pipiens	297	79	3	0	1	0
Culex sp.	50	12	4	0	0	0
Mansonia dyari	20	13	1	0	0	0
Mansonia titilans	2	1	0	0	0	0
Psorophora ferox	2	0	0	0	0	0
sum species	**488**	**159**	**12**	**1**	**1**	**1**

Table S5.5 (continued).

Avian								
Gallus gallus **(chicken)**	***Anas platyrhynchos*** **(duck)**	***Cairina moschata*** **(duck)**	***Dives dives*** **(blackbird)**	***Meleagris gallopavo*** **(turkey)**	***Quiscalus mexicanus*** **(grackle)**	***Ortalis motmot*** **(chachalaca)**	***Turdus grayi*** **(thrush)**	**No match**
4	0	0	0	0	0	0	0	43
1	0	0	0	0	0	0	0	0
0	0	0	0	0	0	0	0	0
0	0	0	0	0	0	0	0	1
0	0	0	0	0	0	0	0	0
6	0	0	0	0	0	0	0	2
132	1	9	1	1	1	0	0	69
10	0	0	0	0	0	1	1	22
1	0	0	0	0	0	0	0	5
0	0	0	0	0	0	0	0	1
0	0	0	0	0	0	0	0	2
154	**1**	**9**	**1**	**1**	**1**	**1**	**1**	**145**